

THE CHARACTERIZATION OF METABOLITES
FROM THREE TROPICAL PACIFIC MARINE
INVERTEBRATES

by

J. Christopher Swersey

A thesis submitted to the faculty of
The University of Utah
in partial fulfillment of the requirements for the degree of

Master of Science

Department of Medicinal Chemistry

The University of Utah

August 1992

Copyright © J. Christopher Swersey 1992

All Rights Reserved

THE UNIVERSITY OF UTAH GRADUATE SCHOOL

SUPERVISORY COMMITTEE APPROVAL

of a thesis submitted by

J. Christopher Swersey

This thesis has been read by each member of the following supervisory committee and by majority vote has been found to be satisfactory.

8/31/92



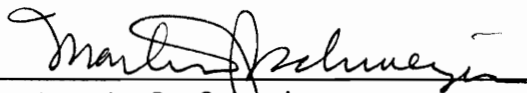
Chair: Chris M. Ireland

8/31/92



Darrell R. Davis

8/31/92



Martin P. Schweizer

ABSTRACT

Marine organisms produce a wide variety of metabolites that display diverse biological activities and represent an astonishing variety of molecular structural classes. As part of the Ireland group's continuing program to discover novel biologically active marine natural products, three sessile invertebrates from the Fijian and Philippine archipelagos were investigated.

Isolation of the compounds described was directed to a large degree by the biological activities displayed by extracts and partitions of the organisms and was accomplished by using standard chromatographic techniques. The structures were solved using standard spectroscopic methods, including one-dimensional (1-D) and two-dimensional (2-D) nuclear magnetic resonance (NMR), infrared (IR) and ultraviolet (UV) spectroscopy, circular dichroism (CD), and low resolution and high resolution fast atom bombardment mass spectrometry (FABMS, HRFABMS).

Mamanuthaquinone, a new member of a class of quinone containing sesquiterpenoid compounds, was the major metabolite of the Fijian sponge *Fasciospongia* sp. Mamanuthaquinone is a potent cytotoxic agent with moderate antimicrobial activity. Chemical rearrangement was utilized to determine the absolute stereochemistry of mamanuthaquinone.

An unidentifiable orange Fijian sponge of mixed taxonomy, having organizational and chemical characteristics of *Axinellidae* and *Jaspidae* families, yielded a new tetracyclic bromopyrrole derivative called epipola-

THE UNIVERSITY OF UTAH GRADUATE SCHOOL

FINAL READING APPROVAL

To the Graduate Council of The University of Utah:

I have read the thesis of J. Christopher Swersey in its final form and have found that (1) its format, citations, and bibliographic style are consistent and acceptable; (2) its illustrative materials including figures, tables, and charts are in place; and (3) the final manuscript is satisfactory to the Supervisory Committee and is ready for submission to The Graduate School.

8/31/92

Date



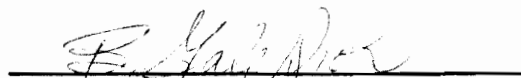
Chris M. Ireland
Chair, Supervisory Committee

Approved for the Major Department



Arthur D. Broom
Chair/Dean

Approved for the Graduate Council



B. Gale Dick
Dean of The Graduate School

sidamide. Epipolasidamide exhibited in vitro cytotoxicity vs. HCT-116 cells, with an IC₅₀ of 0.1 mg/mL.

Mild cytotoxicity exhibited by the crude extract of the Philippino tunicate *Eusynstyela misakiensis* led to the isolation of eusynstyelamide, a novel dimer of a highly modified 6-bromotryptophan and decarboxylated arginine containing dipeptide. Eusynstyelamide was found to be mildly cytotoxic, with an IC₅₀ of 50 µg/mL vs. HCT-116 cells in vitro. The structure was determined by interpretation of 2-D NMR data, including HMBC and COSY45 data. A putative biosynthetic pathway for eusynstyelamide was developed, based on chemotaxonomic and structural evidence.

For Mary, and our Family

TABLE OF CONTENTS

ABSTRACT	iv
LIST OF FIGURES	ix
GLOSSARY OF NMR EXPERIMENTS.....	xiii
ACKNOWLEDGMENTS.....	xv
I. INTRODUCTION.....	1
Background	1
Literature Review.....	5
II. THE CHEMISTRY OF <i>FASCIOSPONGIA</i> SPECIES.....	46
Introduction	46
Sponge Collection and Isolation of Mamanuthaquinone	46
Structure Determination of Mamanuthaquinone	47
Relative and Absolute Configurations of Mamanuthaquinone.....	55
Biological Activity of Mamanuthaquinone	61
III. THE CHEMISTRY OF AN UNIDENTIFIED FIJIAN SPONGE OF MIXED <i>AXINELLIDAE</i> AND <i>JASPIDAE</i> TAXONOMY.....	63
Introduction	63
Sponge Collection and Isolation of Epipolasidamide.....	64
Structure Determination of Epipolasidamide	65
Relative Configuration of Epipolasidamide	71
Molecular Modeling of Epipolasidamide.....	72
Biological Activity of Epipolasidamide.....	77
IV. THE CHEMISTRY OF THE PHILIPPINO ASCIDIAN <i>EUSYNSTYELA MISAKIENSIS</i>	79
Introduction	79

Tunicate Collection and Isolation of Eusynstyelamide.....	80
Structure Determination of Eusynstyelamide.....	80
Other Experiments with Eusynstyelamide.....	96
Biological Activity of Eusynstyelamide	97
V. EXPERIMENTAL.....	98
General Experimental Procedures	98
The Chemistry of <i>Fasciospongia</i> sp.....	99
The Chemistry of an Unidentified Fijian Sponge of Mixed <i>Axinellidae</i> and <i>Jaspidae</i> Taxonomy.....	102
The Chemistry of <i>Eusynstyela misakiensis</i>	105
Appendices	
A. NMR AND CD SPECTRA OF MAMANUTHA- QUINONE AND THE REARRANGED QUINONE SESQUITERPENOIDS	108
B. NMR AND CD SPECTRA OF EPIPOLASIDAMIDE.....	116
C. NMR AND CD SPECTRA OF EUSYNSTYELAMIDE.....	120
REFERENCES.....	127

LIST OF FIGURES

<u>Figure</u>	<u>Page</u>
1. Phyletic distribution of marine natural products reported between 1977-1987	3
2. Phyletic distribution of marine natural products reported between 1986-1987	3
3. Structures of 5,6-secosterols from <i>Hippospongia communis</i>	13
4. Absolute stereochemistry of the dictyoceratins.....	14
5. Derivation of the quinone sesquiterpenoids.....	16
6. Absolute stereochemistry of isospongiaquinone	17
7. Absolute stereochemistry of ilimaquinone.....	18
8. Proposed biosynthesis of mamananthaquinone	19
9. Biologically active cyclic peptides from <i>Theonella</i> sp.....	23
10. Biosynthesis of the phakellins and dibromoisophakellin	31
11. Percentage of nitrogenous metabolites from various phyla	35
12. Derivation of ascidian-produced metabolites.....	35
13. HMBC correlations observed for the quinone substructure of mamananthaquinone	50
14. Partial structures of mamananthaquinone developed by COSY and DQCOSY results.....	52
15. HMBC correlations observed in the terpenoid moiety of mamananthaquinone	53

16.	500 MHz TOCSY spectrum of mamanuthaquinone with spin systems delineated.....	54
17.	Relative stereochemistry of mamanuthaquinone by difference nuclear Overhauser effect spectroscopy	56
18.	Lewis acid catalyzed rearrangement of mamanuthaquinone and ilimaquinone	58
19.	Stacked proton NMR spectra of rearranged quinone sesquiterpenoids.....	59
20.	Stacked carbon NMR spectra of rearranged quinone sesquiterpenoids.....	60
21.	In vitro AIDS inhibition testing of mamanuthaquinone.....	62
22.	Partial structures of epipolasidamide developed from COSY data.....	68
23.	HMBC correlations observed for epipolasidamide.....	69
24.	NOEs observed in epipolasidamide	71
25.	The Karplus relationship	73
26.	Minimized structures of epipolasidamide	74
27.	The dihedral angle between H-7 and H-12.....	75
28.	Comparison of calculated interproton distances and observed NOEs of epipolasidamide.....	76
29.	In vitro HCT-116 testing of epipolasidamide.....	77
30.	Theoretical formation of eusynstyelamide via self-condensation of an achiral precursor	83
31.	Indole proton spin systems of eusynstyelamide by COSY and COSY45.....	87
32.	HMBC correlations observed for the indole moieties of eusynstyelamide	89
33.	The decarboxylated arginine moieties of eusynstyelamide	91

34.	HMBC correlations relating the two dipeptide halves of eusynstyelamide	93
35.	Comparison of α -keto amides and ketone hydrates in eusynstyelamide and cyclotheonamide A	95
36.	Mass spectral fragmentation pathways of eusynstyelamide	96
37.	500 MHz ^1H NMR spectrum of mamanuthaquinone (50).....	109
38.	125 MHz ^{13}C NMR spectrum of mamanuthaquinone (50).....	110
39.	500 MHz ^1H NMR spectrum of rearranged mamanuthaquinone (151_m).....	111
40.	125 MHz ^{13}C NMR spectrum of rearranged mamanuthaquinone (151_m).....	112
41.	500 MHz ^1H NMR spectrum of rearranged ilimaquinone (151_i).....	113
42.	125 MHz ^{13}C NMR spectrum of rearranged ilimaquinone (151_i).....	114
43.	CD spectra of rearranged quinones 151_m and 151_i	115
44.	500 MHz ^1H spectrum of epipolasidamide (88) recorded in d_6 -DMSO	117
45.	125 MHz ^{13}C spectrum of epipolasidamide (88) recorded in d_6 -DMSO	118
46.	CD spectrum of epipolasidamide (88) recorded in methanol.....	119
47.	500 MHz ^1H spectrum of eusynstyelamide (150) recorded in d_6 -DMSO	121
48.	125 MHz ^{13}C spectrum of eusynstyelamide (150) recorded in d_6 -DMSO	122
49.	500 MHz ^1H spectrum of eusynstyelamide (150) recorded in d_4 -methanol.....	123

50.	125 MHz ^{13}C spectrum of eusynstyelamide (150) recorded in d_4 -methanol.....	124
51.	500 MHz DQCOSY spectrum of eusynstyelamide recorded in d_6 -DMSO	125
52.	CD spectrum of eusynstyelamide (150) recorded in methanol.....	126

signal from relatively sensitive protons, as compared to carbon atoms, and is thus much more sensitive than the analogous long range HETCOR and COLOC experiments.

HMQC (Heteronuclear Multiple Quantum Coherence) - Another 2-D reverse detection experiment used to determine direct proton-carbon connectivities. Because signals are detected in the proton domain, this experiment is much more sensitive than the analogous HETCOR experiment.

Difference NOE (Nuclear Overhauser Effect Spectroscopy) - 1-D spectra used to determine which protons of a molecule are proximal in space ($<4 \text{ \AA}$). Irradiation of a particular proton signal, followed by saturation of its usual relaxation pathways, results in dipole-dipole cross relaxation of the irradiated signal and concomitant enhancement of the through-space coupled signal.

Total Correlation Spectroscopy (TOCSY) - A 2-D experiment that utilizes a spin-lock pulse train during which coherence transfer of all proton signals in a coupled proton spin system occurs. The resultant spectrum contains cross peaks between all protons of an isolated proton spin system.

GLOSSARY OF NMR EXPERIMENTS

COSY (Correlated Spectroscopy) - The simplest 2-D NMR experiment, used to determine which signals in a proton spectrum are scalar coupled.

COSY45 - A COSY experiment in which zero quantum coherence is discriminated against. The result of this pulse sequence is the minimization of certain peaks, such as signals along the diagonal.

DEPT (Distortionless Enhancement by Polarization Transfer) - A pulse sequence that allows determination of the multiplicity of relatively insensitive nuclei, such as carbon.

DQCOSY (Double-Quantum Correlated Spectroscopy) - A COSY experiment in which double-quantum coherence is selected for. Undesired coherence is suppressed by phase cycling of the preparation pulses and alternate addition and subtraction of signals, resulting in phase-sensitive spectra.

HMBC (Heteronuclear Multiple Bond Correlation) - A so-called "reverse detection" 2-D experiment used to determine the 2- and 3-bond coupling of protons and carbons. The experiment utilizes detection of

ACKNOWLEDGMENTS

I am extremely grateful to my advisor, Dr. Chris M. Ireland, for his continued support, friendship and guidance during my graduate career. No one in his position is as talented, trusting and capable of sharing as he. It has been my privilege to be associated with him during my development as both a scientist and a better person.

I would like to thank my colleagues in the Ireland group and in the Department of Medicinal Chemistry who contributed advice, answers and the environment in which my work flourished. Drs. Brent Copp, Tadeusz F. Molinski, and Deborah Roll taught me a great deal of science and critical thinking. All of the group members have been more helpful than they can possibly know; they have shown me how to do what I have done. I thank Leonard McDonald in particular for his friendship and chromatographic instinct.

At the best of times, science is demanding of the mind and the soul. My abilities as a scientist have flourished with a concurrent growth in my confidence and self-esteem. I would like to thank my river friends, the best there are, who have aided and allowed me to become happier and more human than I ever believed I could be.

Most importantly, I thank my family for their love and support throughout my education. I thank my parents for their encouragement, and my grandparents for assuring me that my best would be good enough.

Finally, I wish to thank Mary for her love and sacrifices, her dedication to my goals and for the happiness she has brought me during our life together. She is the light of my life, and her support has been inspirational and selfless.

I would like to acknowledge the College of Pharmacy at the University of Utah for their generous fellowship and the National Institutes of Health for funding this research.

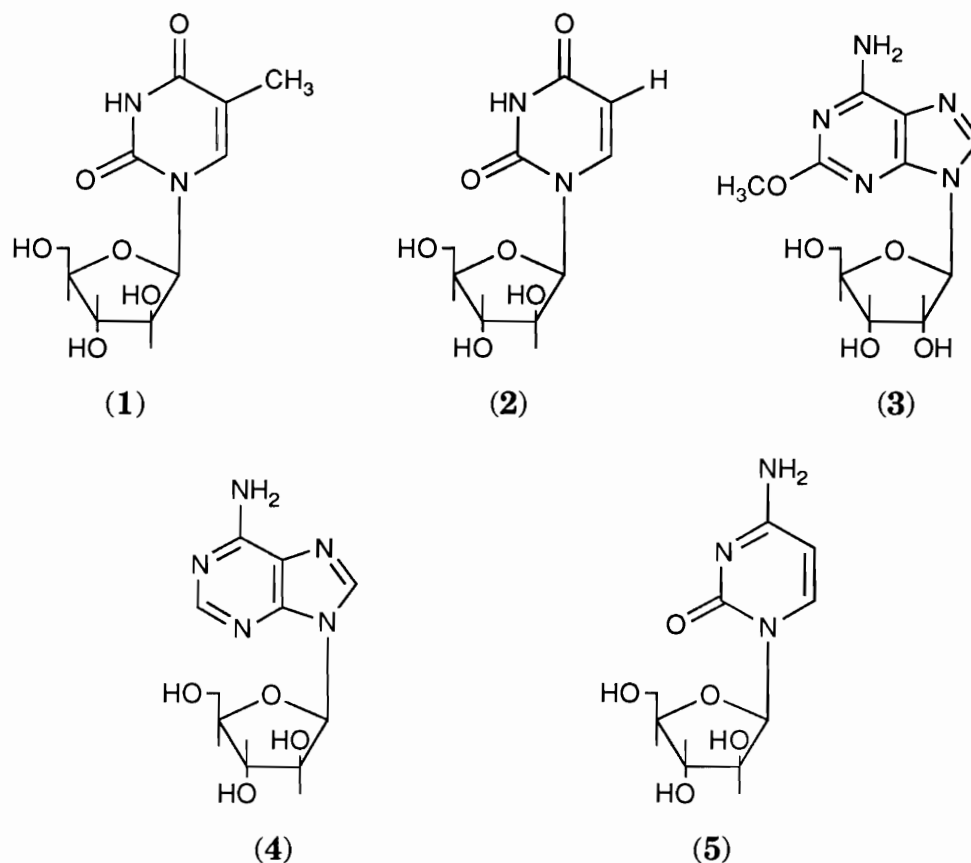
I. INTRODUCTION

Background

The study of marine natural products is relatively new compared to that of compounds from terrestrial origins. The oceans cover 70% of the earth's surface, and only in the last few decades has systematic, routine study of this enormous resource become feasible. As the discovery rate of novel classes of biologically active compounds from terrestrial sources decreases, organisms from the marine environment are becoming an increasingly important source of new metabolites.

The progenitor of the marine natural products field is considered to be Bergmann, who isolated the nucleosides spongothymidine (**1**), spongo-uridine (**2**) and spongosine (**3**) from the large sponge *Tethya crypta* in the early and mid-1950s.¹⁻⁴ These compounds subsequently served as models for the clinically useful synthetic antiviral agents Ara-A (**4**) and Ara-C (**5**).⁵⁻⁷ Since then, the majority of the metabolites isolated from marine organisms have come from invertebrates, such as porifera (sponges), algae and coelenterates.

The earliest field collection efforts concentrated on obvious targets, such as large sponges, soft corals, and algae. An analysis of some 2500 metabolites reported in the 11-year period from 1977 to 1987 shows that these three phyla in particular dominated the focus of marine natural products research (Figure 1). Furthermore, during that period sponges emerged as



the single predominant phylum of study. During the last year of this analysis, sponges alone were responsible for almost as many reported metabolites as coelenterates and algae combined (Figure 2).

Research in the Ireland group has become increasingly focused on more polar biologically active nitrogenous metabolites from sponges and tunicates (a.k.a. ascidians). This trend reflects several developments in marine natural products chemistry and pharmacology. As the field matures, and more compounds are reported, the likelihood of encountering a known compound increases dramatically; this is to be expected in any discovery oriented field. Thus we tend to focus our collection efforts on

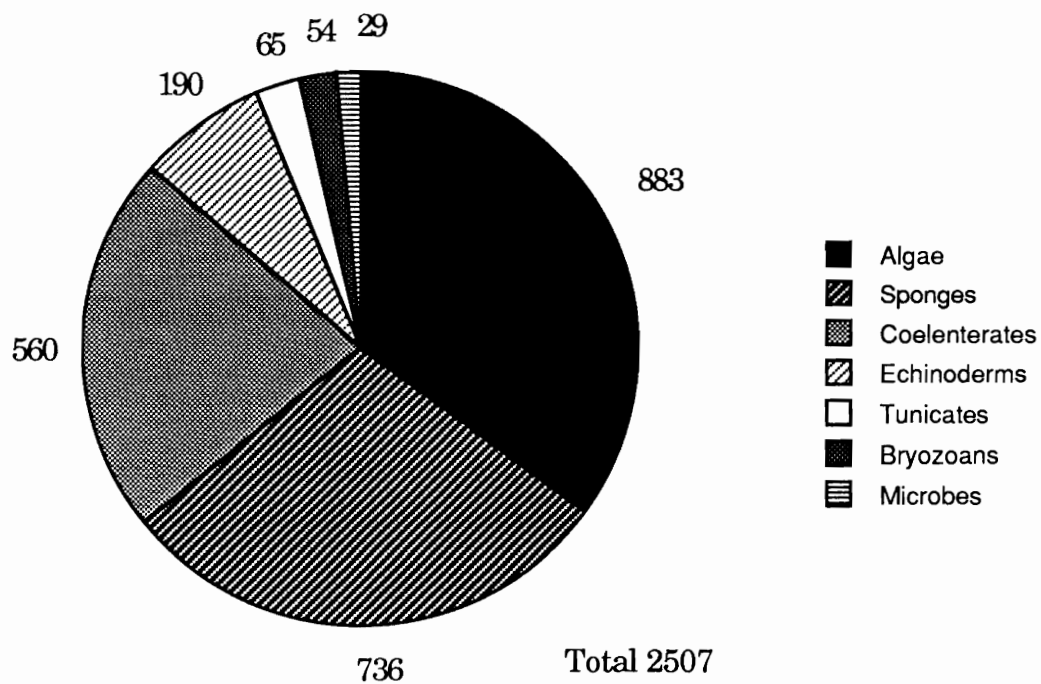


Figure 1. Phyletic distribution of marine natural products reported between 1977-1987.

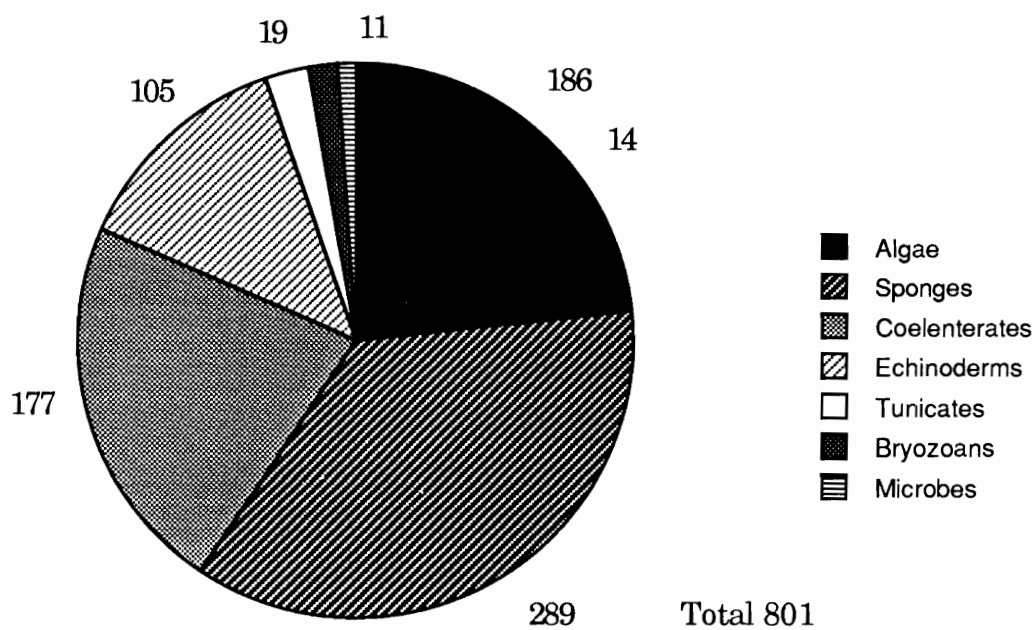


Figure 2. Phyletic distribution of marine natural products reported between 1986-1987.

organisms that are more difficult to collect or are rarely encountered, such as certain types of ascidians, to reduce the chance that we are duplicating the efforts of another group.

Within the context of medicinal chemistry research, we have defined our task as the isolation, structure elucidation, and pharmacological characterization of biologically active substances. To this end, during the past 6 years we have developed or acquired access to increasingly sophisticated testing protocols for crude extracts and pure compounds. For example, "mechanism of action" assays with genetically altered cell lines available in our lab allow us to detect compounds that interact with nucleic acids, either by intercalation or strand scission. Collaborative efforts with other academic groups, commercial pharmaceutical companies, and government agencies allow us to test for in vivo and in vitro antineoplastic activity, protection from Human Immunodeficiency Virus (HIV) infection (which results in acquired immunodeficiency syndrome, or AIDS), and inhibition of tubulin polymerization or depolymerization, among others.

Technological developments have also dramatically affected the *modus operandi* of our group. Recently there has been a dramatic increase in the number of different commercially available chromatographic media. Rational development of a separation strategy for the isolation of pure compounds represents the single most challenging and time-consuming task the natural products chemist performs. The availability of so-called "bonded phase" media has greatly enhanced our ability to handle and separate much more polar compounds. Currently, the likelihood of isolating a known compound seems to decrease as the polarity of the compound increases. Although this is merely an empirical observation, two of the

projects reported herein relied heavily on separation methods afforded by media other than silica and alumina and could not have proceeded without them.

The collection efforts of the Ireland group have expanded from Fiji to include the Philippines archipelago as a new source of tropical marine invertebrates. As part of our continuing effort to find novel biologically active metabolites from these animals, three organisms have been investigated. Two Fijian sponges, including *Fasciospongia* sp. and one of mixed taxonomy in the Families *Axinellidae* and *Jaspidae*, yielded cytotoxic crude extracts, which were investigated further on this basis. Colonial Styelid tunicates of the genus *Eusynstyela* are rarely encountered and difficult to collect. Their habitats are often inaccessible crevices deep in caves, they often occur as rather small colonies, and their anatomical organization renders them difficult to remove intact from the substrate upon which they grow. Crude extracts of several of these organisms, including the orange and red Fijian colonial ascidian *Eusynstyela latericius* and the pink Philippino ascidian *Eusynstyela misakiensis*, exhibited mild cytotoxicity. The Philippino organism *Eusynstyela misakiensis* was collected in sufficient quantity to study, and the compound responsible for its mild biological activity was investigated.

Literature Review

The intention of this introduction is to provide selected background information that is pertinent to the projects described in this thesis, either by taxonomic or structural similarity. Compounds that exhibit remarkable biological activity are also included where appropriate. Comprehensive

reviews of all classes of marine natural products organized by phylum are prepared yearly by Faulkner.⁸⁻¹⁴

The contributions of this thesis to the study of biologically active terpenoid metabolites derived from sponges include the complete characterization of a new member of a class of quinone containing sesquiterpenoid compounds produced by sponges of the Order Dictyoceratida. These sponges are prolific producers of terpenoid compounds; the genus *Dysidea* alone has inspired no less than 70 reports in the last 18 years. This introduction contains brief coverage of Dictyoceratid-derived metabolites which typify those structural motifs characteristic of the Order, such as lactone, furan and phenol terpenoids, and sterols. Quinone sesquiterpenoids and compounds from sponges of the genus *Fasciospongia* are covered more thoroughly.

Work in this thesis in the area of peptidal compounds derived from sponges includes the characterization of epipolasidamide, a novel cytotoxic tetracyclic bromopyrrole-containing compound of peptidal origin from an unidentified Fijian sponge of mixed *Axinellidae* and *Jaspidae* taxonomy. The scope of the present review within this huge area is limited to recently reported peptides isolated from sponges that exhibit remarkable biological activity and those brominated peptidal metabolites from sponges that contain structural similarities to epipolasidamide, or which represent putative biosynthetic precursors.

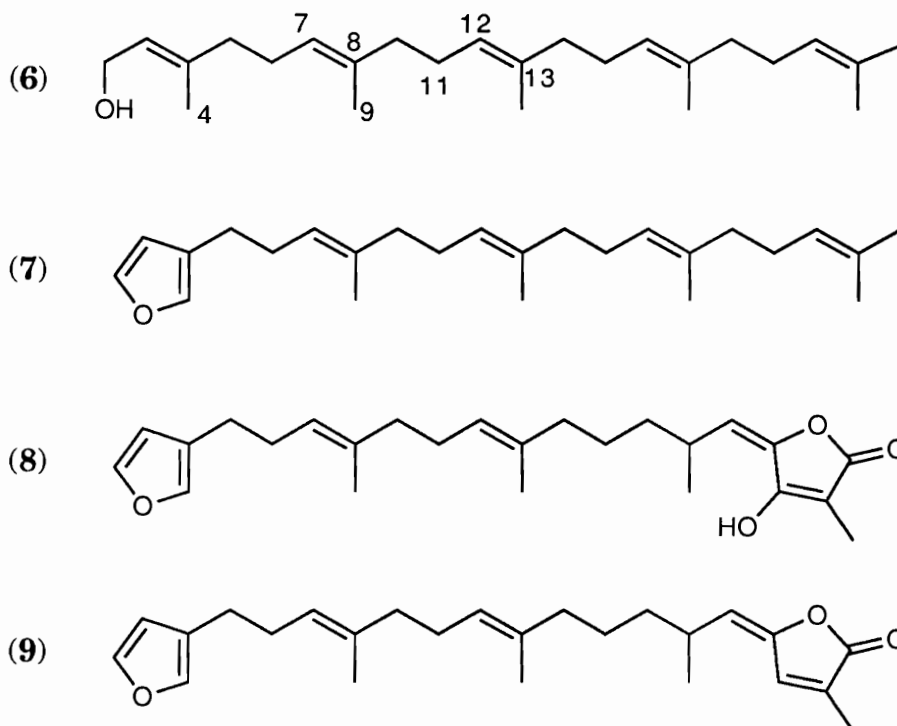
The final research project described in this thesis details the isolation and characterization of eusynstyelamide, a highly polar peptide-derived metabolite isolated from the colonial tunicate *Eusynstyela misakiensis*. This introduction contains comprehensive coverage of those ascidian-derived indole alkaloids or amino acid-derived compounds that incorporate

structural motifs similar to those found in eusynstyelamide, as well as selective coverage of other tunicate-derived peptidal metabolites that exhibit remarkable biological activity.

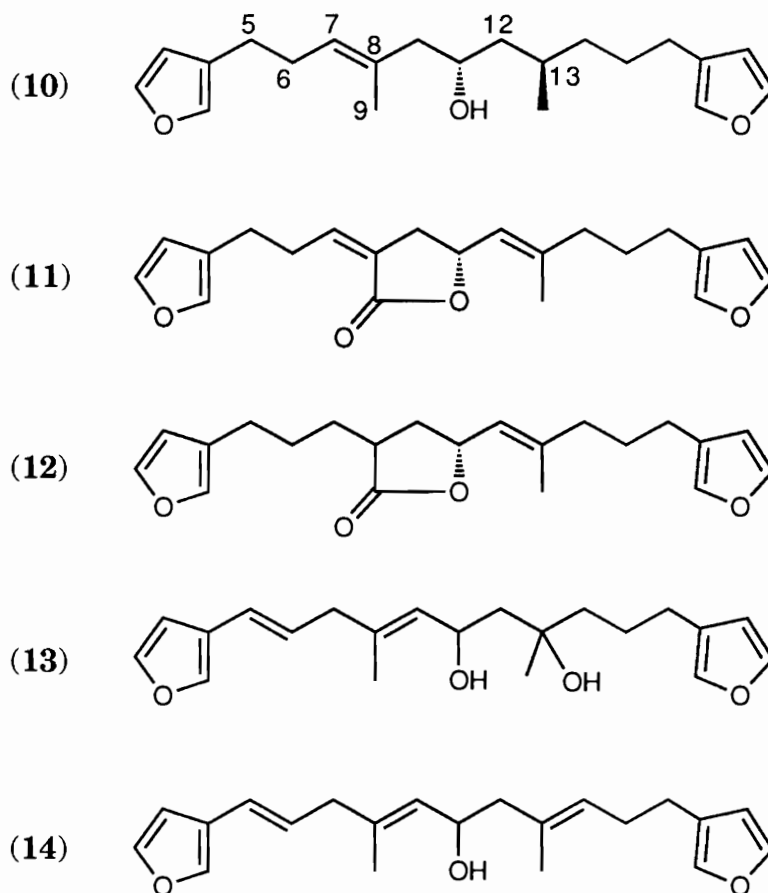
Natural Products from Marine Sponges of the Order Dictyoceratida

Dictyoceratid sponges specialize in the production of terpenoid metabolites with a range of biological activities. Many can be grouped in series of increasingly complex oxidation or ring closure products of simple linear terpenoid precursors, like the 25 carbon terpenoid geranylarnesol (**6**). Sesterterpenes had been considered rare in nature, but by 1976 at least five had been isolated from a variety of Dictyoceratidae.¹⁵ This trend has continued, as contemporary reports describe terpenoids with varied structures and biological activities.

The first reported example of geranylarnesol (**6**) from marine sources came from the Australian sponge *Fasciospongia fovea*.¹⁶ The sponge also contained the previously described compounds furospinulosin-1 (**7**) and variabilin (**8**).^{17,18} Furospinulosin-1 results from ring closure at C-4 of **6** and loss of two molecules of hydrogen. Variabilin appears to result from further elaboration of furospinulosin. Another derivative of **8**, 22-deoxyvariabilin (**9**), was recently isolated from the New Zealand sponge *Thorecta* sp.¹⁹ 22-Deoxyvariabilin displayed mild antimicrobial activity towards *Staphylococcus aureus*, *Bacillus subtilis*, and *Candida albicans* at 100, 50, and 100 µg/disk, respectively.



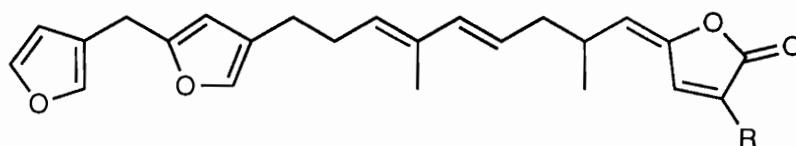
One of the earliest hypotheses regarding the biogenesis of marine natural products was inspired by the series of compounds furospongin-1 (10), nitenin (11), and dihydronitenin (12). Furospongin-1, isolated from the Dictyoceratidae *Spongia officinalis* and *Hippospongia communis*, is a furanoterpene with antibacterial activity against *Diplococcus* and *Streptococcus* strains.²⁰ It is believed that the nitenins, originally isolated from a sample of *Spongia nitens*, arise from furospongin-1 via oxidation and further elaboration of C-9, olefin formation via oxidation of C-12 and C-13, and by reduction of the C-7 and C-8 in the case of 12.²¹



Untenospongins A (**13**) and B (**14**) are furanoterpenes isolated from the Okinawan sponge *Hippospongia* sp.²² The untenospongins exhibit potent coronary vasodilating activity, by inhibiting 40 mM KCl induced contraction in isolated rabbit coronary artery at concentrations of 1 and 2 μ M, respectively. Like the nitenins, **13** and **14** also seem to be derived from furospongins-1, via hydroxylation or oxidation of C-13, isomerization of the olefin about C-8, and oxidation of C-5 and C-6 to another olefin.

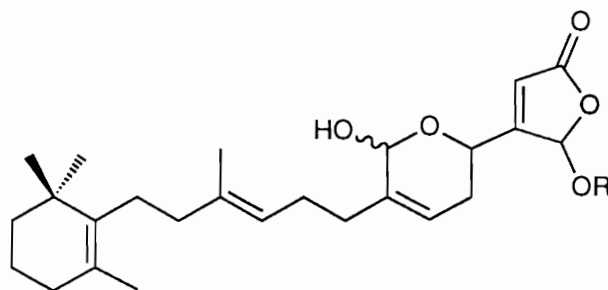
Sesterterpene butenolides have been isolated from several genera of Dictyoceratid sponges. The first of these, ircinolide (**15**) and 24-hydroxyircinolide (**16**), were isolated from an Australian sponge originally ident-

ified as *Thorecta marginalis*.¹⁵ The identity of the sponge that produced ircinolides **15** and **16** was recently established as *Taonura marginalis*.²³ In fact, many Dictyoceratidae are characteristically difficult to identify at the genus and species levels; this has led to several instances of misidentification in reports concerning them.²⁴



(**15**): R=Me
(**16**): R=CH₂OH

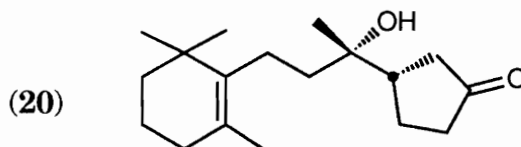
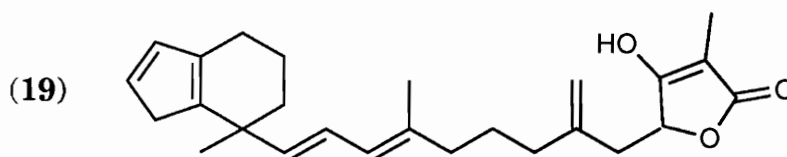
Manoalide (**17**) is a biologically active metabolite of *Luffariella variabilis*.²⁵ Manoalide has been credited with unique analgesic activity, in that it inhibits phorbol-induced inflammation, but not arachidonic acid-induced inflammation.²⁶



(**17**): R=H
(**18**): R=CO₂CH₃

Manoalide was subsequently shown to inhibit phospholipase A₂ (PLA₂) in vitro at extremely low concentrations (IC₅₀ 0.55 μM) and is currently being used to study the role of PLA₂ in the inflammatory reaction, as well as biochemical and physical properties of PLA₂ itself.²⁷ The analog manoalide monoacetate (**18**) was recently isolated from the Australian sponge *Thorectandra excavatus*.²⁴ Unfortunately, because the biological activity of **18** was not reported, the importance of the 24-OH group in the biological activity of **17** remains unknown.

Hippospongins (**19**), a butenolide recently isolated from the Okinawan sponge *Hippospongia* sp., is the first antispasmodic marine natural product isolated lacking either a guanidine or sulfone group.²⁸ Contractile response of guinea-pig ileum to 10⁻⁷ M carbachol and 10⁻⁷ M histamine were abolished by 5 x 10⁻⁶ M **19**. Hippospongins also inhibited the growth of Gram-positive bacteria (21 mm zone at 100 μg/disk vs. *Bacillus subtilis*), but not that of Gram-negative bacteria (*Escherichia coli*) or yeast (*Saccharomyces cerevisiae*).



Sessile marine invertebrates have adapted chemically to a highly competitive predatory environment.²⁹ For instance, the sponge *Fasciospongia cavernosa* from Papua New Guinea produces cavernosine (**20**), a novel ichthyotoxic terpenoid lactone.³⁰ Cavernosine is responsible in part for the toxicity of the dichloromethane extract of the sponge against the fish *Lebistes reticulatus*, (LD=20 mg/L) and was presumed to act as an antifeedant.

Other unique compounds produced by *Dictyoceratidae* include a series of novel 5,6-secosterols (**21** - **29**) isolated from the sponge *Hippospongia communis* (Figure 3).^{31,32} Only a few reports exist to date describing other marine sterols in which bonds of the tetracyclic nucleus have been cleaved. These compounds are 9,11-secosterols isolated from two types of cnidarians and from another Dictyoceratid sponge, *Dysidea herbacea*.³³⁻³⁶ Compounds **21** - **29** represent the first 5,6-secosterols described as natural products.

Dictyoceratin-A (**30**) and -B (**31**), antimicrobial hydroquinone-containing sesquiterpenoids, were recently isolated from the Okinawan sponge *Hippospongia* sp.³⁷ Dictyoceratin-A was more potent than Dictyoceratin-B, with minimum inhibitory concentrations (MIC's) of 6.3 and 3.1 µg/mL vs. *S. aureus* and *B. subtilis*, respectively. The absolute configurations of **30** and **31** were deduced by optical comparison (CD spectrum) of their common ozonolysis product to that derived from the previously described ilimaquinone (**32**).³⁷ The terpenoid moieties of the dictyoceratins were found to be enantiomeric to that of **32** (Figure 4). A similar hydroquinone (**33**) with a linear terpenoid moiety was recently isolated from the New Caledonian sponge *Fasciospongia* sp.³⁸ Hydroquinone **33** exhibited weaker antimicrobial activity than the **30** and **31** (MIC 100 µg/mL vs. *S. aureus* , *B. subtilis*).

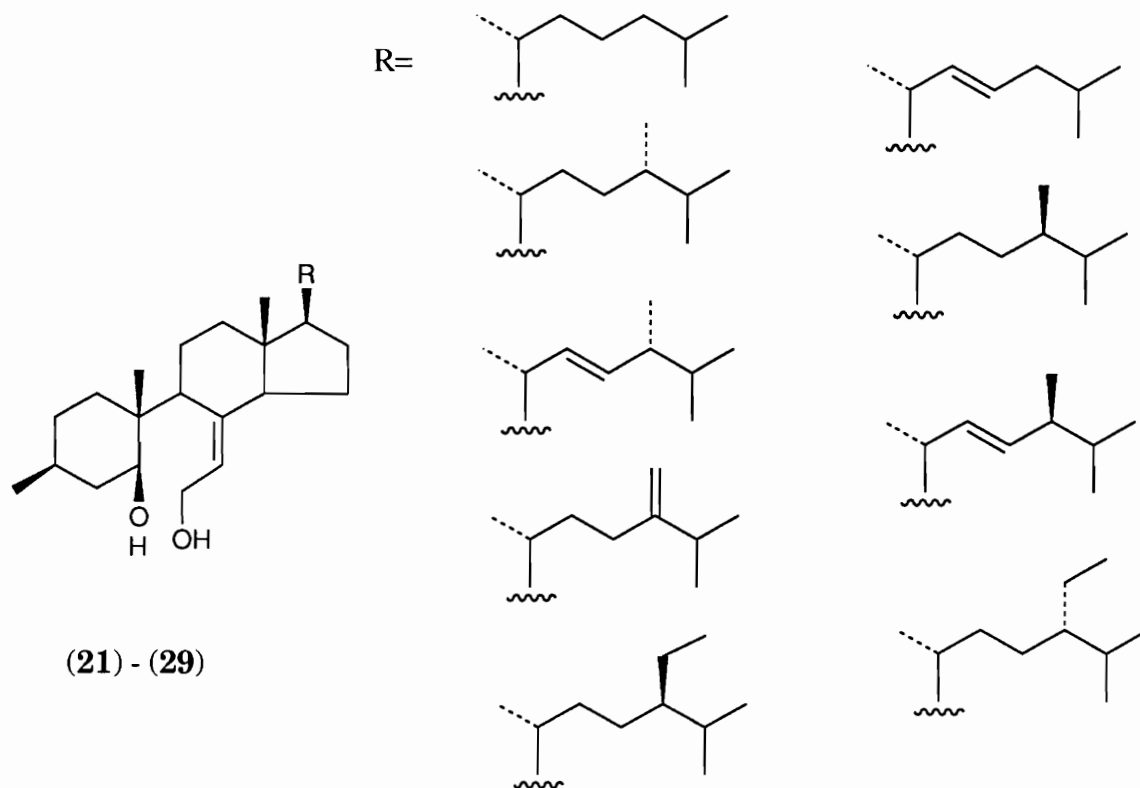


Figure 3. Structures of 5,6-secosterols from *Hippospongia communis*.

As a class, the quinone sesquiterpenoids isolated from Dictyoceratidae are thought to arise from functionalization of polyprenyl quinols of the form **34** - **39**.³⁹ Cyclization of the polyprenyl chain and oxidation of the aromatic moiety of **35** yield the quinone drimane sesquiterpenoids. The drimane moiety may then undergo rearrangement, while the aromatic moiety is elaborated further by hydroxylation, methoxylation, or cyclization to a site on the drimane skeleton. Polyprenyl quinol **36** has been isolated from *Ircinia muscarum*, and quinols **37** - **39** have been isolated from *Ircinia*

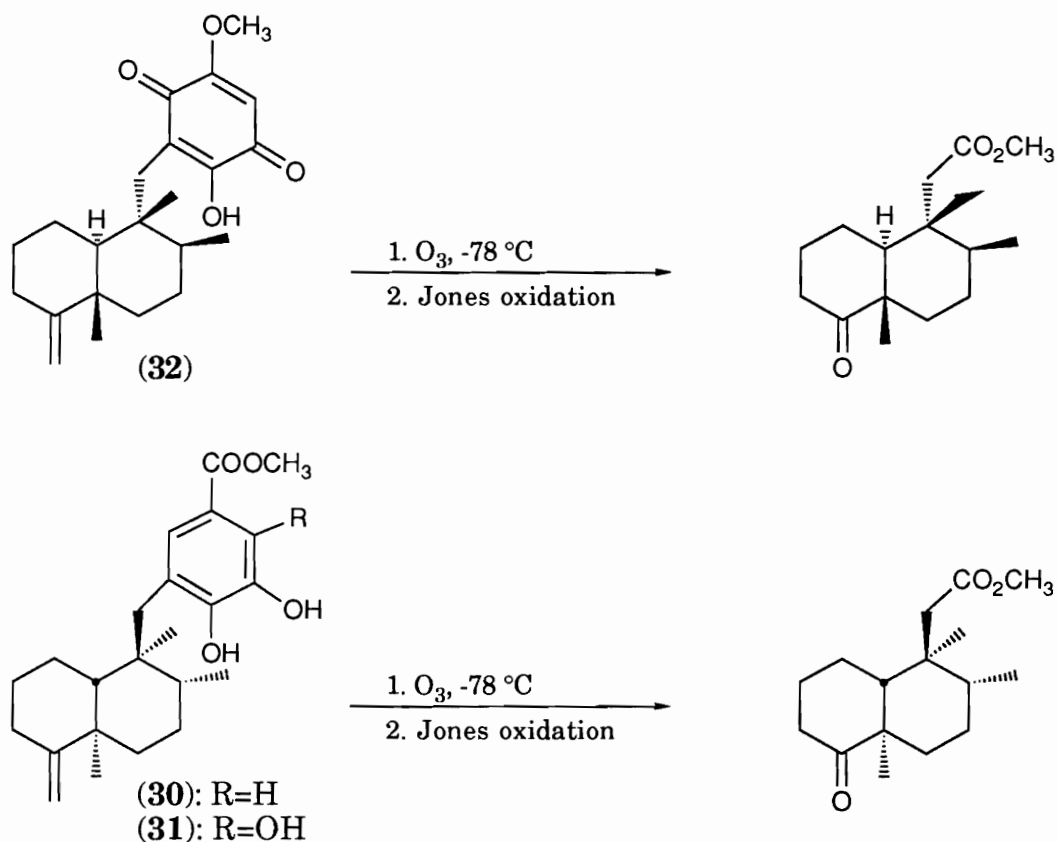
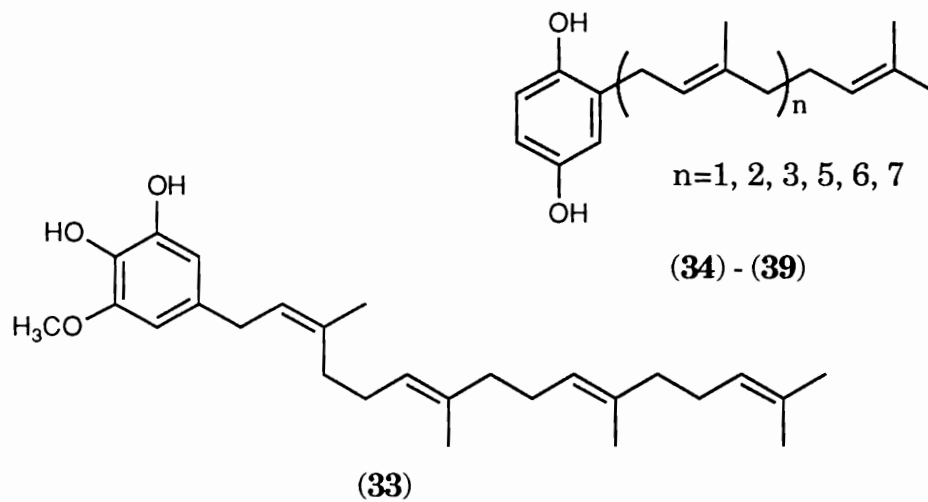


Figure 4. Absolute stereochemistry of the dictyoceratins.

spinulosum.^{40,41} Quinol **34** has been isolated only from two ascidians of the genus *Aplydium*.^{39,42} Isomerization or other chemical reactions of the polyprenyl quinols can also occur. Linear hydroquinol **33**, which represents the unusual *E*-isomer of the C-2/C-3 olefin, is the result of such a process. Linear polyprenyl quinols of the type **35** have not been reported; perhaps this is because they are requisite precursors to the quinone sesquiterpenoids.



The yellow form of *Stelospongia* (= *Fasciospongia*) *conulata* produced the first reported quinone sesquiterpenoids.³⁹ Spongiaquinone (**40**), isospongiaquinone (**41**), cyclospongiaquinone-1 (**42**), cyclospongiaquinone-2 (**43**) and dehydrocyclospongiaquinone-1 (**44**) were isolated on the basis of widespread mild antimicrobial activity in extracts of this sponge. The compounds may all arise from the common intermediate (**45**), which would give **42** directly by cyclization.³⁹ A simple hydride shift from C-9 to C-8 would give rise to **40** via loss of H-11 and **43** by cyclization. Concerted rearrangement of the terpenoid moiety of intermediate **45** would give rise to **40** (Figure 5). Recently, the absolute stereochemistry of **41** was determined by comparison of its acid rearrangement product **46** with the same compound formed from ilimaquinone (Figure 6).⁴³

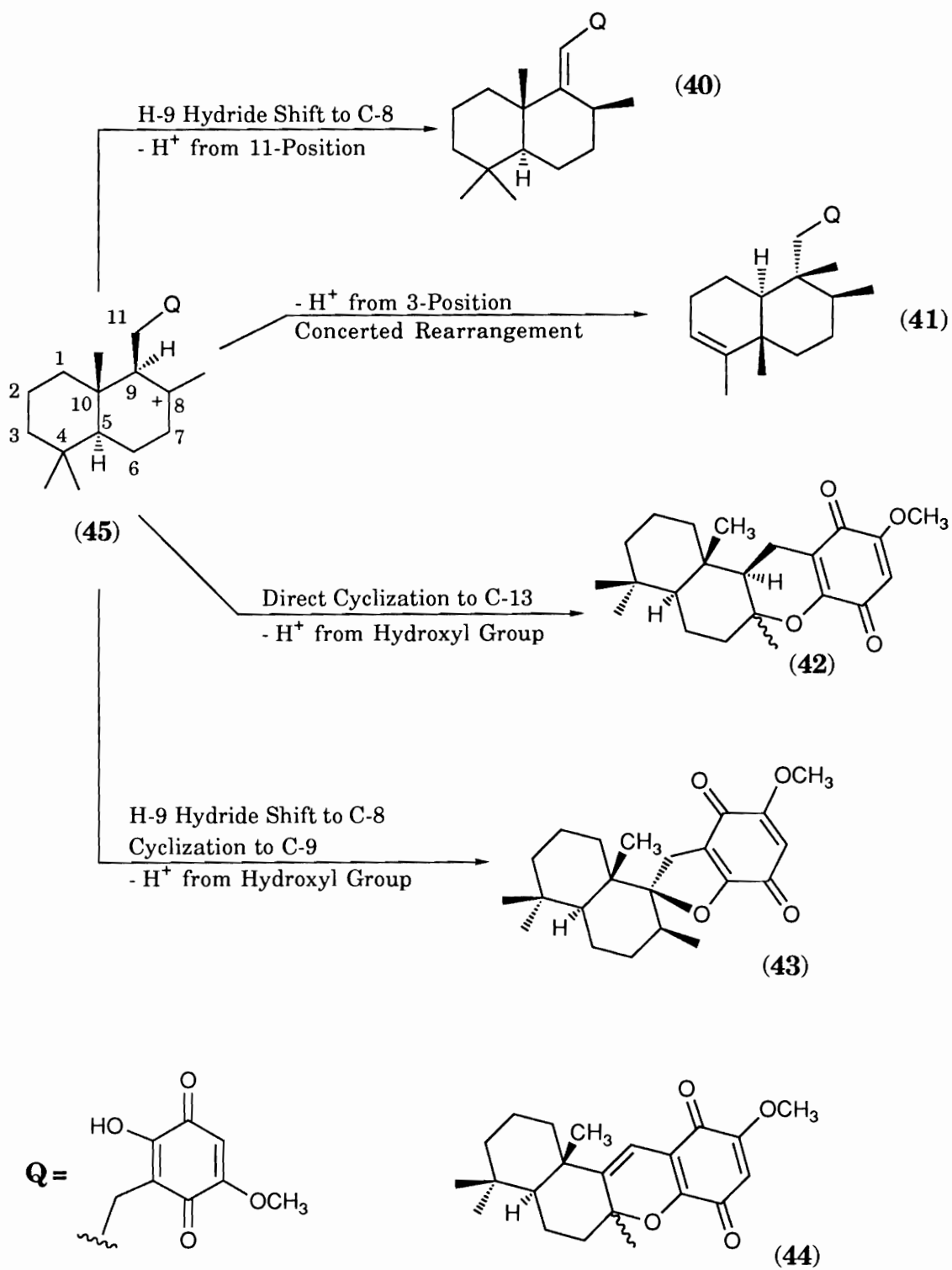


Figure 5. Derivation of the quinone sesquiterpenoids.

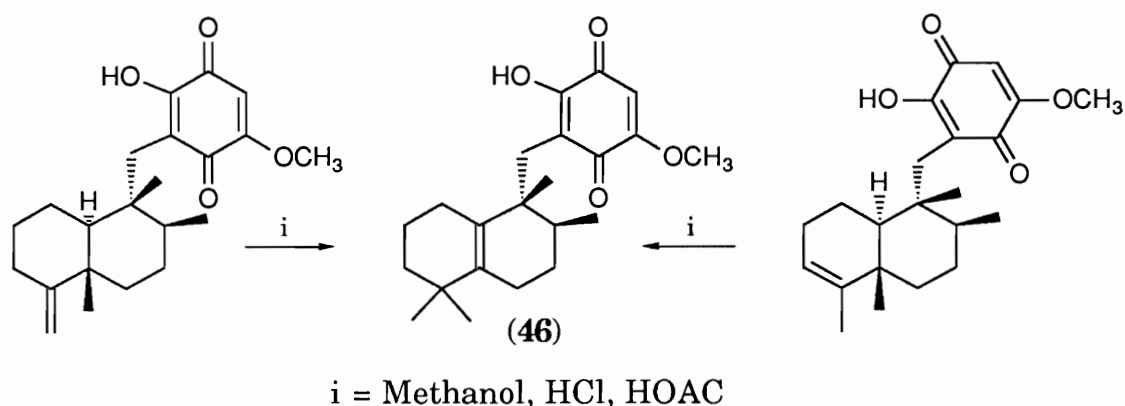


Figure 6. Absolute stereochemistry of isospongiaquinone.

Ilimaquinone (**32**) is the major lipophilic component (4% of dry wt.) of the Hawaiian sponge *Hippospongia metachromia* and exhibits mild anti-microbial activity against *S. aureus*, *C. albicans*, and *Mycobacterium smegmatus*.⁴⁴ The relative stereochemistry of **32** was determined by x-ray crystallography, although the absolute stereochemistry was incorrectly assigned by interpretation of the weak CD effect of ozonolysis degradation product **47**. The absolute configuration of **32** was correctly determined by comparison of the acid catalyzed rearrangement product **48** derived from ilimaquinone to that obtained from aureol (**49**) (Figure 7).⁴⁵ The absolute configuration of **49** had been previously determined by x-ray analysis of its bromoacetate derivative.⁴⁶

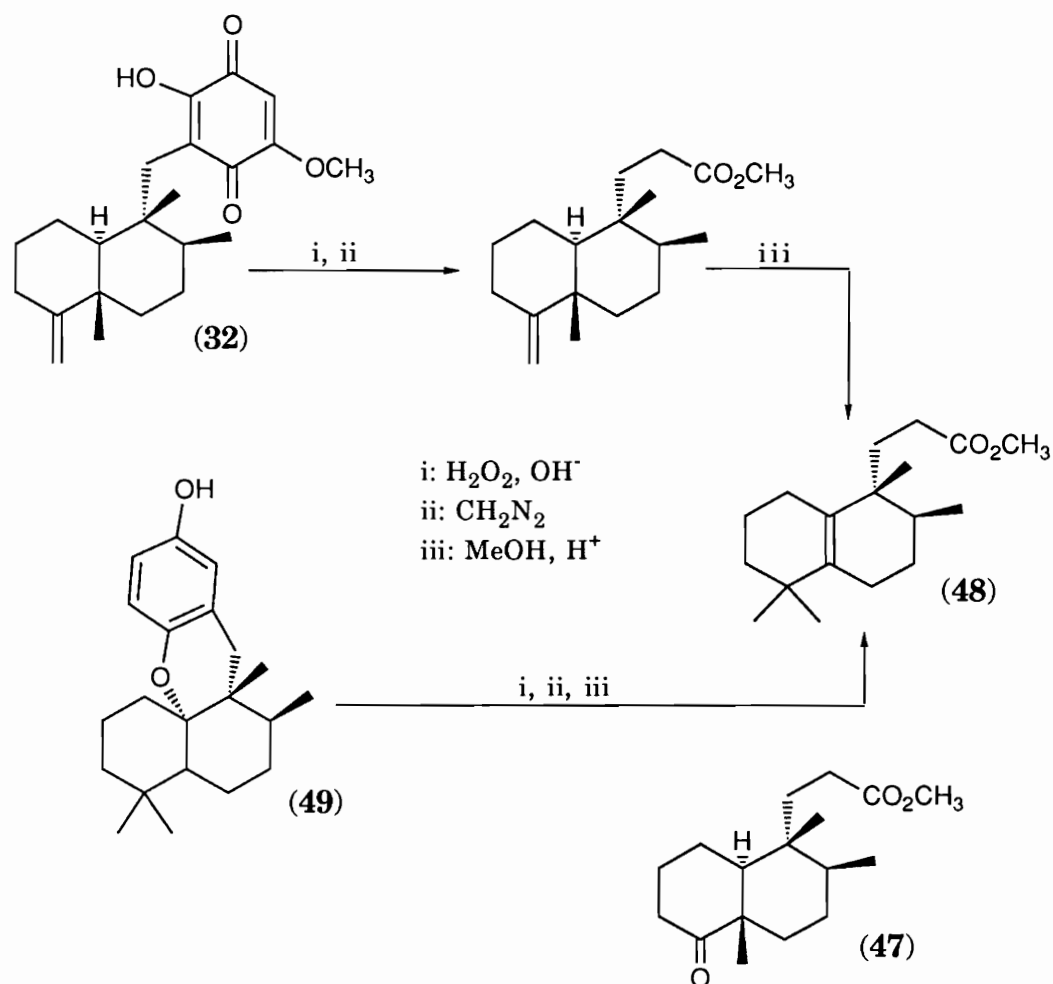


Figure 7. Absolute stereochemistry of ilimaquinone.

The Fijian sponge *Fasciospongia* sp. produced mamananthaquinone (50), another cytotoxic quinone sesquiterpenoid.⁴⁷ The absolute configuration of mamananthaquinone was determined by comparison of its Lewis acid-catalyzed rearrangement product (46) with that derived from 32. Mamananthaquinone could also arise via the same cationic intermediate (45) that was proposed for the derivation of the spongiaquinone series. Loss of a methylene proton from position 6, followed by concerted rearrange-

ment, would yield **50** (Figure 8). Mamanuthaquinone was cytotoxic to HCT-116 cells in vitro (IC_{50} 2.0 $\mu\text{g/mL}$). This work is described in greater detail in this thesis.

5-*epi*-Ilimaquinone (**51**), another antimicrobial quinone isolated from *Fenestraspongia* sp., represents an oxidized hydroxylated form of the previously described arenarol.^{48,49} 5-*epi*-Ilimaquinone was isolated as a 6:4 mixture with **32**. The absolute configuration of **51** was also determined by chemical degradation and acid-catalyzed rearrangement of this mixture.

Metachromins A (**52**) and B (**53**), isolated from *Hippospongia metachromia*, possess potent vasodilating activity (IC_{50} 3×10^{-6} M against 40 mM KCl induced contraction of isolated rabbit coronary artery) and cytotoxicity (IC_{50} 2.40 and 1.62 $\mu\text{g/mL}$ vs. L1210 cells in vitro, respectively).⁵⁰ Metachromin B represents the ring closure product of a reduced methylated quinol form of **52**. Metachromin A occurred in 16-fold excess of

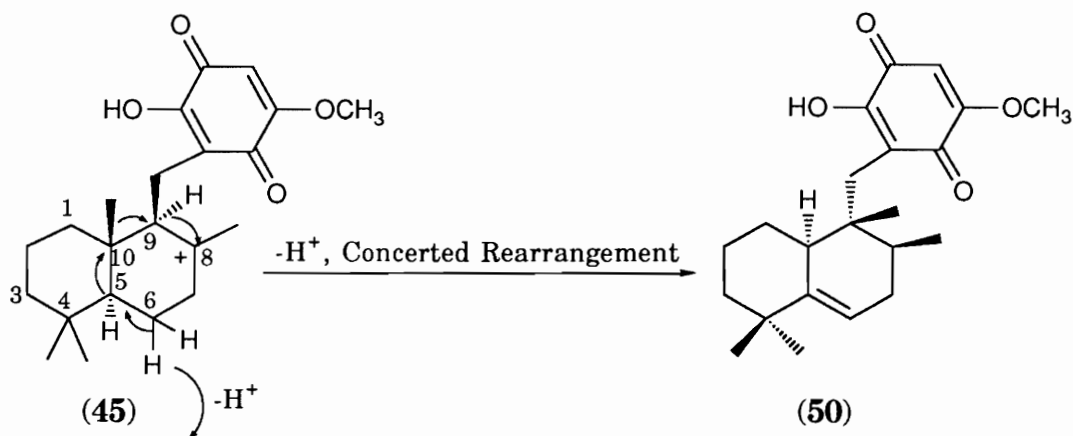
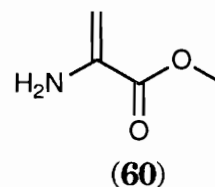
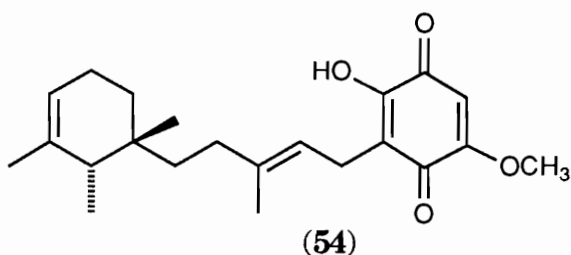
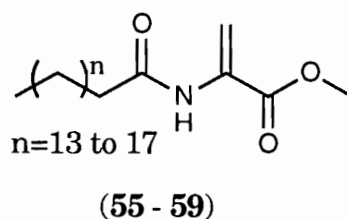
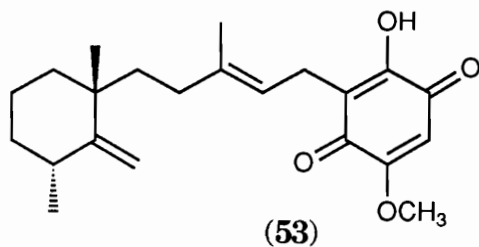
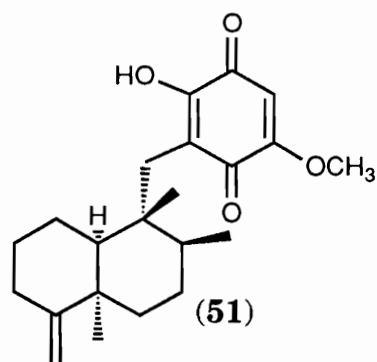
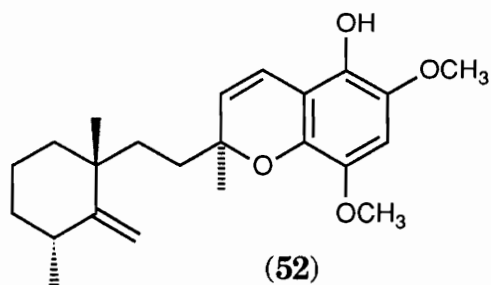


Figure 8. Proposed biosynthesis of mamanuthaquinone.



metachromin B in the sponge, along with the known **41**, which also showed unspecified coronary vasodilating activity. Metachromin C (**54**), an olefinic isomer of **52** also isolated from *H. metachromia*, possesses vasodilating activity and cytotoxicity comparable to those of its congeners **52** and **53**.⁵¹

The only report of a nonterpenoid or nonsteroidal metabolite isolated from any *Fasciospongia* concerns a series of acylated 2-methylene- β -alanine methyl esters (**55 - 59**) produced by *F. cavernosa*.⁵² Esters **55 - 59** appeared in the sponge in unusually high concentrations, between 1-2% of

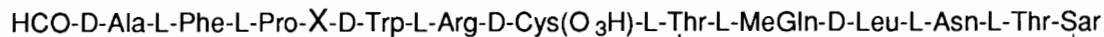
dry weight. The structures of the *N*-acylated methyl esters were solved by elemental analysis, NMR, and GC MS of the aliphatic fatty acids produced by acid hydrolysis of the mixture. Both the *N*-acylated amino acids **55** - **59** and the amino acid 2-methylene- β -alanine methyl ester (**60**) were toxic to mice (80-160 mg/kg, injected intraperitoneally).

Biologically Active Peptides From Marine Sponges

Marine sponges from the Families *Theonellidae*, *Axinellidae*, and *Jaspidae* specialize in the production of novel biologically active peptides and peptide-derived metabolites. Most of the Theonellid-produced molecules are high molecular weight linear and macrocyclic peptides; many contain amino acids without terrestrial precedent. Almost all bromopyrrole-containing compounds described from *Axinellidae* are derived from linear precursors and contain bromopyrrole moieties. The compounds reviewed herein represent some of the diverse structural motifs utilized by sponges and demonstrate a wide variety of biological activities.

Discodermin A (**61**), a metabolite of the Theonellid sponge *Discodermia kiiensis*, was the first biologically active peptide isolated from a marine sponge.^{53,54} This tetradecapeptide contains 5 D-amino acids, and the unusual *t*-butyl leucine, and inhibits *B. subtilis*, *S. aureus*, *Escherichia coli*, and *Pseudomonas aeruginosa* at 1 μ g/disk. Three related metabolites, discodermins B-D (**62** - **64**), were subsequently isolated.⁵⁵ Peptides **61** and **63** were found to inhibit the development of starfish embryos at 5 μ g/mL. The structures of the discodermins were determined by NMR, FAB and EI MS, and amino acid analysis (HCl hydrolysis, chiral GCMS, and paper electrophoresis). Polydiscamide A (**65**) is a more recent example of a high mol-

ecular weight cytotoxic depsipeptide, isolated from the abyssal (deep water) Lesser Antilles sponge *Discodermia* sp.⁵⁶ The structure of **65** was determined largely by 1-D and 2-D NMR methods and amino acid analysis. In polydiscamide A, the rare 3-methylisoleucine replaces a *t*-butyl leucine of **61**, and the leucine, threonine, and sarcosine of the discodermins are replaced by valine and proline. Polydiscamide A inhibits the human lung cancer cell line A549 in vitro (IC₅₀ 0.7 μg/mL), and *B. subtilis* (MIC 3.1 μg/mL).

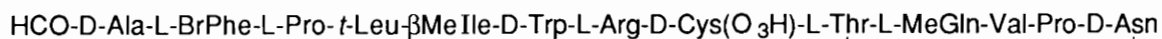


(**61**): -X- = -D-*t*-Leu-L-*t*-Leu-

(**62**): -X- = -D-Val-L-*t*-Leu-

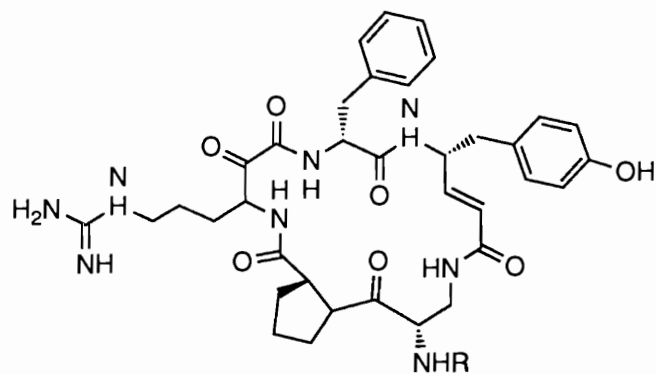
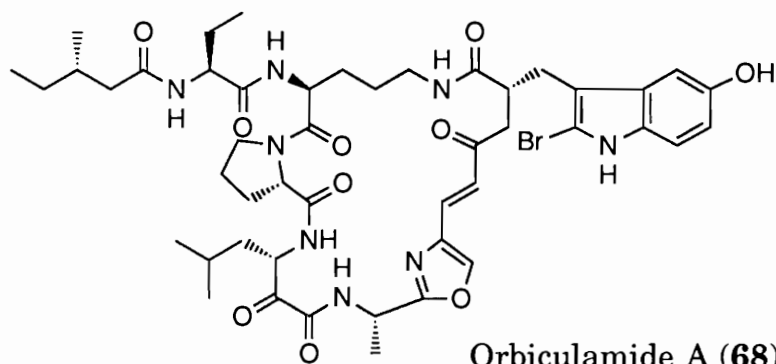
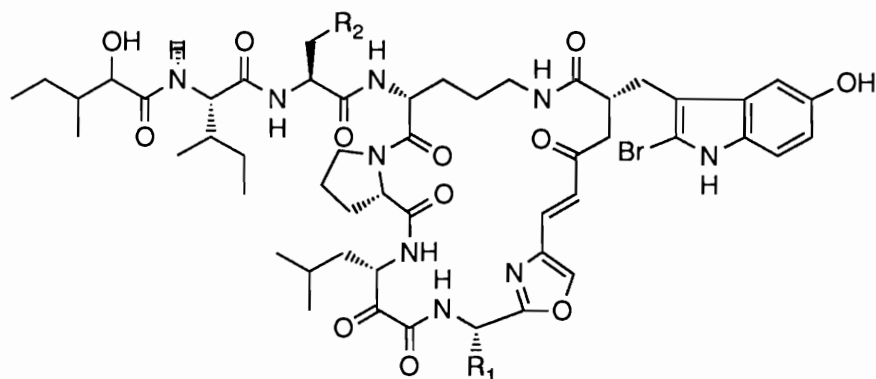
(**63**): -X- = -D-*t*-Leu-L-Val

(**64**): -X- = -D-Val-L-Val



(**65**)

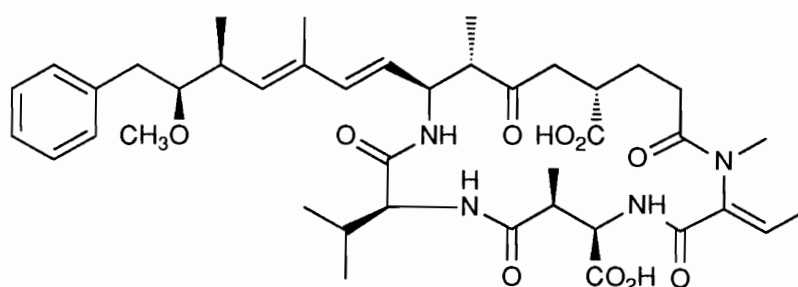
As mentioned above, sponges of the genus *Theonella* produce a variety of biologically active cyclic and bicyclic peptides, some of which were recently reviewed.⁵⁷ The more recently reported examples seem to be characterized by remarkable enzyme inhibitory activities and include chemically interesting α-keto-β-amino acids (Figure 9).

Cyclotheonamide A (**66**): R=CHOCyclotheonamide B (**67**): R=AcOrbiculamide A (**68**)Keramamide B (**69**): R₁=CH₂CH₃, R₂=CH₂CH₃Keramamide C (**70**): R₁=CH₂CH₃, R₂=CH₃Keramamide D (**71**): R₁=CH₃, R₂=CH₃Figure 9. Biologically active cyclic peptides from *Theonella* sp.

Cyclotheonamides A (**66**) and B (**67**) are potent thrombin inhibitors (IC₅₀ 0.076 µg/mL for **66**) isolated from the Japanese sponge *Theonella* sp.⁵⁸ The structure elucidation of the cyclotheonamides relied heavily on NMR techniques and FABMS. Cyclic peptide **66** and its acetate **67** incorporate α-keto-β-arginine and a highly modified tyrosine derivative. This same sponge also produced orbiculamide A (**68**) and keramamides B-D (**69-71**).^{59,60} Each of these biologically active cyclic peptides incorporates 3 novel amino acids, including 2-bromo-5-hydroxytryptophan, an oxazole containing moiety called theonalanine, and another α-keto-β-amino acid, called theoleucine. Interestingly, **68** is cytotoxic against P388 murine leukemia cells (IC₅₀ 4.7 µg/mL), while its congeners **69 - 71** lack cytotoxicity against murine L1210 and human epidermoid KB cells in vitro at concentrations as high as 10 µg/mL. However, the keramamides selectively inhibit the superoxide generation response of human neutrophils elicited with *N*-formyl-Met-Leu-Phe (fMLP), a chemotactic peptide; **69 - 71** do not inhibit the response induced by phorbol myristate acetate or ovalbumin-immunoglobulin G₂ antibody complex. These results suggest that some factor involved in the intracellular signal transduction process initiated by fMLP is inhibited by the keramamides.

The Papua New Guinea sponge *Theonella swinhoei* produced motuporin (**72**), a potent inhibitor of protein phosphatase-1 (PP1).⁶¹ Motuporin incorporates valine and glutamic acid with the unusual β-methylaspartic acid, *N*-methyl-*Z*-dehydrobutyrine, and the previously described aromatic amino acid Adda in a macrocyclic pentapeptide. Adda is a constituent of the blue-green algal toxins microcystin-LR and nodularin.^{62,63} This raises the obvious question of whether the Adda residue in **72** is produced by the

sponge or fixed by the sponge from an algal symbiont. Motuporin displays nonselective cytotoxicity towards a variety of cancer cell lines, with IC_{50} 's ranging from 2-12 $\mu\text{g/mL}$ against six different strains. Motuporin is one of the most potent known inhibitors of PP1, with a MIC < 1 nM, and is currently being used to study protein phosphatases, which regulate hormone and growth factor intracellular signaling pathways.

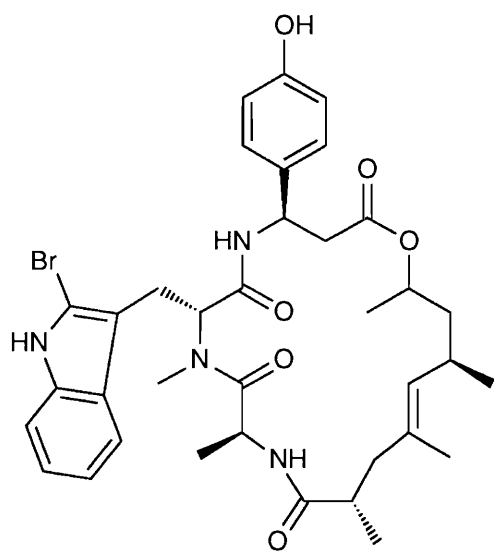


(72)

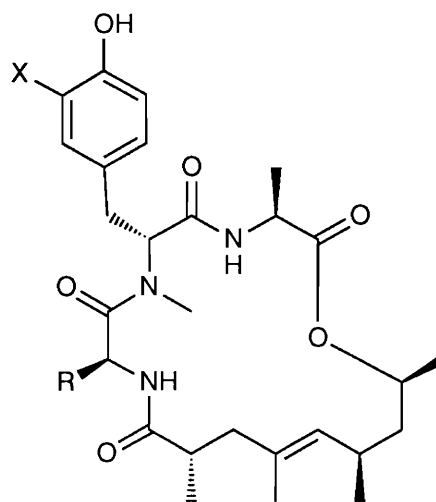
The first metabolite of mixed peptide/polyketide biosynthesis reported from a marine sponge was Jaspamide (73) isolated from the sponge *Jaspis johnstoni* collected in Fiji and Palau.^{57,64} Jaspamide incorporates L-alanine, the novel 2-bromoabrine (D-2-bromo- α -N-methyltryptophan) and a rare β -tyrosine with a 12-carbon polypropionate unit in a 19-membered macrocycle of unprecedented mixed biosynthetic origin. Jaspamide displayed potent insecticidal activity against *Heliothis virescens* at 4 ppm and good in vivo antifungal activity; a 2% topical solution vs. *C. albicans* vaginal infection in mice was comparable to miconazole nitrate.⁶⁵ Another report credits 73 with in vitro antihelminthic activity (ED<1 $\mu\text{g/mL}$ vs. *Nippo-*

strongylus braziliensis) and cytotoxicity (IC₅₀ 0.32 and 0.01 μg/mL vs. larynx epithelial carcinoma and human embryonic lung cells, respectively).⁶⁶

Geodiamolides A-F (**74** - **79**) incorporate the same 12-carbon polypropionate unit found in jaspamide with a halotyrosine-containing tripeptide into 18-member macrolides.^{67,68} Peptides **74** and **75** were isolated from *Geodia* sp. gathered in the West Indies, while **76** - **79** were isolated from the geographically and taxonomically remote Papua New Guinea Axinellid sponge *Pseudaxinyssa* sp. Like jaspamide, the geodiamolides also exhibited



(73)

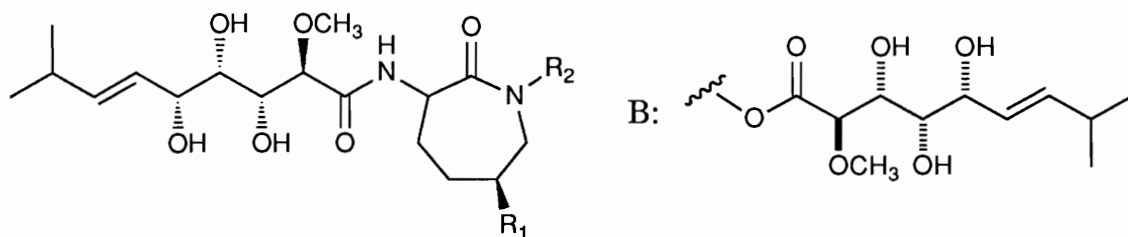


- (74): X=I, R=Me
 (75): X=Br, R=Me
 (76): X=Cl, R=Me
 (77): X=I, R=H
 (78): X=Br, R=H
 (79): X=Cl, R=H

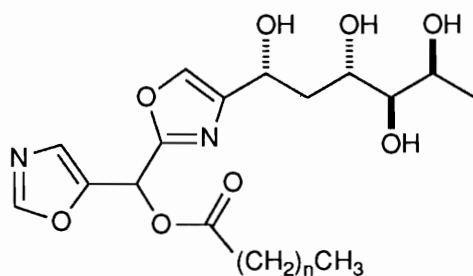
antifungal activity vs *C. albicans*. The geodiamolides possess considerable antineoplastic activity. Crude extracts of *Pseudaxinyssa* sp. exhibited in vivo antineoplastic activity (T/C=153 vs P388 @ 50 mg/kg dose in mice). The pure geodiamolides were active in vitro (ED₅₀=3.2, 2.6, 2.5, 39, 14, and 6.0 ng/mL vs. L1210 cells, for **74** - **79** respectively) but were isolated in insufficient quantity for in vivo testing.

Bengamides A-F (**80** - **85**), isolated from an orange Fijian sponge, exhibit cytotoxic, antihelminthic, and antimicrobial activity.⁶⁹ The bengamides contain a novel caprolactam formed by cyclization of lysine or δ -hydroxylysine. This same sponge also produced the mildly antihelminthic bengazoles A (**86**) and B (**87**).⁷⁰ The sponge was not readily identifiable, although taxonomic characteristics of the family *Jaspidae* were noted.

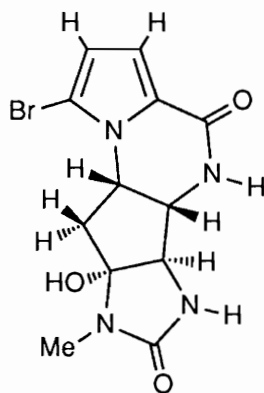
Crude methanolic extracts prepared in our lab of this same atypical orange Fijian sponge possessed potent in vivo antineoplastic activity in P388 infected mice (T/C=135 @ 45 mg/kg, T/C=142 @ 135 mg/kg). Investigation of the polar organic partitions of this extract led to the isolation and characterization of the bromopyrrole derivative epipolasidamide (**88**), while the less polar partitions yielded **80** and other related compounds. The isolation and structure elucidation of epipolasidamide is described in detail later in this thesis. Epipolasidamide is a member of a group of biosynthetically related bromopyrrole-containing compounds of peptidal origin typically isolated from the sponge Family *Axinellidae*.^{71,72} The only terpenoid compound produced by an Axinellid sponge, which is reviewed herein, is included because of its interesting biological activity.



- (80): $R_1=O_2C(CH_2)_{12}CH_3$ $R_2=H$
 (81): $R_1=O_2C(CH_2)_{12}CH_3$ $R_2=CH_3$
 (82): $R_1=B$ $R_2=H$
 (83): $R_1=B$ $R_2=CH_3$
 (84): $R_1=H$ $R_2=H$
 (85): $R_1=H$ $R_2=CH_3$

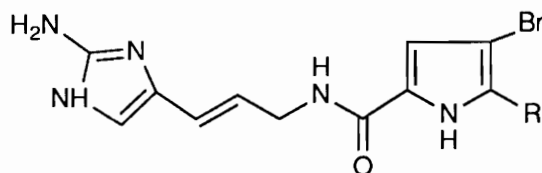
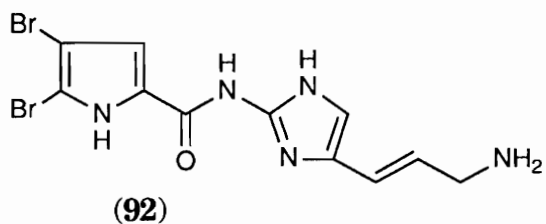
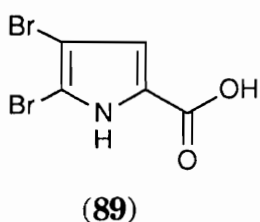


- (86): $n=12$
 (87): $n=11$



(88)

The simplest bromopyrroles produced by sponges are 4,5-dibromopyrrole-2-carboxylic acid (**89**) and oroidin (**90**), originally isolated from *Agelas oroides* collected in the Bay of Naples.⁷³ The structure of oroidin originally proposed (**92**) was shown to be incorrect. Synthetic efforts produced a compound bearing spectral similarities to the natural product, which was reassigned the structure **90** on this basis.⁷⁴ Debromooroidin (**91**) was subsequently isolated from the sponges *Hymeniacidon* sp. and *Agelas clathrodes*.^{75,76}

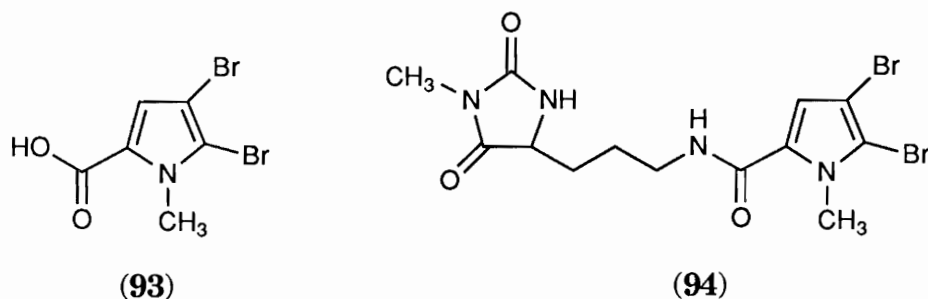


(90): R=Br

(91): R=H

The related compounds *N*-methylpyrrole carboxylic acid (**93**) and midpacamide (**94**) were isolated from an unidentified orange sponge gathered in the Marshall Islands.⁷⁷ Midpacamide is a dipeptide consisting of ornithine, in the form of a methylformamide hydantoin moiety, and

bromopyrrole **93**. Midpacamide is related to oroidin via olefin reduction and carbonylation of the amino imidazole moiety of **90**.



Dibromophakellin (**95**) and monobromophakellin (**96**), mildly antimicrobial alkaloids isolated from the sponge *Phakellia flabellata*, appear to be biosynthetically related to the oroidins.⁷⁸ The structure of the tetracyclic skeleton of the phakellins was established by x-ray crystallography of monoacetylated **95**.⁷⁹ The phakellins behave as weak bases, with anomalously low pKa values <8, compared to >13.5 for other guanidine containing compounds. A biosynthetic mechanism was proposed to explain the formation of the phakellins from the oroidins via activated intermediate **97** (Figure 10).⁷⁸

An intriguing structural isomer of **95** is dibromoisophakellin (**98**), isolated from the Madagascar Axinellid sponge *Acanthella carteri*.⁸⁰ Heterocycle **98** may also be derived from dibromooroidin (Figure 10). A putative mechanism in which the π -excessive pyrrole acts as an enamine during concerted ring closure of the dihydrooroidin-like activated intermediate **97** is offered herein (Figure 10).

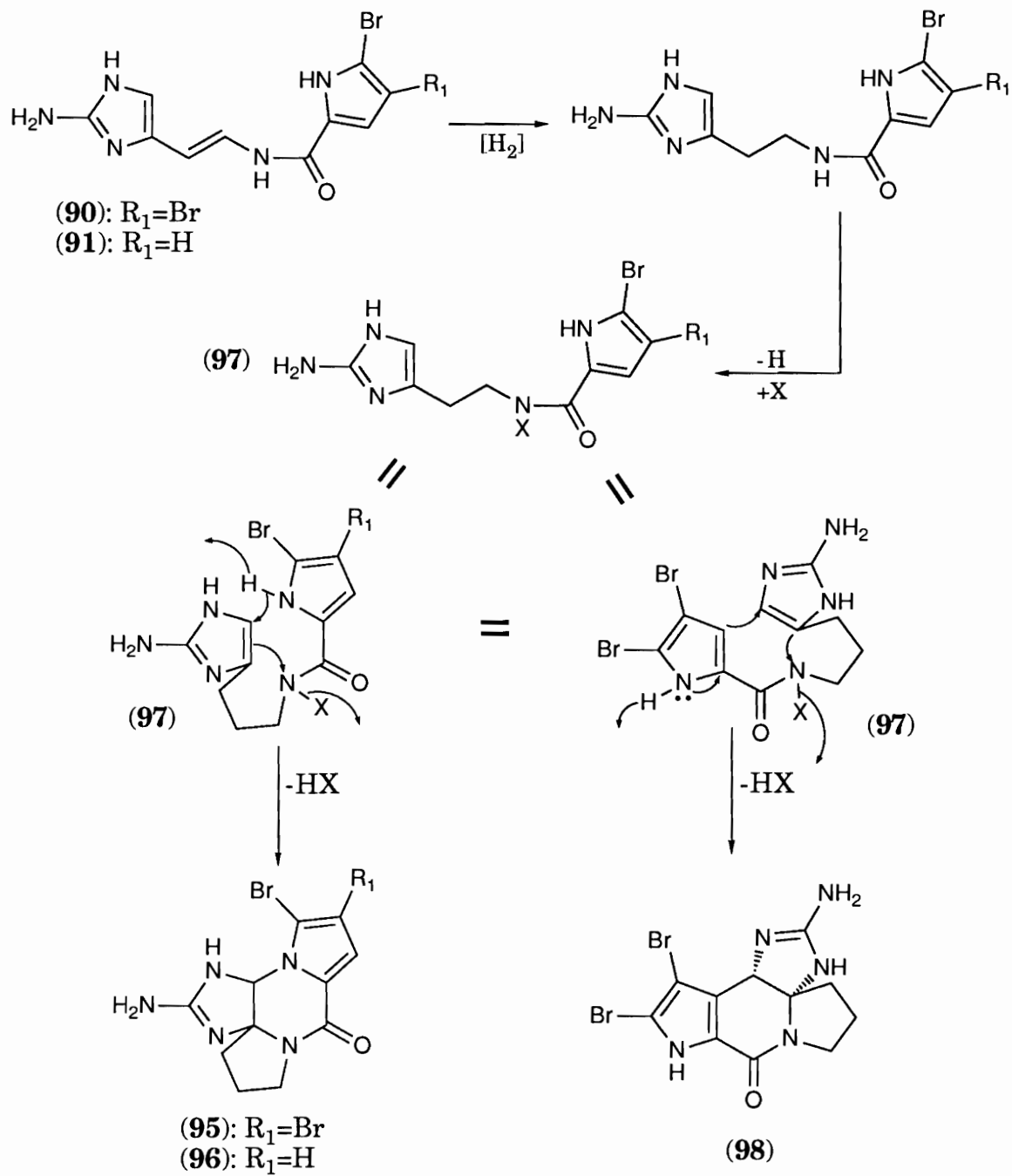
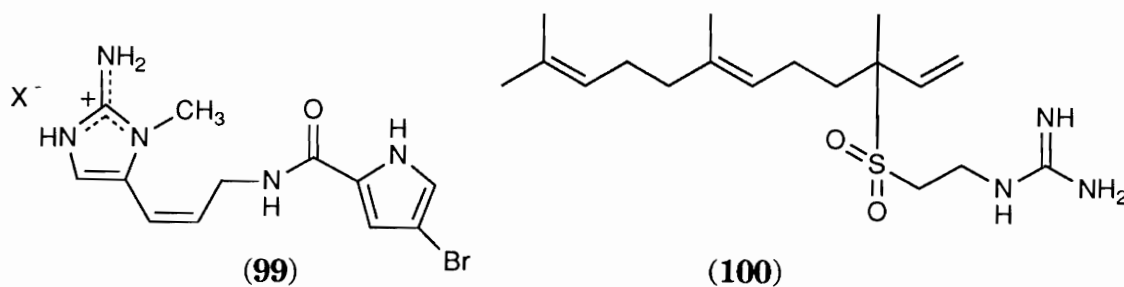


Figure 10. Biosynthesis of the phakellins and dibromoisophakellin.

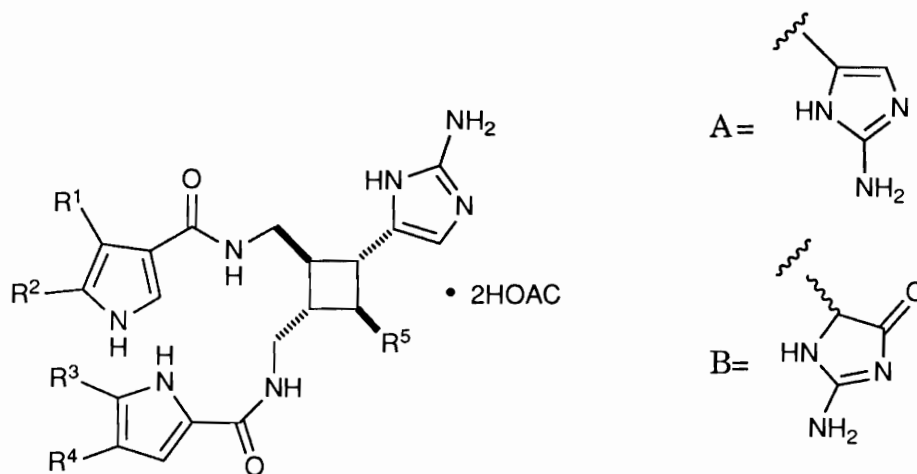
The oroidin congener keramidine (**99**), isolated from an Okinawan *Agelas* sp., possesses serotonergic receptor antagonistic activity.⁸¹ The structure of **99**, in which the olefin is cis unlike that in **90**, was established by spectral means. The contractile response of isolated rabbit aorta to 10^{-6} M serotonin was abolished by 1.5×10^{-6} M keramidine, whereas the responses to 0.04 M KCl and 10^{-6} M epinephrine were not.

Agelasidine-A (**100**) is a unique antispasmodic terpenoid metabolite isolated from an Okinawan *Agelas* sp.⁸² Its structure represents an unusual acyclic sesquiterpene, substituted with sulfone and guanidine functional groups, and may arise from the coupling of farnesol with cysteine. The structure of agelasidine-A was determined by mass spectrometry, NMR spectroscopy and chemical degradation.



Sceptrin (**101**), an antimicrobial alkaloid isolated from *Agelas sceptrum*, represents a head-to-head [2+2] cycloaddition product of debromoroidin.⁸³ The structure of **101** was established by x-ray crystallography. Several attempts to synthesize sceptrin analogs in solution and solid-state from oroidin-like precursors were unsuccessful. Sceptrin displayed anti-

microbial activity at 15 $\mu\text{g/mL}$ against Gram positive bacteria and *C. albicans*.



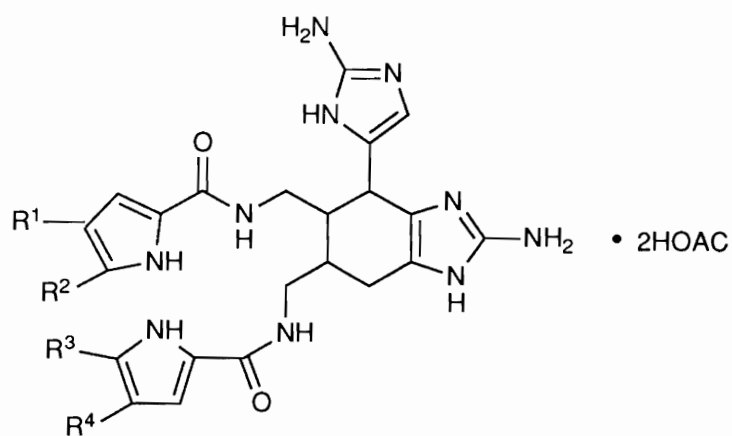
(101): $R^1=\text{Br}$, $R^2=\text{H}$, $R^3=\text{H}$, $R^4=\text{Br}$, $R^5=\text{A}$

(102): $R^1=R^2=R^3=R^4=\text{Br}$, $R^5=\text{A}$

(103): $R^1=\text{Br}$, $R^2=\text{H}$, $R^3=\text{H}$, $R^4=\text{H}$, $R^5=\text{A}$

(104): $R^1=\text{Br}$, $R^2=\text{H}$, $R^3=\text{H}$, $R^4=\text{Br}$, $R^5=\text{B}$

(105): $R^1=\text{H}$, $R^2=\text{H}$, $R^3=\text{H}$, $R^4=\text{Br}$, $R^5=\text{B}$



(106): $R^1=\text{Br}$, $R^2=\text{H}$, $R^3=\text{H}$, $R^4=\text{Br}$

(107): $R^1=R^2=R^4=\text{Br}$, $R^3=\text{H}$

(108): $R^1=R^2=R^3=R^4=\text{Br}$

Dibromosceptrin (**102**) and debromosceptrin (**103**) were isolated as diacetate salts from a collection of mixed Caribbean *Agelas* sp. sponges.⁷¹ The same sponge also produced oxysceptrin (**104**), debromooxysceptrin (**105**), and the ageliferins (**106 - 108**). As a class, the ageliferins represent head-to-head [4+2] cycloaddition products of oroidin halo- or dehalo-isomers; a mechanism which accommodates the formation of all the sceptrins and the ageliferins has been presented.⁷¹ All of these bromopyrrole derivatives showed mild antimicrobial activity. The sceptrins and ageliferins were active against *Herpes simplex* type 1 and *Vesicular stomatitis* viruses at 20 and 100 µg/disk respectively, whereas the oxysceptrins (**104** and **105**) were somewhat less active against both viruses.

Selected Indole and Amide-containing Alkaloids from Tunicates

As several researchers have noted, tunicates specialize in the production of amino acid-derived metabolites.^{57,84} Almost 90% of reported metabolites from these semichordates are nitrogenous, a proportion larger than any other phylum (Figure 11). These range in complexity from single amino acids to highly modified peptides, such as the patellamides produced by *Lissoclinum patella*.^{57,84-86} Most of the reported metabolites are derived directly from amino acids or modified peptidal precursors (Figure 12). Indole and amide-containing alkaloids derived from tryptophan or from cyclization of tyrosine make up the rest of this group.

These nitrogenous metabolites appear to perform a variety of functions. Many serve as antifeedants, which protect the sessile, often fragile tunicates in predator-rich reef environments.⁸⁷⁻⁹⁰ Others perform primary

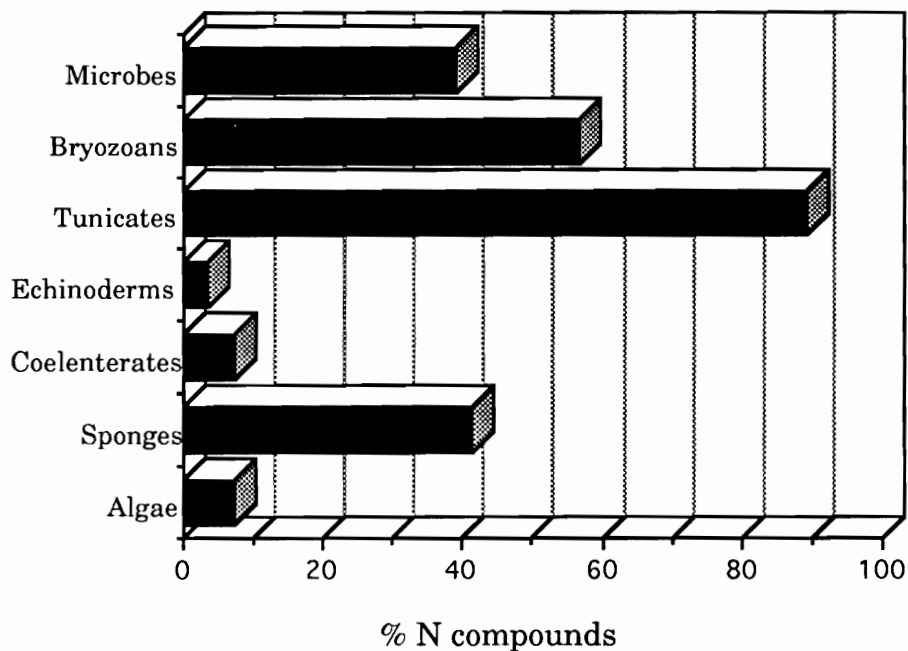


Figure 11. Percentage of nitrogenous metabolites from various phyla.

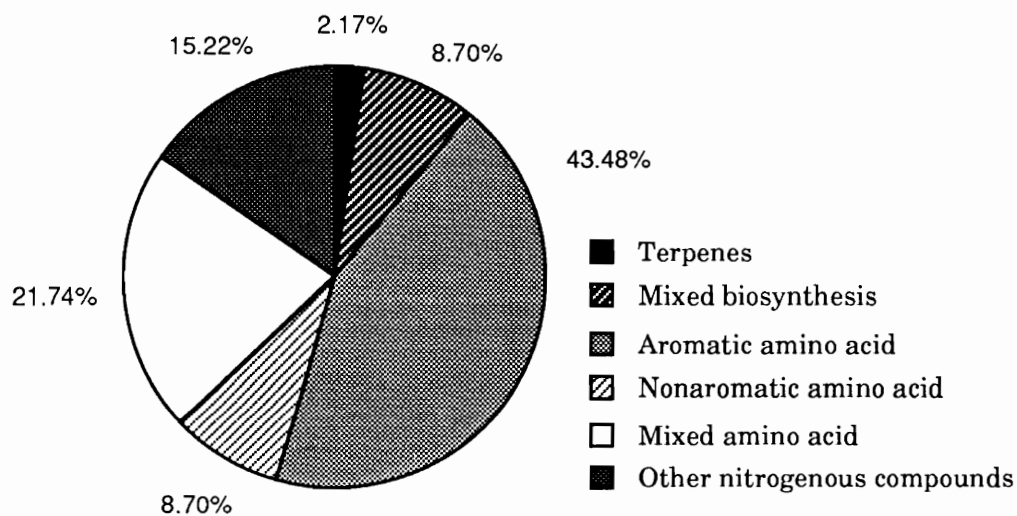
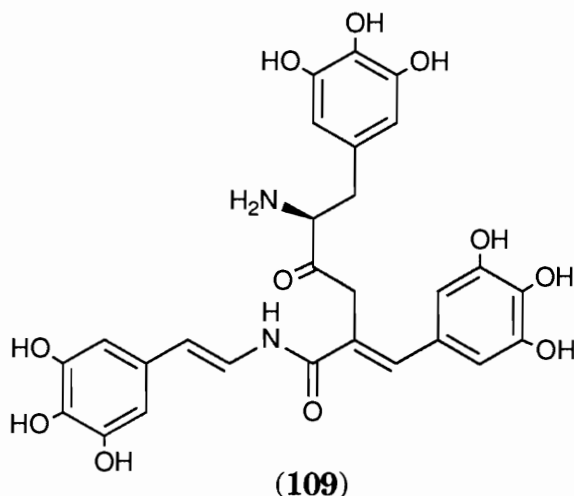
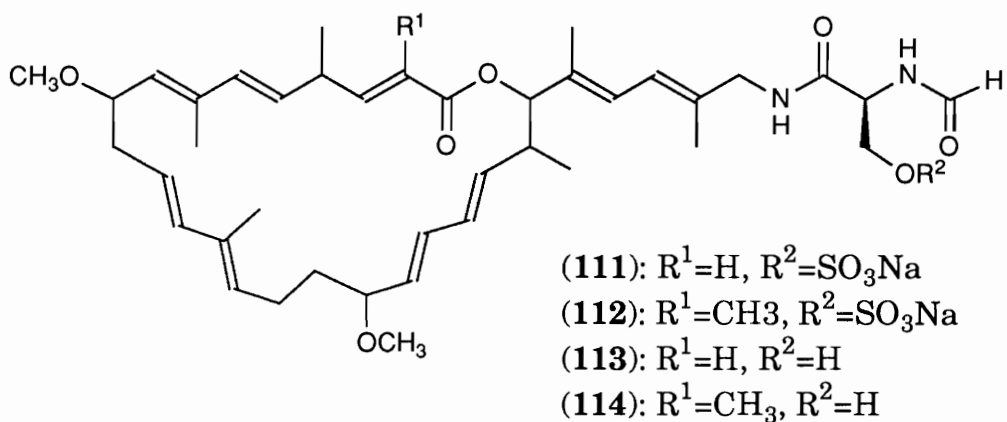
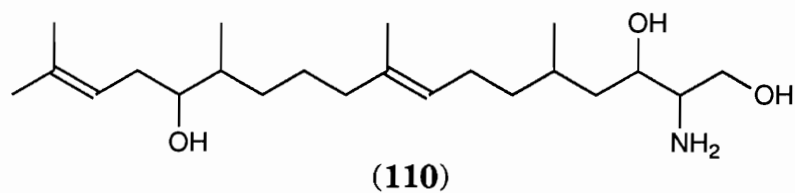


Figure 12. Derivation of ascidian-produced metabolites.

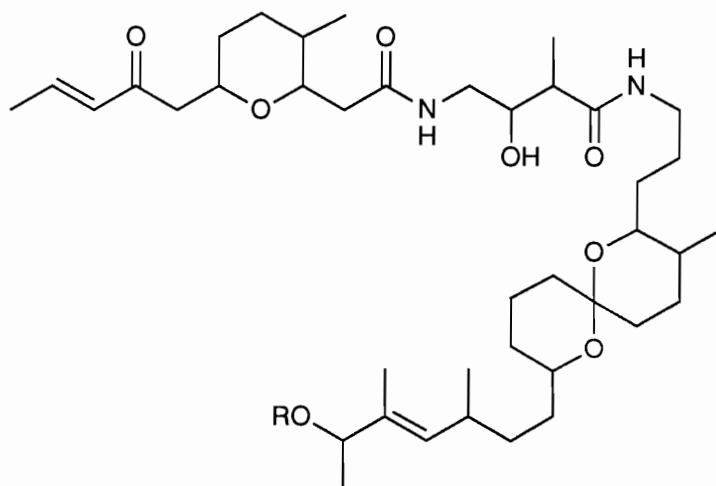
metabolic functions in these highly specialized organisms. For instance, the circulatory system of *Ascidia nigra* employs vanadium at reduced V(III) and V(IV) states; these labile ions are readily oxidized above pH 2.5. Tunichrome B-1 (**109**), a bright yellow pigment found in the tunicate blood, was recently described as a modified dopa peptide.^{91,92} Tunichrome B-1 is a member of a family of highly reductive ligands responsible for stabilizing vanadium (III) in the relatively elevated pH of the blood stream of the organism.^{93,94} Other tunichromes that stabilize iron have also been described.⁹⁵



Tunicates have produced a limited number of terpenoid and mixed polyketide-derived metabolites with interesting biological activity. These include aplidiasphingosine (**110**), an antimicrobial and cytotoxic derivative of diterpenic acid and serine isolated from the Gulf of California tunicate *Aplydium* sp., and iejimalides A - D (**111 - 114**), antineoplastic macrolides isolated from the Okinawan tunicate *Eudistoma* cf. *rigida*.⁹⁶⁻⁹⁸



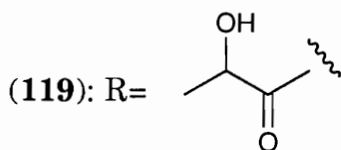
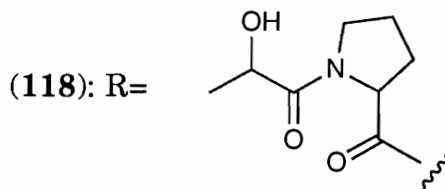
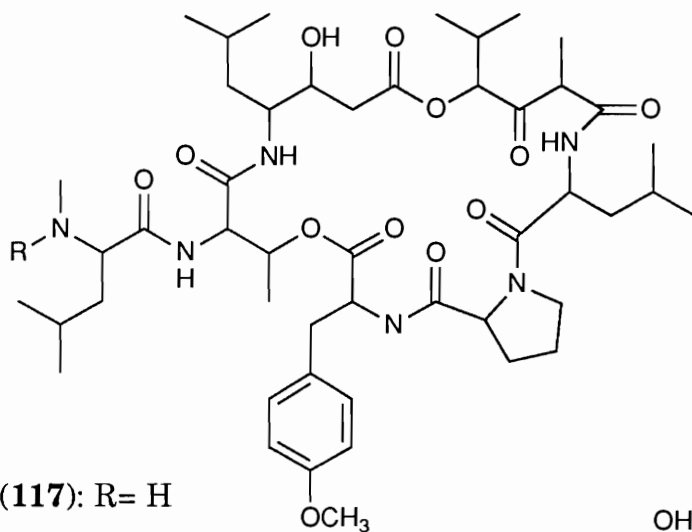
Bistramides A (115) and B (116) are polyketide-derived ethers isolated from *Lissoclinum bistratum*. Their structures were recently corrected on the basis of 2-D NMR experiments, including computer analysis of 2-D



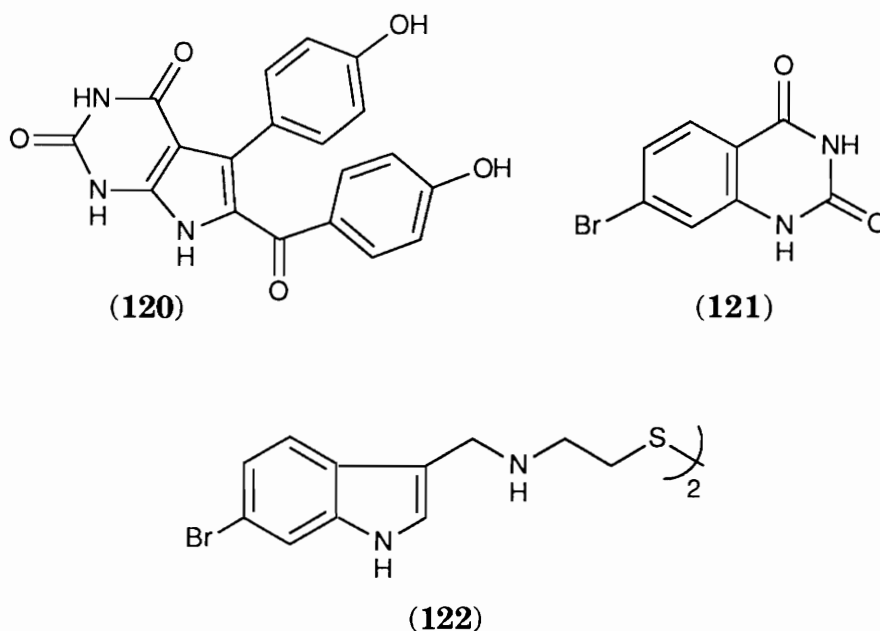
(115): $R=H$
 (116): $R=CO_2CH_3$

INADEQUATE data.⁹⁹⁻¹⁰² Bistramide A modifies the action potentials of cardiac cells and exhibits cytotoxicity towards KB, P388 and epithelial cells (IC₅₀ 45, 20, and 22 nM, respectively).¹⁰¹ Other tunicate-derived terpenoids have been reviewed.⁸⁶

Of the peptidal compounds described from ascidians, didemnins A - C (117 - 119) isolated from the Caribbean tunicate *Trididemnum solidum* remain the most intriguing.¹⁰³⁻¹⁰⁶ Didemnin B, the most active, displays anti-viral, antineoplastic and immunosuppressive activity and is currently in phase II of human clinical trials as a cancer chemotherapeutic agent.¹⁰⁷⁻¹⁰⁹ Didemnins A - C have been synthesized, and their biological activity has been thoroughly reviewed.^{86,110,111}



Rigidin (**120**), a pyrrolopyrimidine alkaloid isolated from the same *E. cf. rigida* that produced the iejimolides, displays potent calmodulin antagonistic activity.¹¹² The structure of **120** was determined by NMR and mass spectral studies. Rigidin inhibits calmodulin-activated brain phosphodiesterase ($IC_{50} 5 \times 10^{-5}$ M). Rigidin represents the first pyrrolo[2,3-d]pyrimidine isolated from a marine invertebrate, although this heterocyclic nucleus has been described in some nucleoside antibiotics isolated from strains of streptomycetes.¹¹³ Interestingly, some synthetic pyrrolo[2,3-d]pyrimidine-2,4-diones have weak affinity for benzodiazepine receptors.¹¹⁴



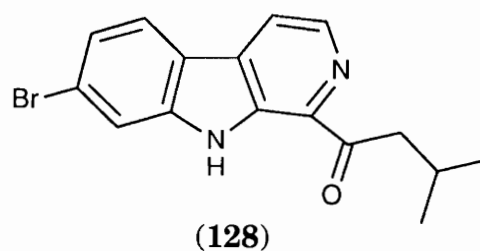
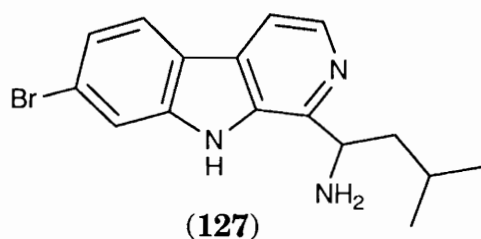
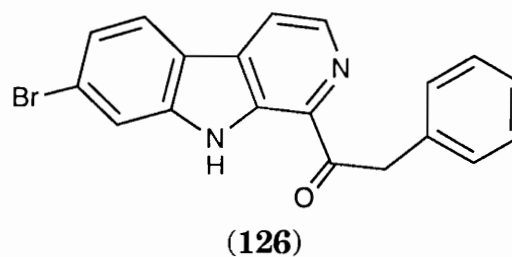
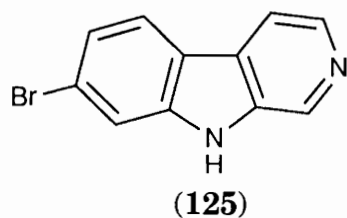
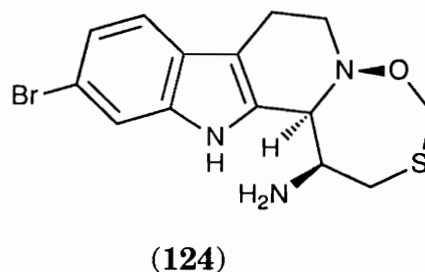
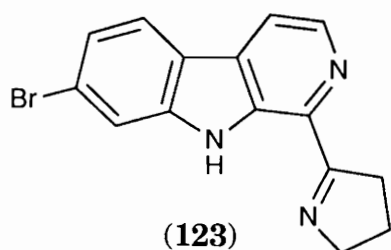
A brominated quinazolinone (**121**) produced by a Japanese tunicate *Pyura sacciformis* represents the only reported metabolite from the tunicate Family *Pyuridae* to date and the first isolation of a brominated quinazolinone from a natural source.¹¹⁵ Compound **121** was isolated in

$3 \times 10^{-4}\%$ yield of dry weight (0.6 mg) from the organism (170 g), along with 6-bromoindole-3-carbaldehyde in 30-fold excess. The structure of **121** was confirmed by synthesis.

Citorellamine (**122**), a cytotoxic and mildly insecticidal bromoindole dimer, was isolated from *Polycitorella mariae*.¹¹⁶ The structure **122** represents a correction of that originally proposed for citorellamine and was determined by synthesis of the natural product.¹¹⁷ The crude methanolic extract of *P. mariae* was mildly insecticidal towards the tobacco budworm. Citorellamine is cytotoxic towards L1210 cells in vitro (IC₅₀ 3.7 µg/mL).

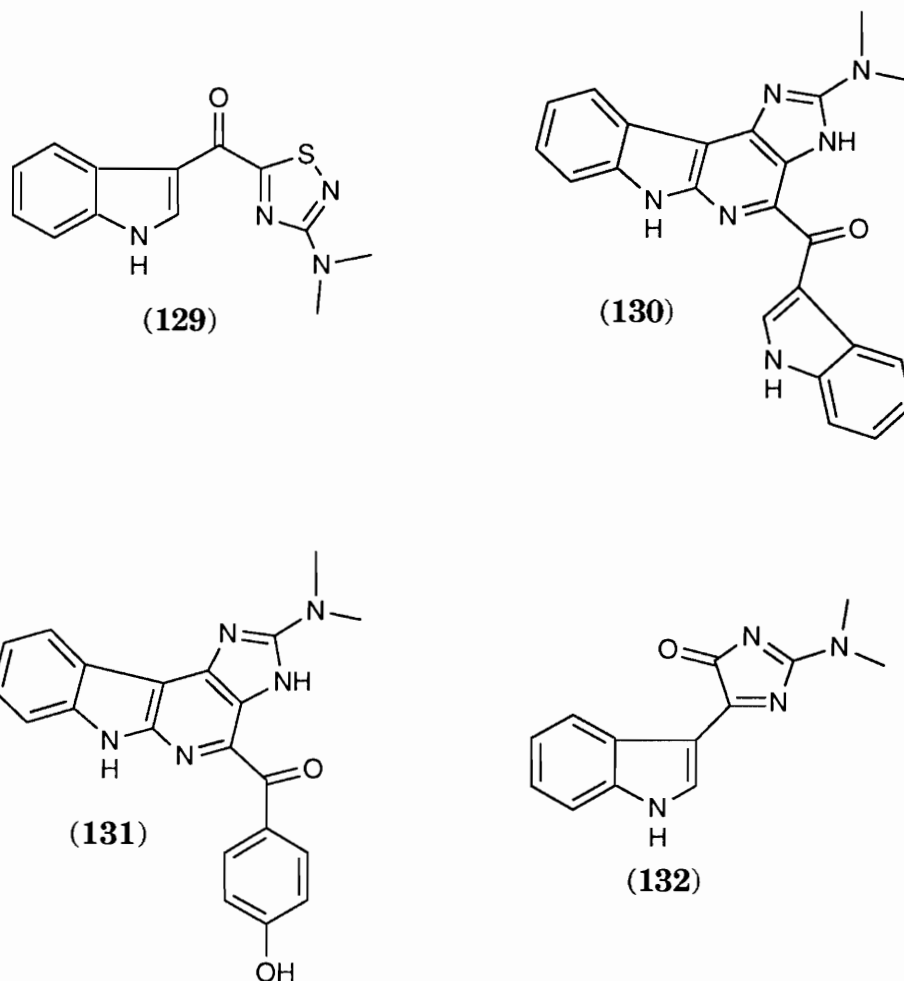
Eudistomins G (**123**), K (**124**), O (**125**) and R (**126**) are members of a series of biologically active indole alkaloids isolated from the Caribbean tunicate *Eudistoma olivaceum*.¹¹⁸⁻¹²⁰ The eudistomins are β-carboline compounds, many of which bear acyl or aromatic substituents at the 4 position; only the 6-bromoindole-containing examples are included herein. Almost all of the eudistomins reported to date are active against *Herpes Simplex* virus type 1 (HSV-1). Eudistomin O, a simple bromo-β-carboline, was also active against *S. cerevisiae* and *B. subtilis* at unspecified levels. Eudistomin K represents the first oxathiazepine containing metabolite from marine sources. Eudistomin F represents the previously unreported 1-pyrrolinyl-β-carboline ring system. Eudistomin R was isolated from a Bermudan collection of *E. olivaceum*.¹²⁰ Isolation of pure compounds proved problematic throughout the original reports describing the eudistomins; many of the structures were solved as intractable mixtures.¹¹⁸ HPLC with aminopropyl bonded phase stationary media allowed several of the eudistomins to be clearly resolved for the first time.¹²⁰

Eudistalbins A (**127**) and B (**128**) were isolated from a New Caledonian tunicate *Eudistoma album*.¹²¹ Compound **127** was found to be cytotoxic to the human nasopharyngeal carcinoma KB cell line, with an ED₅₀ of 3.2 μg/mL. It was suggested that the eudistalbins were derived from tryptophan and leucine.¹²¹



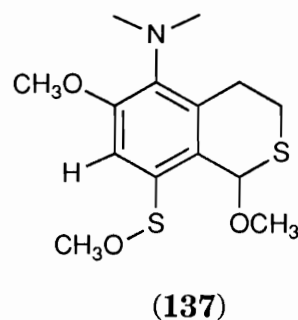
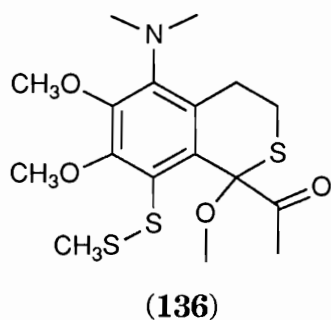
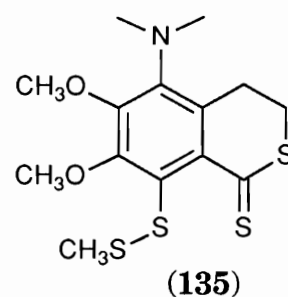
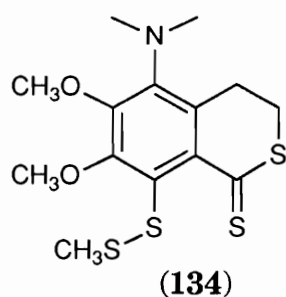
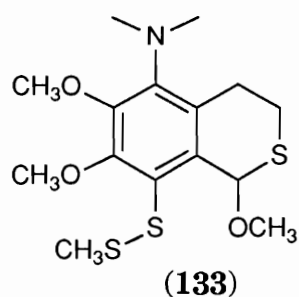
The North Brittany coast solitary red Styelid tunicate *Dendrodoa grossularia* has produced a number of indole alkaloids, including dendrodoine (**129**), grossularine-1 (**130**) and grossularine-2 (**131**), and 3-indolyl-4H-

imidazol-4-one (**132**).¹²²⁻¹²⁵ The structure of dendrodoine, the first natural product incorporating a novel thiadiazole ring, was established by x-ray crystallography. Dendrodoine was subsequently synthesized.¹²⁶ Dendrodoine was found to inhibit L1210 cells and DNA synthesis as measured by incorporation of tritiated thymidine, at unspecified levels. The grossularines are the first natural products possessing an α -carboline skeleton and were cytotoxic towards L1210 cells (IC_{50} 6.0 and 4.0 $\mu\text{g/mL}$, respectively). Grossularine-2 was also found to be more cytotoxic towards

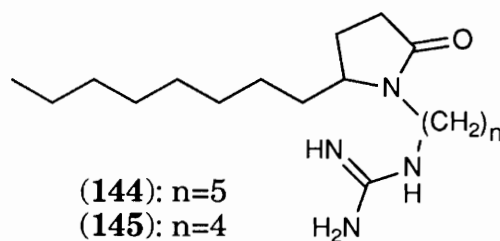
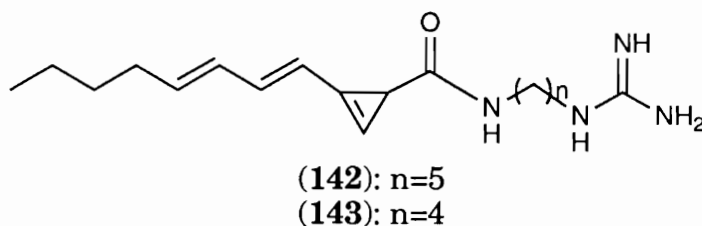
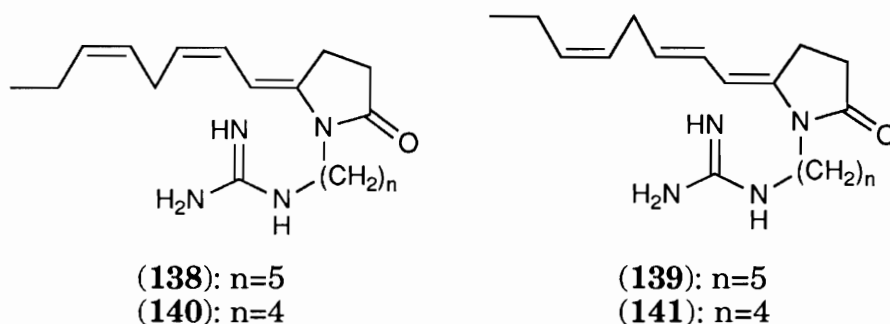


human colon (WiDr) and breast (MCF7) solid tumor cell lines at 10 ng/mL; **131** appears to act as an intercalator.¹²⁷ Compound **132** was isolated from the dichloromethane partition of the extract of *D. grossularia*.¹²⁵ The structure was elucidated by interpretation of NMR and mass spectral data and was confirmed by synthesis of the natural product. Compound **132** represents the first imidazol-4-one from natural or synthetic sources.

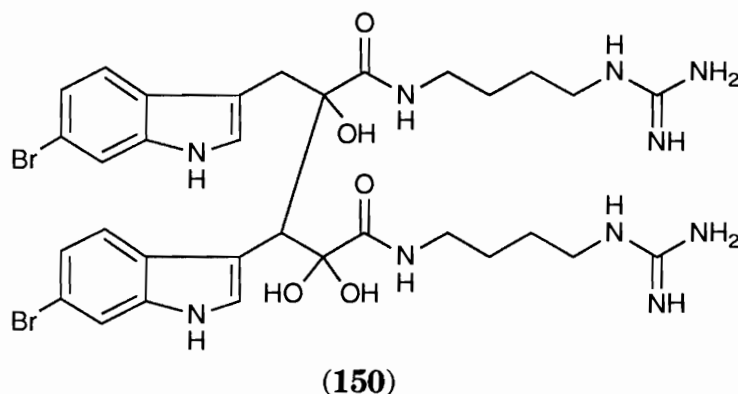
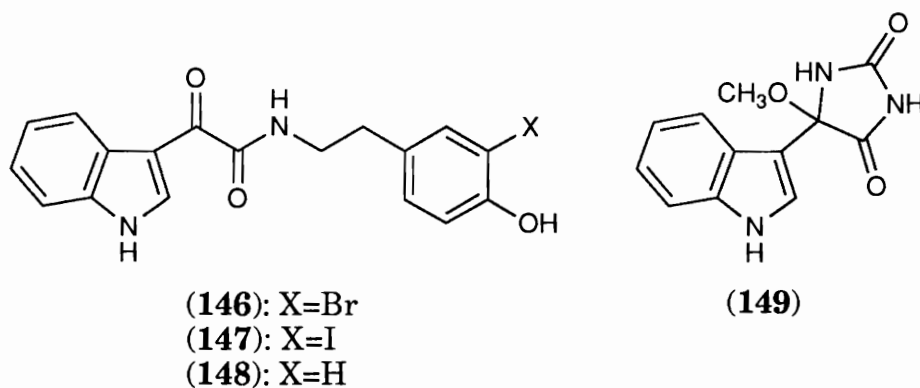
Polycarpamines A-E (**133** - **137**) were isolated from the solitary Philippino ascidian *Polycarpa auzata*. This organism is a highly conspicuous member of Pacific coral reef fauna; individuals as large as 20 cm in length are commonly encountered, and the coloration is a striking blend of orange with purple mottling. Compound **134** was found to be a potent inhibitor of the fungi *S. cerevisiae* and *C. albicans*. Compounds **134** and **135** are believed to be natural products, while **133**, **136** and **137** are thought to be artifacts of isolation.



The red colonial tunicate *Polyandrocarpa* sp. collected in the Gulf of California produces polyandrocarpidines A - D (**138** - **141**).^{128,129} The original structures assigned these compounds included cyclopropenyl acid amides (**142** and **143**) but were revised to *N*-alkyl- γ -alkylidene- γ -lactams **138** - **141**. The polyandrocarpidines are antibacterial and cytotoxic towards L1210 and KB cell lines at unspecified levels. The presence of the lactam moiety



was confirmed by ozonolysis of the 8 carbon polyunsaturated side-chain of **138** - **141** to generate *N*-alkyl succinimides.¹²⁹ The structures of the polyandrocarpidines were confirmed by synthesis of the hexahydropolyandrocarpidines (**144** and **145**).¹³⁰



The rust-colored Philippino colonial tunicate *Polyandrocarpa* sp. produced polyandrocaramides A - D (**146** - **149**).¹³¹ The structures were elucidated by interpretation of NMR and mass spectra, chemical conversions, and synthesis of a phenethylamine analog. The polyandrocaramides contain α -keto-amide functionalities, thus providing a chemotaxonomic precedent for this Family of organisms. The taxonomically and geographically very closely related Philippino ascidian *Eusynstyela misakiensis* produced eusynstyelamide (**150**), another α -keto-amide containing 6-bromoindole alkaloid. The ketone hydrate in **150** was detected by diagnostic NMR spectral data. The isolation and structure elucidation of eusynstyelamide is described in greater detail herein.

II. THE CHEMISTRY OF *FASCIOSPONGIA* SPECIES

Introduction

Sponges of the Order *Dictyoceratidae* have received tremendous attention from natural products chemists. As mentioned above, sponges of the genus *Dysidea* have produced a large number of secondary metabolites, which account for most of the reports concerning the *Dictyoceratidae*. Other genera within the Order, such as *Fasciospongia*, have not been as well represented. *F. cavernosa* has produced cavernosine (**20**) and a series of *N*-acylated β -alanine methyl esters (**55** - **59**).^{30,52} The remaining reported metabolites are aromatic linear or cyclized polyprenyl terpenoids. These include an unnamed polyprenyl quinol (**33**) from a *Fasciospongia* sp. and five quinone sesquiterpenoids (**40** - **44**) isolated from *Stelospongia* (= *Fasciospongia*) *conulata*.^{38,39} Mamanuthaquinone is a new member of this latter class of secondary metabolites typically isolated from sponges of this genus.⁴⁷

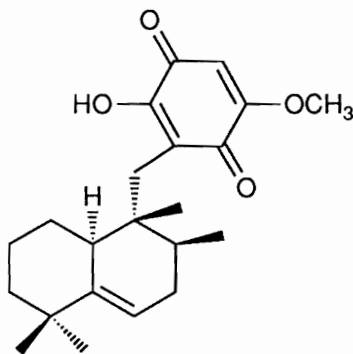
The decision to investigate the small osculed, fibrous purple sponge was based on preliminary cytotoxicity data of the crude methanol extract, with in vitro IC₅₀'s of 0.12 μ g/mL vs. HCT-116 cells. The extract also showed moderate life extension properties in vivo, with a T/C=118 at 115 mg/kg in P388 infected mice when injected intraperitoneally.

Sponge Collection and Isolation of Mamanuthaquinone

The sponge *Fasciospongia* sp. was collected off the Western coast of Mamanutha Island, in the Yasawa group of the Fiji Islands in November

1987. The sponge was a mottled greenish-brown and yellow when collected, but had turned purple after 3 years of frozen storage. Portions of the deep purple methanol extract (1.4 g brown oil) of the sponge were either extracted successively with hexanes, carbon tetrachloride, and chloroform, or applied directly to an LH-20 column and eluted with acidified methanol. Thin layer chromatography (silica gel, 39.9% ethyl acetate/60% hexanes/0.1% acetic acid) showed the single major component of all of these fractions was **50**.

Fractions containing **50** were pooled and purified by HPLC, yielding 243 mg mamanuthaquinone (5% yield by dry weight). Other pigments and minor metabolites were not characterized.



(50)

Structure Determination of Mamanuthaquinone

Solutions of **50** exhibited a characteristic color change from orange to purple in alkali media. This trait is typical of hydroxyl quinone compounds. Coincidentally, Dr. Brent Copp isolated and identified ilimaquinone (**32**) from another sample in our lab. Because the extracts containing **50** and **32**

behaved identically by TLC and coloration, we were fairly certain that **50** was also a quinone sesquiterpenoid.

NMR chemical shift data are summarized in Table I, and full spectra are included in Appendix A. Carbon multiplicities and proton-carbon connectivities were determined via DEPT and HMQC experiments.^{132,133}

Signals corresponding to an aromatic methoxyl group at δ 56.8 and quinone carbonyls at δ 182.0 and 182.4 were observed in the ^{13}C NMR spectrum of **50**. Signals in the ^1H NMR spectrum at δ 7.45 (exch s, 1H), 5.85 (s, 1H) and 3.86 (s, 3H) indicated the substitution pattern of the quinone moiety of **50** was identical to that in **32**, **40** and **41**.^{39,44} Low resolution positive ion FAB mass spectrometry yielded a spectrum with little fragmentation and distinct molecular ions at m/z 358 (M^+) and 359 (MH^+). The only major fragmentation peak at m/z 191 is characteristic of the drimane portion of the molecule; the same fragmentation pathway was observed in the FAB and EI mass spectra of dictyoceratin A, spongiaquinone and isospongiaquinone, and gave rise to the base peak in the EI spectra of the cyclospongiaquinones **42** and **43**.³⁷ High resolution FAB mass measurements of both M^+ and MH^+ established a molecular formula of $\text{C}_{22}\text{H}_{30}\text{O}_4$ (found M^+ 358.2146, Δ 0.2 mmu, $\text{C}_{22}\text{H}_{30}\text{O}_4$; MH^+ 359.2223, Δ 0.1 mmu, $\text{C}_{22}\text{H}_{31}\text{O}_4$), identical to that of other described quinone sesquiterpenoids, such as ilimaquinone.⁴⁴

The quinone portion of **50** was the simplest substructure to assign. A 2-D homonuclear correlation (COSY) experiment at 200 MHz showed extremely weak coupling between the singlet at 5.85 ppm and the *O*-methyl singlet at 3.86 ppm.¹³⁴ A phase-sensitive double quantum-filtered COSY (DQCOSY) experiment at 500 MHz showed the 13 Hz doublets at 2.45 and

Table I
 ^1H and ^{13}C NMR Assignments of Mamanuthaquinone

C#	^{13}C (ppm) (mult) ^{a,b}	^1H (ppm) (mult, J (Hz)) ^c
1	30.6 (t)	A- 0.90 (m) B- 1.79 (bd, 8.5)
2	22.7 (t)	A- 1.40 (m) B- 1.46 (m)
3	41.2 (t)	A- 1.13 (dt, 13.25, 4.25) B- 1.32 (m)
4	36.3 (s)	
5	146.3 (s)	
6	114.8 (s)	5.35 (bs)
7	31.5 (t)	A- 1.73 (ddt, 18.0, 6.5, 2.5) B- 1.95 (dt, 18.0, 5.0)
8	36.4 (d)	1.36 (m)
9	40.9 (s)	
10	41.7 (d)	2.08 (d, 13.0)
11	16.5 (q)	0.92 (s)
12	29.7 (q)	0.99 (s)
13	27.9 (q)	0.96 (d)
14	16.0 (q)	0.73 (s)
15	32.7 (t)	A- 2.45 (d, 13.5) B- 2.58 (d, 13.5)
16	118.3 (s)	
17	152.8 (s)	7.45 (s)
18	182.4 (s)	
19	102.0 (s)	5.85 (s)
20	161.5 (s)	
21	182.0 (s)	
22	58.8 (q)	3.86 (s)

^a measured at 125 MHz; referenced to CDCl_3 (77.0 ppm).

^b multiplicity determined by DEPT experiment.

^c measured at 500 MHz; referenced to residual CHCl_3 (7.24 ppm).

2.58 ppm corresponding to the two diastereotopic benzylic methylene protons (H-15) couple only to each other.¹³⁵ Evidence provided by a heteronuclear multiple bond correlation (HMBC) experiment allowed the unequivocal assignment of the attachment point of C-15 to the quinone and confirmed the substitution pattern of the quinone.¹³⁶ The HMBC correlations observed for the quinone substructure are shown in Figure 13.

The allylic methylene H-15 protons both showed intense correlations from carbon signals at 152.8, 118.3 and 182.0 ppm; these were assigned as C-17, C-16 and C-21, respectively. The lone quinone proton (H-19) at 5.85 ppm showed intense correlations from carbon signals at 152.8 (C-17) and 182.0 (C-21) ppm and weaker 2-bond correlations from signals at 182.4 and 161.5 ppm; these signals are assigned as C-18 and C-20. Correlations were also observed from C-20 to the three proton methyl singlet at 3.86 ppm and from C-17 to the broad hydroxyl singlet at 7.45 ppm.

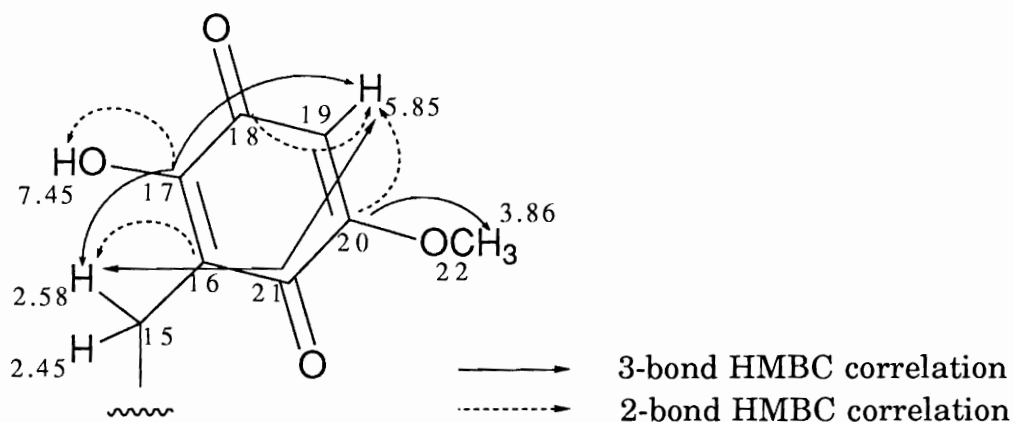


Figure 13. HMBC correlations observed for the quinone substructure of mamanuthaquinone.

Data from DQCOSY, HMQC, HMBC and TOCSY experiments were used to establish the carbon skeleton of the terpenoid portion of maminuthaquinone, which proved to be a less straightforward task. The salient HMBC and COSY correlations are indicated in Figures 14 and 15. The DQCOSY spectrum contained unambiguous correlations establishing the proton system from methine H-6 to both protons borne by C-7 (1.95, 1.73 ppm), and from these methylene protons to methine H-8 at 1.36 ppm. This proves that the methine carbon at 36.4 ppm that bears H-8 must be C-8, removing any ambiguity caused by the presence of two very close carbon signals in this region. The multiplicity of C-8 was confirmed by DEPT results; quaternary C-4 at 36.3 ppm did not appear in this experiment. A correlation in the DQCOSY spectrum between H-8 and the only methyl doublet in the proton spectrum at 0.96 ppm completed this spin system (Figure 14). DQCOSY correlations from H-10 to the methylene signal at 0.90 (H-1) allowed assignment of C-1. Signals from both H-3 and H-1 into a complex two proton multiplet at 1.40-1.46 ppm allowed assignment of the methylene carbon bearing these protons as C-2. Finally, H-10 and H-6 showed allylic coupling in the 200 MHz COSY spectrum. This observation and correlations in the HMBC spectrum of **50** from carbon signals at 114.8 and 146.3 ppm to H-10 at 2.08 ppm facilitated assignment of C-5 and C-6.

HMBC correlations from carbon signals at 41.7, 16.0, 36.4 and 40.9 ppm to both H-15 doublets indicated one of these carbons must be the attachment point of the quinone to the drimane skeleton. The only arrangement that accommodates the multiplicity of these atoms is that in which the quaternary carbon at 40.9 (C-9) ppm bears methyl C-14, methines C-8 and C-10, and methylene C-15 (Figure 15). Strong correlations to the H-14

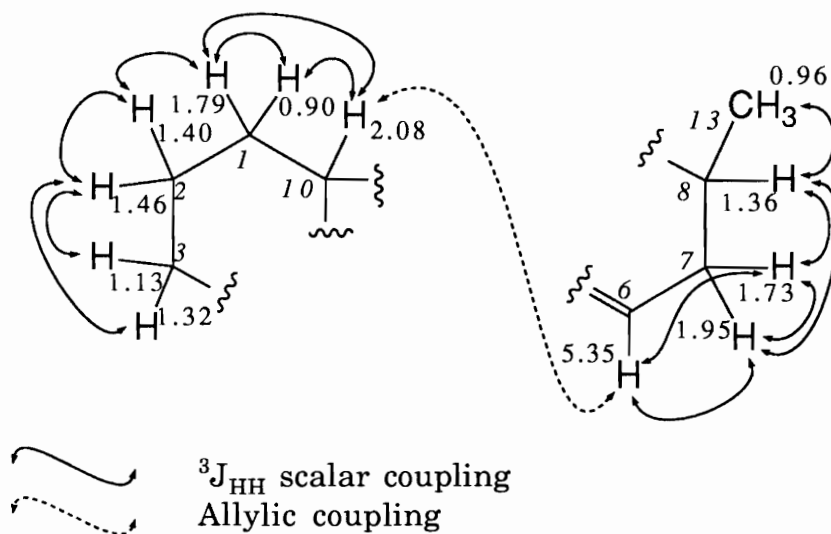


Figure 14. Partial structures of mamanuthaquinone developed by COSY and DQCOSY results.

methyl singlet at 0.73 ppm from C-8, C-9, C-10 and C-15 confirm this arrangement. Further correlations observed in the HMBC spectrum of mamanuthaquinone established the carbon skeleton of the terpenoid moiety.

HMBC correlations from C-11 to H-12, from C-12 to H-11 and from the quaternary carbon signal at 36.3 ppm to both H-11 and H-12 indicated that C-11 and C-12 are geminal methyls attached to the quaternary center. HMBC correlations from this quaternary carbon to H-6 established that the carbon signal at 36.3 ppm corresponded to C-4. Strong correlations from the methylene carbon at 41.2 ppm to both H-11 and H-12 allowed assignment of C-3. Further confirmation of the proton spin systems delineated by H-10/H-1/H-2 /H-3 and H-13/H-8/H-7/H-6 was provided by the results of a total correlation spectroscopy (TOCSY) experiment.^{137,138} The TOCSY pulse sequence utilizes a so-called “spin-lock” pulse train of variable mixing time, during which an isotropic mixing Hamiltonian is created which allows

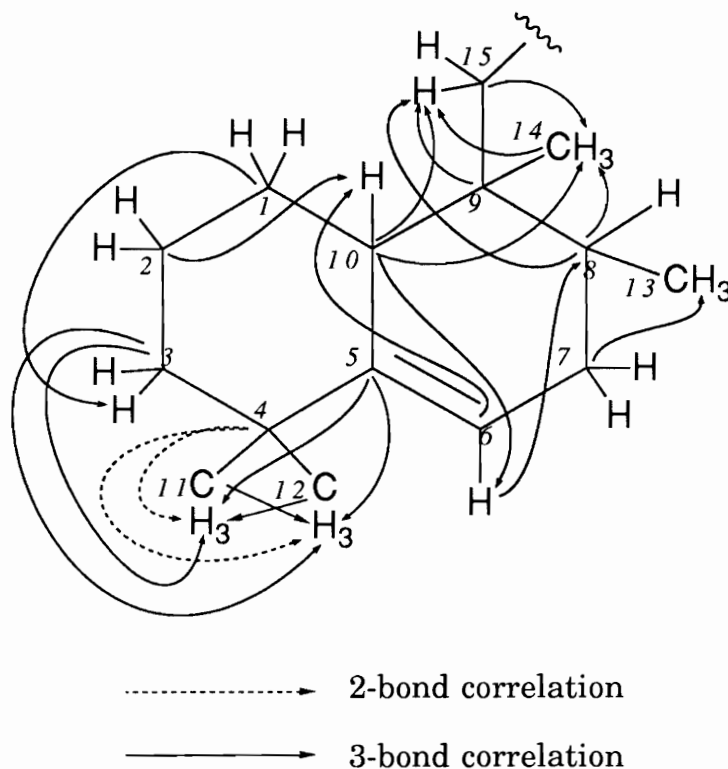


Figure 15. HMBC correlations observed in the terpenoid moiety of mamanuthaquinone.

transfer of magnetization between all protons of an isolated spin system. The quaternary carbons at C-9, C-4 and C-5 effectively divide **50** into two distinct spin systems. The use of a typical mixing time (50 msec) produced a spectrum with correlations entirely consistent with only those spin systems implied by structure **50** (Figure 16). The mixing time utilized was sufficiently short that the relatively inefficient allylic coupling between H-6 and H-10 was not observed.

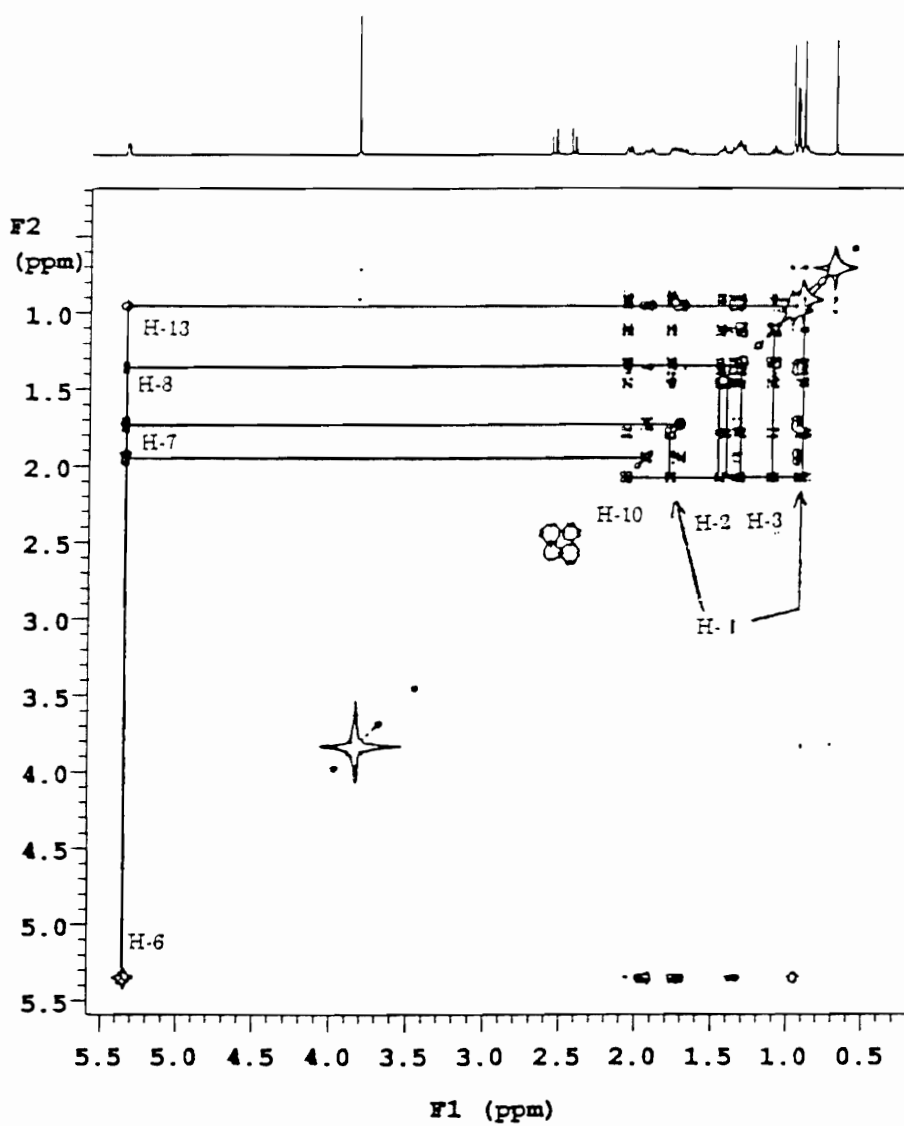


Figure 16. 500 MHz TOCSY spectrum of mamanuthaquinone with spin systems delineated.

Relative and Absolute Configurations
of Mamanuthaquinone

The absolute stereochemistry of few quinone sesquiterpenoids has been determined.^{43,45} Historically, compounds reported in the literature have been shown with a particular absolute stereochemistry without basis of chemical or spectroscopic evidence, or based on comparison to other structures which later proved to be incorrect.^{44,48} Our goal was to unequivocally establish the absolute stereochemistry of mamanuthaquinone, using chemical and spectral methods.

The relative stereochemistry of C-8, C-9 and C-10 was readily established by interpreting the results of several difference nuclear Overhauser effect (NOE) difference experiments at 200 MHz.¹³⁹ The NOE arises from transfer of magnetization by dipole-dipole cross relaxation. In these experiments, irradiation of one particular proton signal produces enhancement of only those signals corresponding to protons which are relatively close ($<3.5 \text{ \AA}$) in space. Partial structures summarizing all enhancements observed are shown in Figure 17. In particular, irradiation of the H-15 methylene at 2.45 ppm produced a 6.8% enhancement of the H-10 signal at 2.08 ppm, indicating H-10 and C-15 (which bears H-15) exist in a *syn* relationship. Also observed was a 2.8% enhancement of the H-14 methyl doublet at 0.96 ppm upon irradiation of the H-13 methyl singlet at 0.73 ppm, indicating these two methyl groups are also *syn* to one another. These results established that the relative stereochemistry of mamanuthaquinone is similar to that of ilimaquinone and provided two possible enantiomeric structures consistent with the biosynthetic origins of compounds in this class.

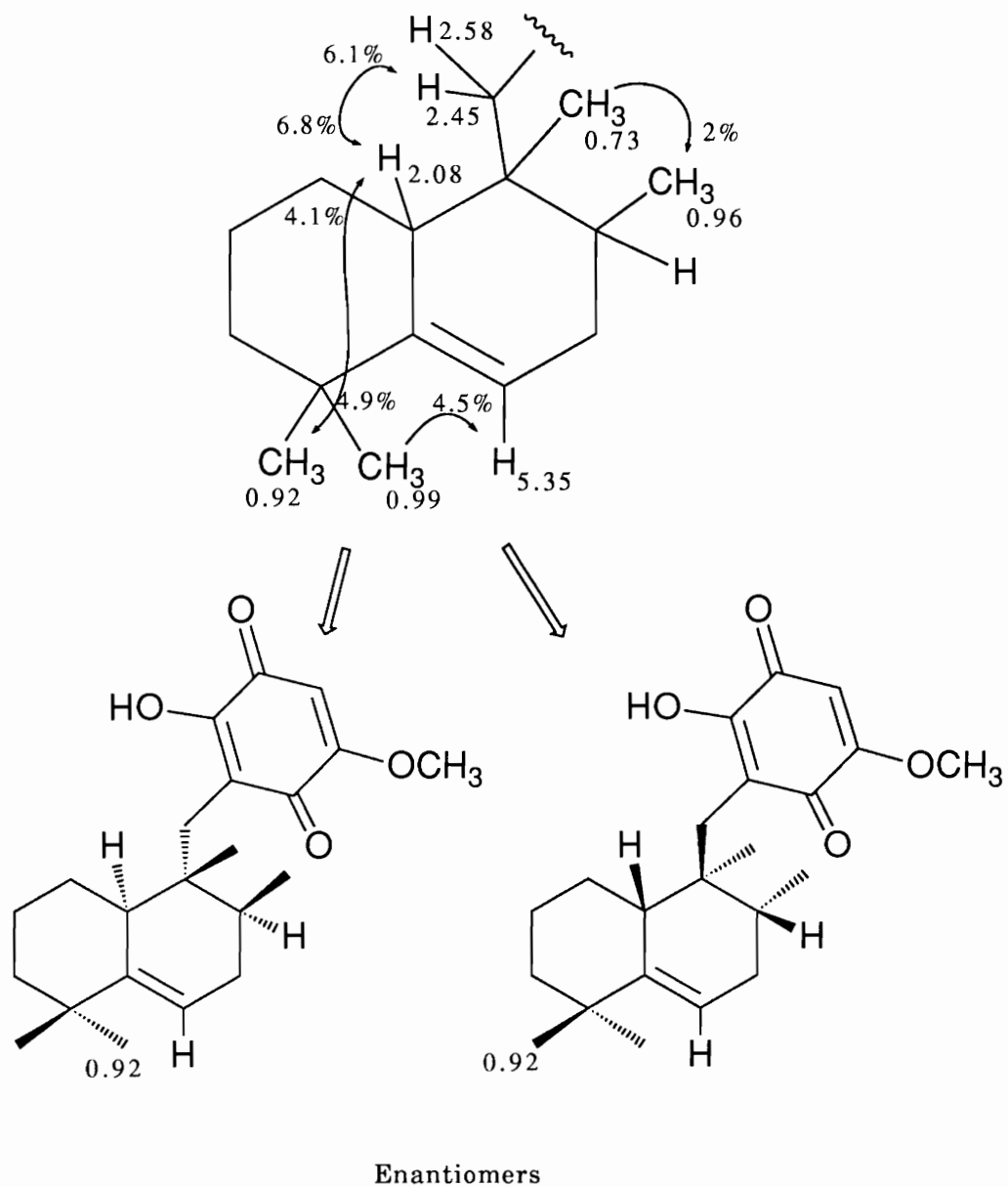


Figure 17. Relative stereochemistry of mamanuthaquinone by difference nuclear Overhauser effect spectroscopy.

Determining the absolute stereochemistry of **50** was accomplished by comparing the optical properties of structurally isomeric compounds (**151_m** and **151_i**) derived from mamananthaquinone and ilimaquinone, respectively. Rearranged quinone sesquiterpenoids of the general form **151** were afforded by Lewis acid-catalyzed (BF₃-etherate) rearrangement (also known as a Nametkin rearrangement) of either **50** or **32**. Our procedure was a simplification of one reported previously, and details are included in the experimental section.⁴⁸

The general scheme is depicted in Figure 18. We first had to determine that **151_m** and **151_i** were isomeric. In fact, rearrangement products **151_m** and **151_i** were chemically indistinguishable. They exhibited similar mass spectra and behaved identically in several TLC systems. The compounds yielded identical NMR spectra; 1-D proton and carbon NMR spectra of **151_m** and **151_i** are included in Appendix A and are compared in Figures 19 and 20. In particular, the ¹³C spectrum of both compounds displayed new signals at 131.4 and 134.9 ppm, corresponding to a tetra-substituted olefin between C-5 and C-10. Neither compound displayed signals for terpenoid olefinic protons in their ¹H spectra.

The next step was to determine if **151_m** and **151_i** shared the same or opposite absolute configuration. Because the absolute configuration of **32** is known, the absolute stereochemistries at C-8 and C-9 of **151_i** are fixed. Identical UV spectra ($\epsilon=620/\text{mol}/\text{cm}$ at 430 nm, CHCl₃) and similar O.R.D. values were obtained for **151_m** ($[\alpha]_{546} +28.3^\circ$) and **151_i** ($[\alpha]_{546} +31.5^\circ$). CD spectra of the rearranged quinones **151_m** and **151_i** are included in Appendix A. The CD curves (CHCl₃) produced by the rearranged quinones exhibited maxima at 347 nm, minima near 400 nm, and nodes at 374 nm. If **151_m** and

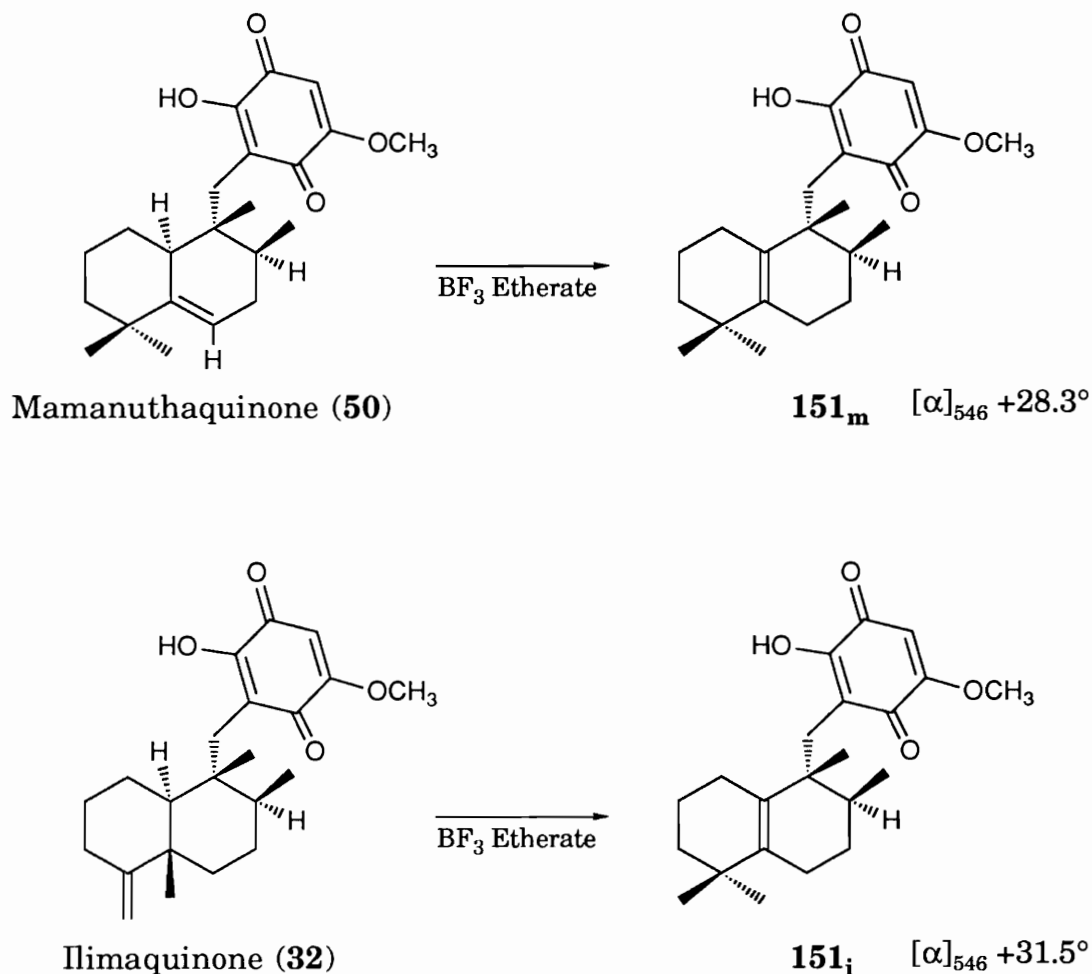


Figure 18. Lewis acid catalyzed rearrangement of mamanuthaquinone and ilimaquinone.

151_i were of opposite absolute stereochemistry, the specific rotation values would have been of opposite sign, and the CD curves would have been of opposite phase. The optical data indicate that **151_m** and **151_i**, and therefore the compounds from which they are derived, are of identical absolute configuration. By virtue of their optical behavior, and the difference NOE results concerning the relative configuration of C-8, we established that the absolute configuration of mamanuthaquinone is 8S, 9R, 10S.

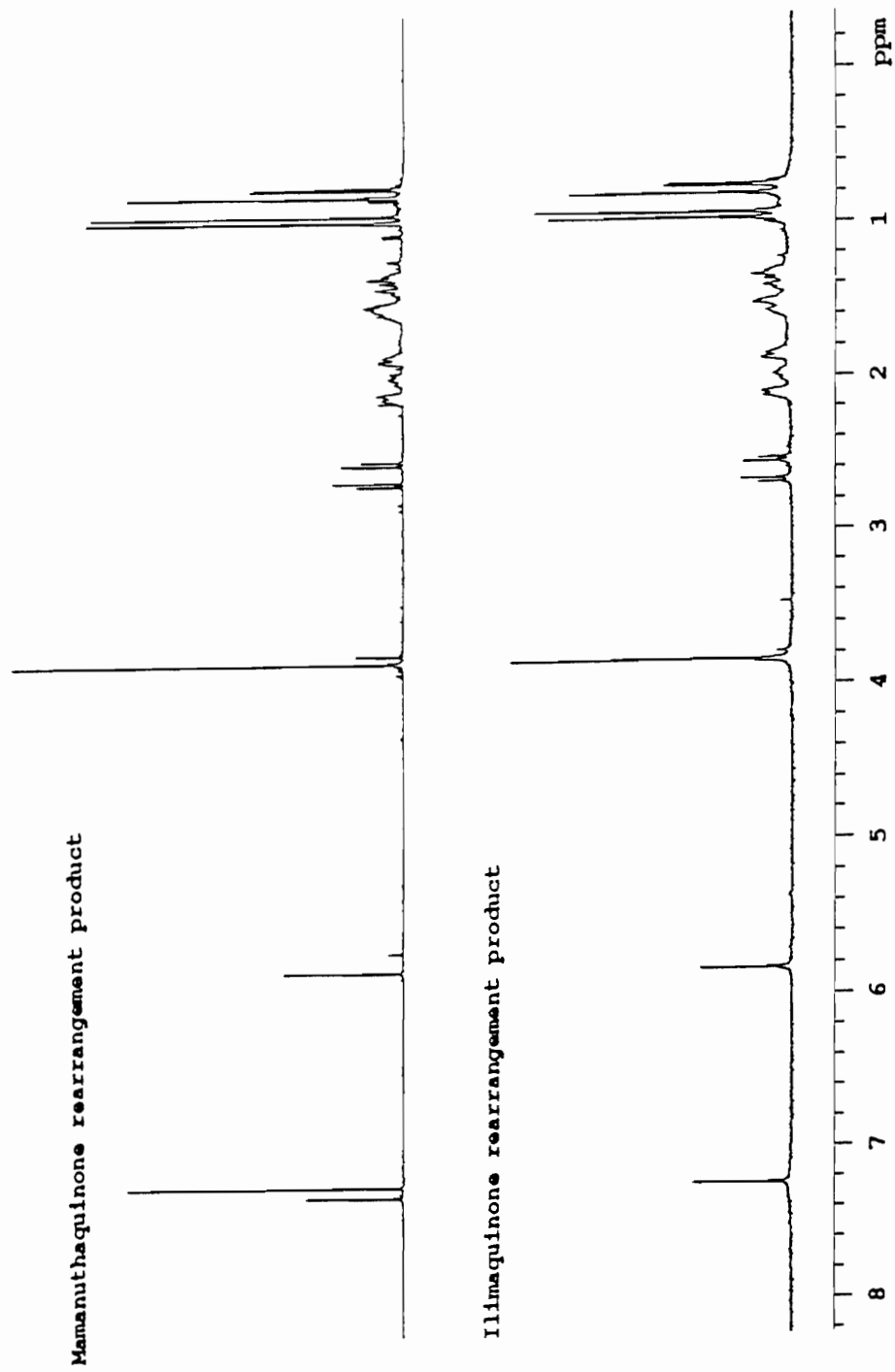


Figure 19. Stacked proton NMR spectra of rearranged quinone sesquiterpenoids.

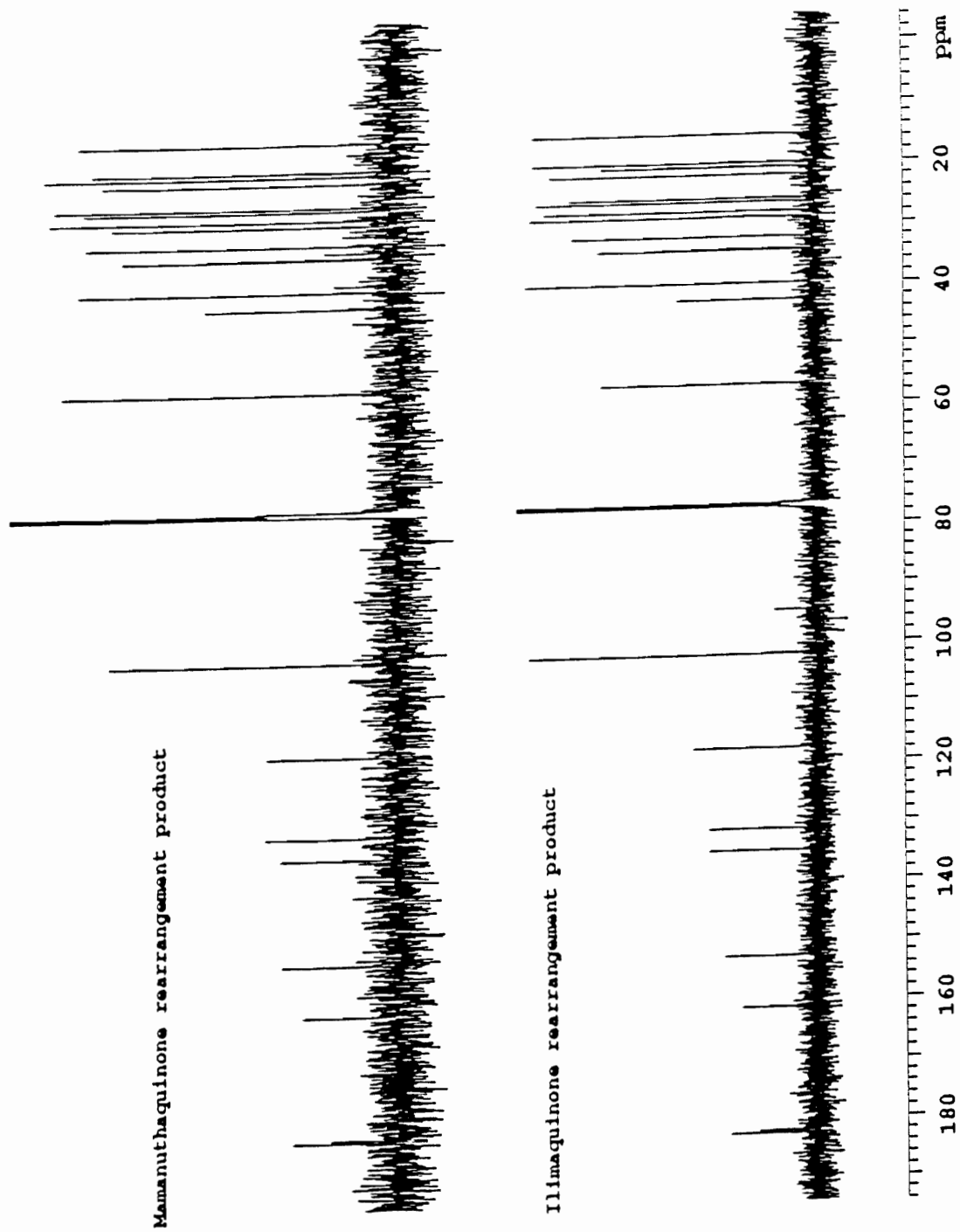
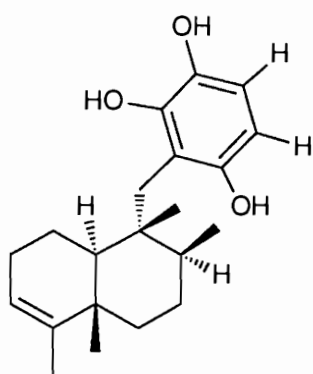


Figure 20. Stacked carbon NMR spectra of rearranged quinone sesquiterpenoids.

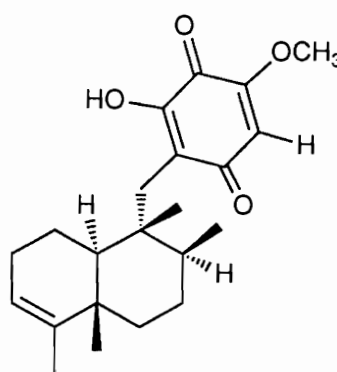
Biological Activity of Mamanuthaquinone

Because mamanuthaquinone was the single major component of *Fasciospongia* sp., it was expected to be responsible for the cytotoxic activity exhibited by extracts of the sponge. In fact, **50** showed moderate to good levels of cytotoxicity against a variety of cell lines, at roughly one-tenth the levels exhibited by the crude extract. Compound **50** exhibited an IC_{50} of 2.0 $\mu\text{g/mL}$ vs. the HCT-116 cell line.

Our interest in mamanuthaquinone as a potentially therapeutic substance in the treatment of acquired immuno-deficiency syndrome (AIDS) was raised by a report that analogs of **50**, such as avarol (**152**) and avarone (**153**), inhibited the enzymatic activities of Human Immuno-deficiency Virus Reverse Transcriptase (HIV-RT) (IC_{50} 7.0 and 1.0 $\mu\text{g/mL}$, respectively).¹⁴⁰



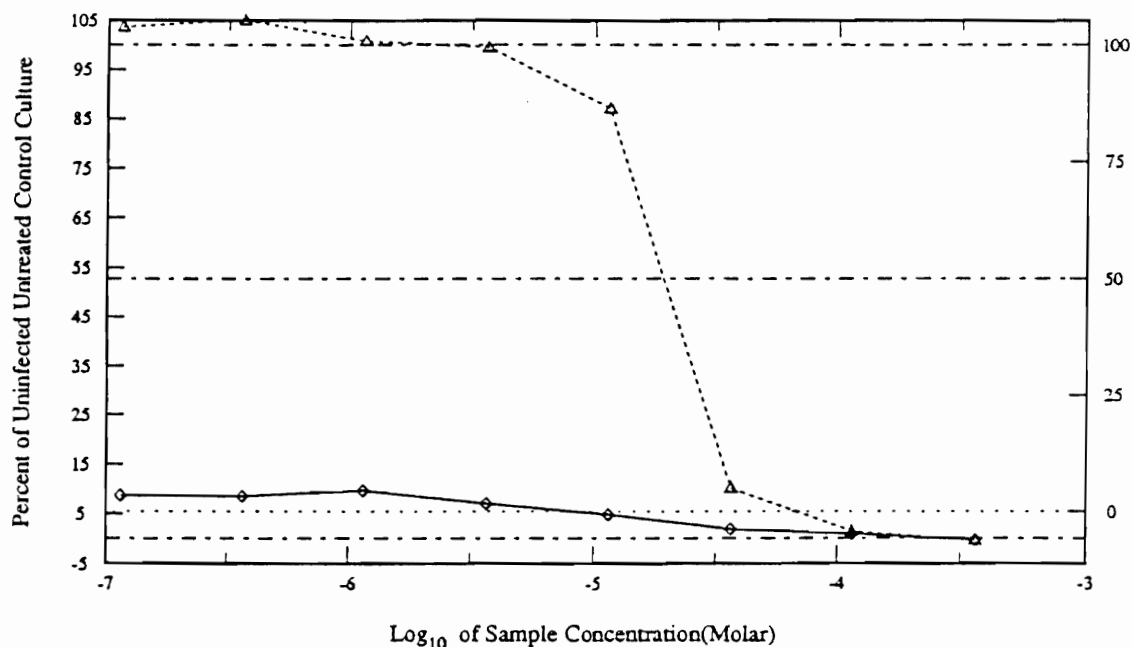
Avarol F (**152**)



Avarone E (**153**)

This enzyme is responsible for converting the viral genomic RNA into proviral double-stranded DNA and is crucial to the reproductive cycle of the virus. Because reverse transcriptases are unique to retroviruses and

no endogenous cellular homologues are known, substrates that inhibit them should bear selective lethality to retroviruses, such as HIV. Unfortunately, mavanuthaquinone provided no measureable protection for an HIV-treated culture of T4 lymphocytes (CEM cell line) vs. an untreated control culture (Figure 21). Mavanuthaquinone was found to be cytotoxic to the cultured CEM cells, with an IC_{50} of $6.7 \mu\text{g/mL}$.¹⁴¹



Viral Cytopathic Effect

.....

Infected Treated Culture

—————

Uninfected Treated Culture

.....

Figure 21. In vitro AIDS inhibition testing of mavanuthaquinone.

III. THE CHEMISTRY OF AN UNIDENTIFIED FIJIAN SPONGE OF MIXED *AXINELLIDAE* AND *JASPIDAE* TAXONOMY

Introduction

Systematists studying all manner of invertebrate animals and plants have relied occasionally on chemical profiles of particular specimens to enable or strengthen the taxonomic classification of those specimens. Identification of an organism under study is crucial for scientific accuracy and repeatability. Our study of marine invertebrates is no different, in that many organisms which appear identical macroscopically may actually belong to entirely different genera or even families. Chemotaxonomic traits of certain families of sponges have developed in tandem with our understanding of the chemistry of these families.¹⁹

Bromopyrrole-containing compounds have been isolated only from sponges of the Order Axinellida, such as *Agelas*, *Axinella*, and *Phakellia*.^{71,142} Different collections of the orange sponge from which we isolated epipolasidamide (**88**) contained varying amounts of the metabolite as measured by percentage of dry weight, while all collections contained the bengamide series (e.g., **80**) in roughly the same abundance. Further, we had taxonomic evidence from several sources that the sponge had organizational and physical characteristics of more than one species. For this reason, we believe the specimen represents either an undescribed species or an epizoic complex of two poorly resolved or new species in varying pro-

portions. The ecology of such associative relationships between sponges has been discussed.¹⁴²

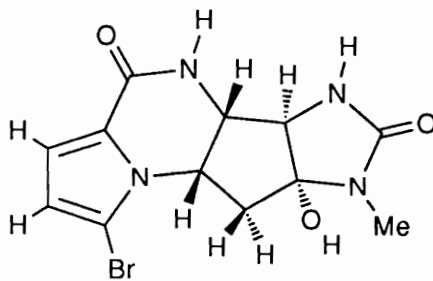
Our decision to investigate this organism was prompted by the potent *in vivo* antineoplastic properties of its crude methanol extract. This extract significantly extended the lives of P388 infected mice (T/C 142 at 135 mg/kg dose, T/C 135 at 45 mg/kg dose).

Sponge Collection and Isolation of Epipolasidamide

The orange crunchy sponge was collected on four separate occasions in reef waters of the Mbenga passage, off Mbenga Island of the Fijian Archipelago from November 1986 to January 1992. The sponge invariably exhibited evidence of a tubeworm symbiont whose protective calcareous tubes (1-3 mm diameter, 4-10 mm long) are responsible for the crunchy texture and white spotted pattern of the sponge. Methanol extracts of the homogenized sponge were reduced *in vacuo*, taken up in 20% aqueous methanol, and subjected to a solvent partition scheme with hexanes, carbon tetrachloride, chloroform, and ethyl acetate. The hexane and carbon tetrachloride partitions contained carotenoid pigments, the known bengamide A (**80**), and a series of related compounds that were not investigated further.

Cytotoxicity testing indicated much of the activity exhibited by the crude extract of the sponge was concentrated in the chloroform and ethyl acetate partitions. Chromatography of this material with amino or octadecyl bonded-phase flash column media yielded **88** and a slightly more polar related compound. The related compound was extremely labile, and we were unable to purify and characterize this metabolite before it degraded. ¹H NMR spectra of the partially purified compound showed most

of the signals found in the NMR spectrum of **88**, except that the signal of the *N*-methyl group was absent. Final purification of epipolasidamide was achieved by HPLC with an amino Dynamax column. Epipolasidamide was isolated as a colorless glassy solid (21 mg).



(88)

Structure Determination of Epipolasidamide

The low resolution FAB mass spectrum (glycerol matrix) of **88** showed a doublet of peaks with similar heights at m/z 341 and 343, indicating the molecule contained one bromine atom. The high resolution FAB mass measurement of the peak at m/z 341 gave an exact mass of 341.0246, suggesting a formula of $C_{12}H_{14}N_4O_3^{79}Br$ (Δ .35 mmu) for the protonated molecular ion MH^+ . This formula incorporates 8 degrees of unsaturation (double bond equivalents, or DBE's).

The IR spectrum of **88** showed two very strong absorbances at 1670 and 1643 cm^{-1} , typical of amide functionalities. The UV spectrum of **88** showed absorbance maxima ($\log \epsilon$) at 277 (4.01), 228 (3.91) and 207 (3.87) nm,

which compare favorably to the published values of bromopyrrole **93** at 272 (4.09), 240 (3.98) and 207 (3.97) nm.⁷⁷

The ¹H and ¹³C NMR spectra are included in Appendix B. Proton-carbon connectivities were established by the results of HMQC experiments. These results are summarized in Table II. The ¹³C and ¹H NMR data were in full accord with the formula provided by mass spectroscopy. Twelve carbon-bound protons and three exchangeable protons were observed in DMSO.

Table II
¹H and ¹³C NMR Assignments of Epipolasidamide

C#	¹³ C (ppm) (mult) ^{a,b}	¹ H (ppm) (mult, J (Hz)) ^c
2	104.5 (s)	
3	111.8 (d)	6.33 (d, 4.0 Hz)
4	113.3 (d)	6.72 (d, 4.0 Hz)
5	123.6 (s)	
6	52.5 (d)	4.35 (m, 6.0, 5.5, 1.0)
7	60.3	3.94 (d, 5.5)
N8		NH- 8.01 (s)
9	157.7 (s)	
10	38.9 (t)	A- 1.91 (dd, 12.5, 12.5) B- 2.44 (ddd, 12.5, 6.0, 0.65)
11	93.3 (s)	OH- 6.5 (brs)
12	65.0 (d)	3.75 (d, 2.5)
14	158.5 (s)	
N15		NH- 7.12 (d, 2.5)
16	23.5 (q)	2.62 (s)

^a measured at 125 MHz; referenced to DMSO-*d*₆ (39.5 ppm).

^b multiplicity determined by DEPT experiment.

^c measured at 500 MHz; referenced to residual DMSO (2.49 ppm).

A striking feature of both the proton and carbon spectra was the anomalous chemical shifts associated with the *N*-methyl group at position 16 of epipolasidamide. Typical proton chemical shift values for this hetero-substituted functionality are from 3.3-3.9 ppm, and typical carbon values are 35-43 ppm. The *N*-methyl group in **88** gives rise to signals at 2.62 and 23.5 ppm, respectively. This indicates either that the magnetic environment of this group is significantly shielded or that this methyl group receives electron density from neighboring groups. *N*-methyl hydantoin-containing compounds such as midpacamide (**94**) and the naamidines have been described.^{77,143,144} NMR spectra of all these compounds contain similar anomalous signals corresponding to shielded *N*-methyl groups.

A DQCOSY experiment established the proton spin systems of **88**, and facilitated the establishment of the partial substructures shown in Figure 22. Two aromatic protons at 6.33 and 6.72 ppm couple at 4.0 Hz, a typical value for pyrrole protons in this configuration.¹⁴⁵ Because these signals are simple doublets, N-1 must be tertiary, and C-2 and C-5 must be quaternary. Another proton spin system observed in the DQCOSY experiment involved the amide exchangeable 2.5 Hz doublet signal at 7.12 ppm (H-15) coupled to a 2.5 Hz doublet methine signal at 3.75 ppm (H-12). The final coupled proton spin system observed in the DQCOSY spectrum consisted of a methine doublet at 3.94 ppm (H-7; 5.5 Hz) coupled to a complex multiplet at 4.35 ppm (H-6); H-6 was further coupled to both methylene protons H-10 and H-10' at 2.44 and 1.91 ppm respectively, which showed geminal coupling ($J=12.5$ Hz).

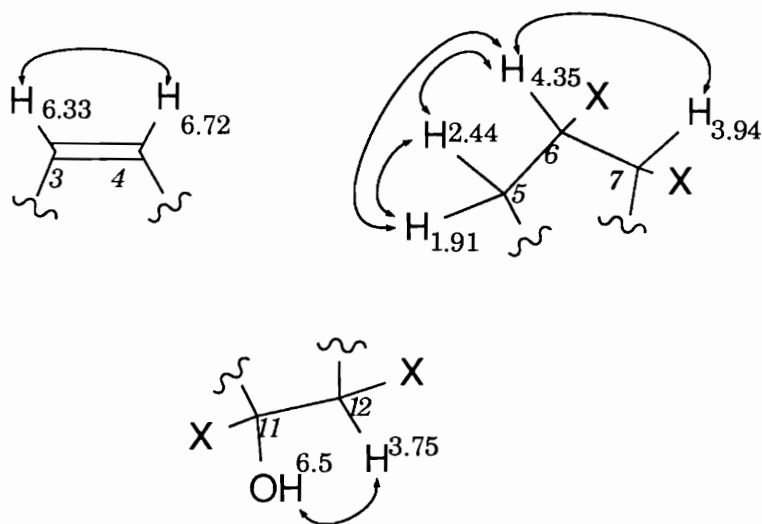


Figure 22. Partial structures of epipolasidamide developed from COSY data.

The remainder of the structure of **88** was deduced primarily by interpretation of the results of HMBC spectra optimized at 6 and 10 Hz. The salient correlations are summarized in Figure 23. A strong correlation to H-6 from C-2 and C-5 indicated that the alkyl substituent of N-1 was C-6. The chemical shift of methine C-6 at 52.5 is entirely consistent with N-substitution. Furthermore, this provided unambiguous evidence that the 2 and 5 positions of the pyrrole moiety were quaternary, as expected from the coupling constant and splitting pattern of the signals corresponding to H-3 and H-4. Further correlations from C-2 and C-5 to both H-3 and H-4 confirmed the pyrrole ring existed as shown. The chemical shifts of C-3 and C-4 are typical of protonated carbons in the 3 and 4 positions of a pyrrole ring. The chemical shift of C-2 (δ 104.5) is not typical of a carbon in the 2-position of a pyrrole ring (usually 120-122 ppm). This reflects the substitution of this position with a large polarizable bromine atom, which con-

tributes electron density back to the carbon that bears it, resulting in an upfield chemical shift.

Further correlations from both C-10 and C-7 to H-6 confirmed the arrangement of the aliphatic system H-7/H-6/H-10 (derived from COSY data above). A correlation from the carbonyl signal at 157.7 ppm to H-4 established amide carbonyl C-9 as the substituent of quaternary C-5, while other signals from C-5, C-6 and C-7 to the exchangeable proton at 8.00 ppm allowed generation of the amide containing 6-membered ring.

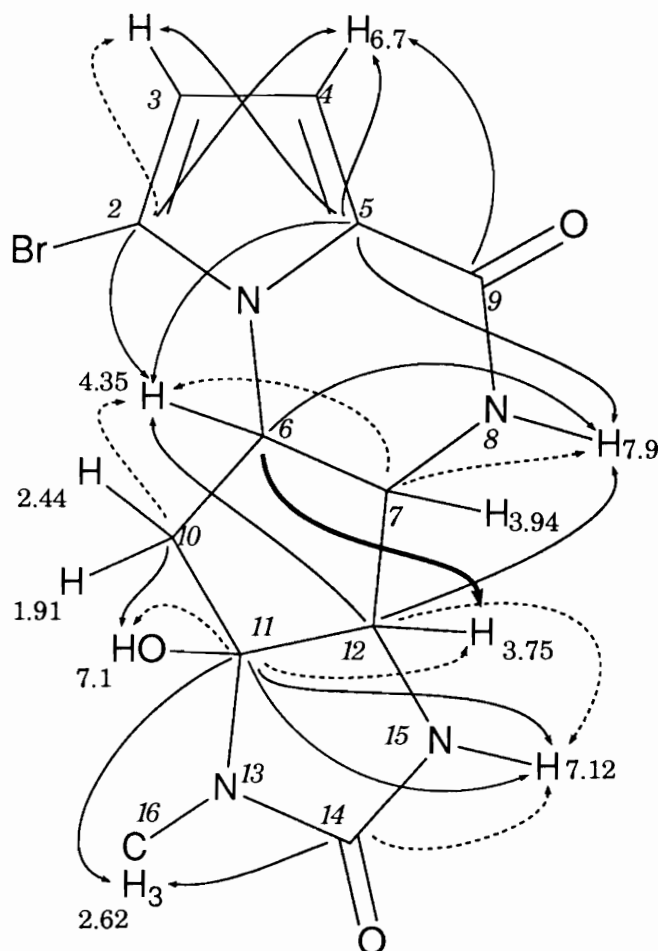


Figure 23. HMBC correlations observed for epipolasidamide.

Unambiguous 3-bond HMBC correlations from C-12 to both H-6 and H-8 allowed attachment of the methine C-12 at 65.0 ppm to C-7. A crucial connectivity shown in Figure 23 from C-6 to H-12 confirmed this attachment. No signals indicating scalar coupling between H-7 and H-12 were ever observed in DQCOSY, COSY and COSY45 experiments; this implies H-12 and H-7 are orthogonal. Molecular modeling experiments, which indicate this is indeed the case, are described.

Coupling of carbon signals at 38.9 and 93.3 ppm to the exchangeable proton signal at 6.5 ppm (H-11) indicated that methylene C-10 must be attached to quaternary C-11 and that C-11 must bear a hydroxyl group (OH-11). The 2-bond HMBC correlation from C-11 to H-12 and the coupling of H-11 and H-12 observed in the DQCOSY spectrum allowed attachment of C-12 to C-11, and confirmed the architecture of this 5-membered ring.

Crucial connectivities observed in the HMBC spectrum allowed generation of the *N*-methyl hydantoin portion of **88**. Specifically, correlations from only C-11 and the urea carbonyl signal at 158.5 ppm to the *N*-methyl protons (H-16, 2.62 ppm) placed N-13 unequivocally between C-11 and C-14. The chemical shift of C-11 is typical of that for an sp^3 hybridized carbon bearing two heteroatoms. Correlations from C-11 and C-12 to the exchangeable proton signal at 7.12 ppm allowed attachment of N-15 to C-12. The final correlation from C-14 to H-15 allowed closure of this 5-membered ring, with C-14 as a urea type carbonyl. The chemical shift of C-14 is consistent with this assignment. The proximity of O-14 and O-11 to the *N*-methyl group C-16 is responsible for increased electron density at this position and the concomitant anomalous chemical shifts of the methyl protons and carbon.

Relative Configuration of Epipolasidamide

The relative configuration at C-6, C-7, C-11 and C-12 was determined by interpretation of 200 MHz difference NOE proton NMR spectra of **88**. Results of these experiments are shown in Figure 24. The observed enhancements indicated that C-6 and C-7 define a cis ring fusion as expected and confirmed that C-11 and C-12 define a requisite 5-5 cis ring fusion. Irradiation of the H-6 signal at 4.35 ppm produced enhancement of H-7 and only the H-10 signal at 2.44 ppm (5.3% and 2.3%, respectively). Because this experiment did not result in enhancement of the H-10' signal at 1.91 ppm,

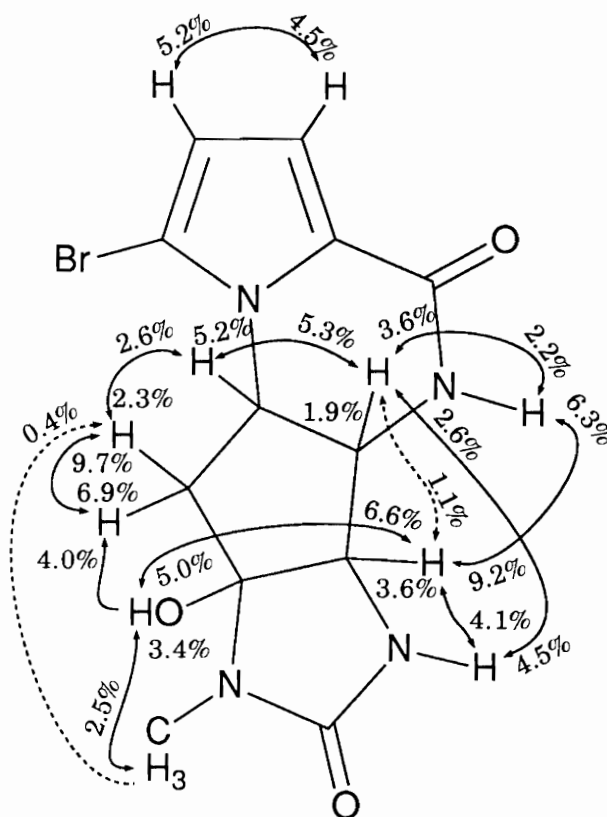


Figure 24. NOEs observed in epipolasidamide.

we knew that H-10, H-7 and H-6 were *syn* and that H-10' was *anti* to all of these. Irradiation of H-10 and the H-11 exchangeable signal at 6.52 ppm resulted in enhancement of H-10' (6.9% and 4.0%, respectively). Irradiation of H-11 produced enhancement of methine H-12 at 3.75 ppm. These results indicate that H-11 and H-12 are *syn* to one another and confirmed that C-11 and C-12 define a *cis* ring fusion. Because irradiation of H-7 and H-12 resulted in negligible enhancement of one other, we determined that these protons were *trans*. The ability to “walk the NOE chain” on one side of C-7, C-6 and C-10, down to the other side of C-10 to C-11 and then to C-12 fixed the relative stereochemistry of C-6, C-7, C-11 and C-12 and led to structure **88** for epipolasidamide. The strong ellipticity observed in the CD spectrum of **88** indicated that it was chiral and not a mixture of diastereomers (Appendix B). The absolute stereochemistry of epipolasidamide was not determined.

Molecular Modeling of Epipolasidamide

Initially, we were unable to explain the lack of scalar coupling between H-7 and H-12. Theoretically, the Karplus relationship indicates that protons that are orthogonal to one another will not be coupled (Figure 25).^{146,147} The particular form of the Karplus relationship used to generate this figure was developed by Abraham and McLauchlan.^{148,149} This model was chosen because it describes the behavior of carbon-bound protons in a relatively rigid system. Molecular modeling, dynamics and minimization were performed to determine if the minimum energy conformation of **88** was consistent with this arrangement of protons. The details of the computer modeling and dynamics run are included in the experimental section. In

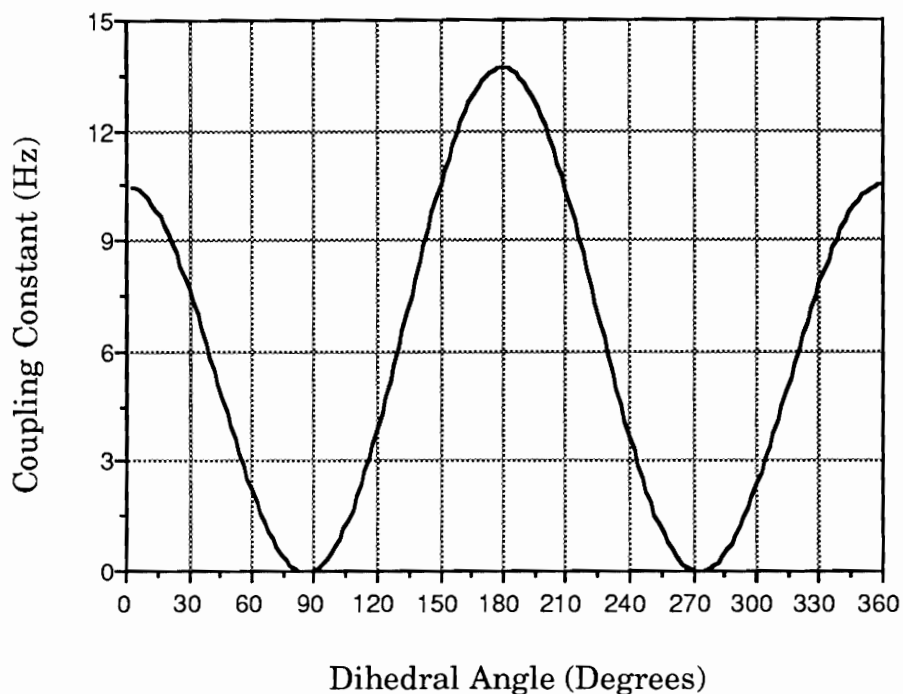


Figure 25. The Karplus relationship. This function illustrates the dependence of scalar coupling magnitude on the dihedral angle between two scalar coupled protons.

essence, the molecule was “heated” to a temperature of 1000 K, and then allowed to sample different conformations accessible at that temperature. The various conformations attained were then stored as individual data sets. Individual conformers that deviate significantly from the average conformation were chosen for minimization. A least-squares energy minimization algorithm was applied to these structures to find the local minima into which they fall. The overall free energy and conformation of these minimized structures can be compared to determine the conformation that most likely represents the global minimum energy state of the structure.

The results of this exercise are summarized in Figures 26-28. Animation of the 200 high temperature species showed relatively few major conformational changes. Ten of the most dissimilar high energy conformers of **88** were chosen for minimization. All converged to two distinct minimized species that differed by a negligible amount of free energy ($\Delta G_{\text{max}} = 0.012$ Kcal/Mol). The minimized structures are shown overlapped in Figure 26. The only appreciable conformational difference between the two nominally isoenergetic states arose from rotation of H-11 around the C-11/O-11 bond.

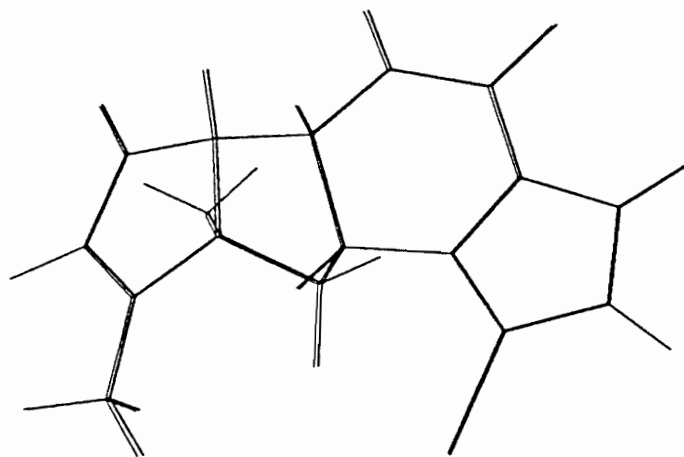


Figure 26. Minimized structures of epipolasidamide. Rotation of H-11 about the O-11/C-11 bond results in the two nominally isoenergetic conformers shown.

Molecule **88** appears to be relatively inflexible; this rigidity limits the range of motion available to its constituent atoms. The pyrrole “A” ring is nearly planar, as expected. A side view of **88** shows that the 6-membered “B” ring is roughly coplanar with the pyrrole moiety, and nearly orthogonal to the hydantoin “D” ring; the cyclopentyl “C” ring describes a diagonal plane intersecting the “B” and “D” rings. Protons H-7 and H-12 are in fact nearly orthogonal, as shown in Figure 27. The perspective along the C-7 to C-12 bond clearly shows the dihedral angle between these protons, which was calculated at -94.2 degrees. This could explain why no coupling was observed between these two protons.

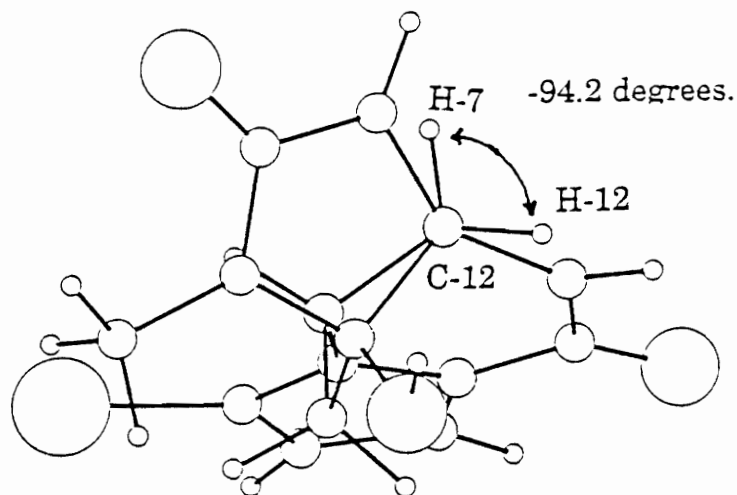


Figure 27. The dihedral angle between H-7 and H-12.
This perspective is along the C-12/C-7 bond.

The rigidity and relative stereochemistry of **88** confer some intriguing constraints on the spatial orientations of what appear to be adjacent protons. The minimized structures also contain distance information, some of which is shown in Figure 28. Interestingly, although H-7 appears to be closer to H-12 than to any other proton, it was found to be closer to H-15. Similarly, H-8 is closer to H-12 than to H-7. These modeling data are consistent with the NOE enhancements observed.

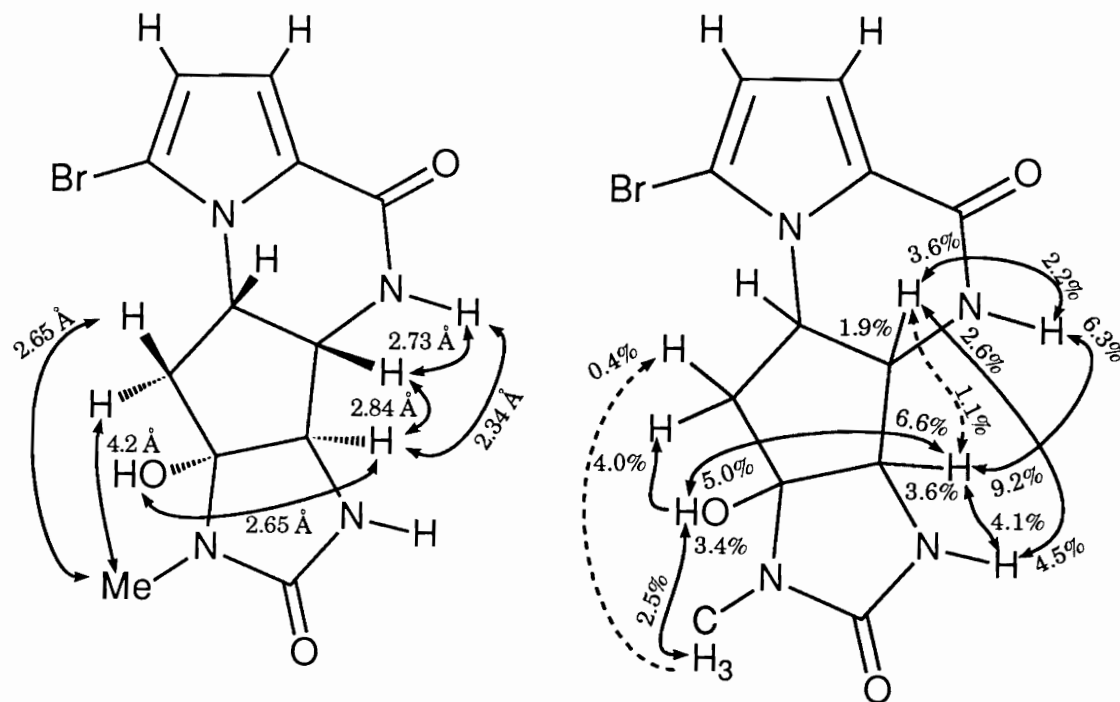


Figure 28. Comparison of calculated interproton distances and observed NOEs of epipolasidamide.

Biological Activity Of Epipolasidamide

Epipolasidamide was found to be cytotoxic towards HCT-116 cells in vitro, with an apparent IC_{50} of $0.1 \mu\text{g/mL}$. A dose-response curve of this test is shown in Figure 29. A striking feature of this graph is the very broad response to increasing concentrations of epipolasidamide. Generally, dose-response data of this type result in sigmoidal shaped curves, in which most or all of the cytotoxic effect of the drug develops within one order of magnitude or less (e.g., Figure 21, in which mavanuthaquinone demonstrates cytotoxicity towards the CEM cell line).

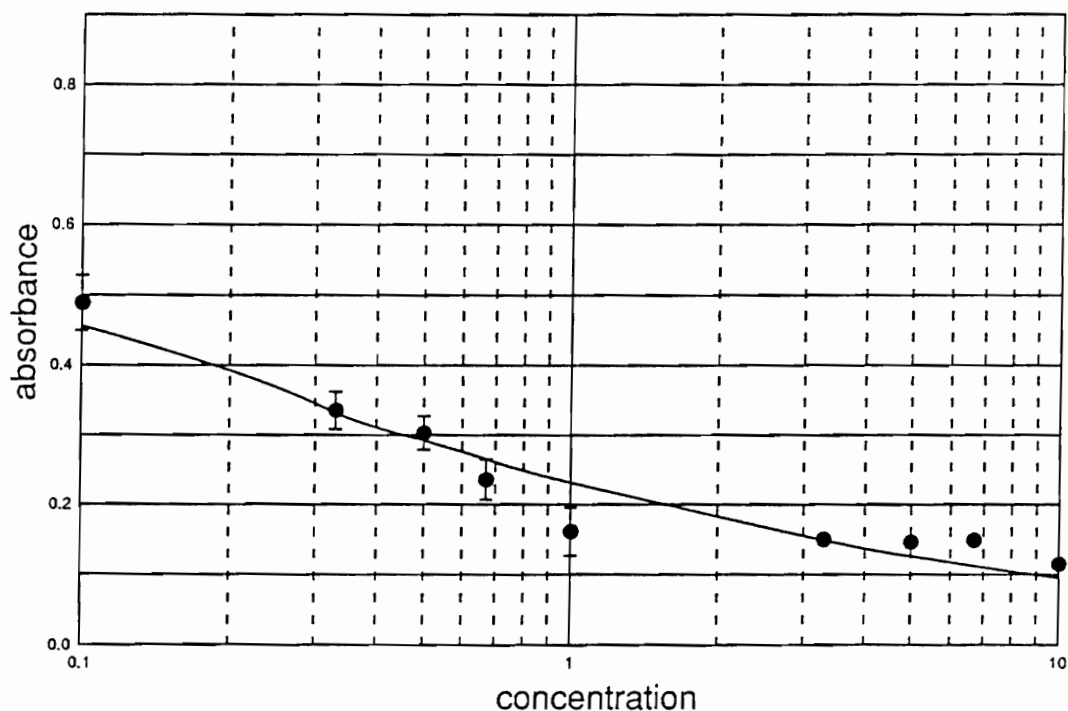


Figure 29. In vitro HCT-116 testing of epipolasidamide.

The dose-response effect of **88** appears to develop over 3 or more factors of 10; this result was repeated several times, indicating the phenomenon was not a chance occurrence. Through a personal communication with Dr. Ernest Hamel, several researchers within the Ireland group learned that broad dose-response curves of this type are often associated with compounds that inhibit the polymerization and/or depolymerization of tubulin. Unfortunately, a 200 μg sample of epipolasidamide was inactive in Dr. Hamel's tubulin inhibition assay at the National Cancer Institute. Epipolasidamide was not tested in any in vivo models.

IV. THE CHEMISTRY OF THE PHILIPPINO ASCIDIAN

EUSYNSTYELA MISAKIENSIS

Introduction

Ascidians (or tunicates) of the genus *Eusynstyela* are colonial sessile organisms belonging to the Family *Styelidae*. These invertebrates are infrequently encountered in reef habitats, unlike many of the related styelids; often they are hidden in caves, small in size, and are well camouflaged.¹⁵⁰ Styelids have been the subject of all but one report concerning ascidians of the order *Stolidobranchia*; the other two families within the order are clearly underrepresented. The *Pyuridae* and *Molgulidae* are difficult to collect, either due to their fragile nature or because many are abyssal.¹⁵⁰ The only non-Styelid tunicate of the Order *Stolidobranchia* investigated to date is the Okinawan ascidian *Pyura sacciformis*.¹¹⁵

Our interest in these tunicates began with the collection of a relatively abundant red and orange specimen of *Eusynstyela latericius* from Fijian waters in November 1987. Crude extracts of this organism exhibited mild cytotoxicity. The activity was traced to a labile sample, which our group was unable to characterize. The taxonomically related and organizationally similar Baja California tunicate *Polyandrocarpa* sp. yielded polyandrocarpidines A - D.^{128,129} A rust-colored Philippino species of *Polyandrocarpa* collected near Siquijor Island yielded polyandrocarpamides A - D (133 - 136).¹³¹ In March 1991, we collected relatively large quantities of the pale pink colonial Styelid ascidian *Eusynstyela misakiensis* at the Northern

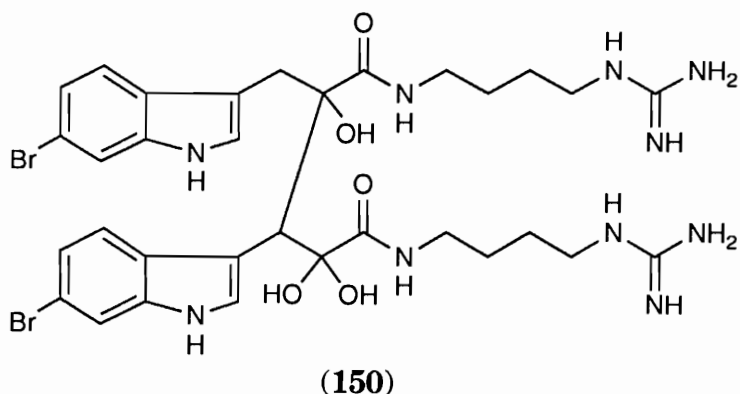
reef of Siquijor Island. Our decision to investigate this organism further was prompted by the mild *in vitro* cytotoxicity of its crude extract ($IC_{50} > 100 \mu\text{g/mL}$ vs. HCT-116) and by the presence of an unusually strong UV chromophore in the aqueous partition of the crude extract.

Tunicate Collection and Isolation of Eusynstyelamide

The pale pink leathery ascidian collected at Siquijor Island was frozen until worked up. During storage, the sample became a burnt orange-red color. The ascidian (56 g dry weight after extraction) was homogenized in methanol, extracted four times and filtered. The combined extracts were subjected to a solvent partitioning scheme with hexane, carbon tetrachloride, chloroform and ethyl acetate. The remaining aqueous partition was reduced to dryness *in vacuo* and triturated three times with cold methanol. The triturate was filtered through a plug of glass wool and reduced *in vacuo* to yield 1.3 g of a tan foam. This material was chromatographed on a reverse phase flash column eluting with 50% aqueous methanol to remove salts and highly polar species, followed by exhaustive washing with methanol to yield 135 mg of a glassy green solid. Further reverse phase flash column chromatography and repeated gel filtration chromatography using LH-20 media eluting with methanol yielded 50.8 mg eusynstyelamide (**150**) as a pale yellow oil.

Structure Determination of Eusynstyelamide

The low resolution FAB mass spectrum of eusynstyelamide (3-nitrobenzyl alcohol [NBA] matrix) exhibited an isotopic cluster of three peaks at m/z 787, 789 and 791 with relative intensities of 1:2:1, diagnostic of



a molecule containing two bromine atoms. Also observed was an intense fragmentation peak cluster at m/z 629, 631, 633 and a one bromine doublet at m/z 394, 396, which is half the mass of the molecular ion. The FAB mass spectrum of eusynstyelamide from a glycerol matrix also contained an isotopic cluster of two peaks at m/z 709, 711, diagnostic of the parent molecule containing one bromine atom following hydride exchange [$MH^+ - H_2O - Br + H$]. Reductive dehalogenation of aromatic moieties has been observed previously on many occasions, particularly with a glycerol matrix.^{71,151,152} This observation strengthens the placement of the bromine atoms on the aromatic indole moieties of eusynstyelamide.

A high resolution mass measurement of the molecular ion peak at m/z 787 established a formula of $C_{32}H_{41}^{79}Br_2N_{10}O_4$ (found $MH^+ - H_2O$ m/z 787.1661, Δ 1.8 mmu). The nominal molecular species with a mass of 786 must therefore have a formula of $C_{32}H_{40}^{79}Br_2N_{10}O_4$, which implies 17 degrees of unsaturation (DBE). HRFABMS of the monomer peak at m/z 394 established a formula of $C_{16}H_{21}^{79}BrN_5O_2$ (found $(M^+ - H_2O)/2 + H^+$ 394.0875, Δ 2.9 mmu). Finally, HRFABMS of the fragmentation peak at m/z 629 estab-

lished a formula of $C_{26}H_{27}^{79}Br_2N_6O_3$ (found $((M^+ - H_2O) - C_6H_{13}N_4O)$ 629.0531, Δ 2.4 mmu).

The complex IR spectrum of **150** contained a very broad strong band from 3500-3000 cm^{-1} indicative of exchangeable functionalities such as hydroxyl or guanidine protons and a complex series of ten peaks from 1700-1620 cm^{-1} , typical of the sp^2 carbon-heteroatom stretches observed for amide or guanidine functional groups.

A positive O.R.D. measurement and ellipticity observed in the CD spectrum of eusynstyelamide indicated that the compound was chiral. We were concerned that perhaps eusynstyelamide had resulted from acid or base-catalyzed condensation of two molecules of a dipeptide precursor, as shown in Figure 30. However, the conceivable precursor (**154**) is achiral, and any condensation of **154** and its achiral enol (**155**) would result in a racemic mixture. The optical activity of **150** belies its formation by such a simple mechanism, both in vivo and during isolation, and indicates that eusynstyelamide results from some discrete, as yet undetermined metabolic event within the organism.

All signals in the proton and carbon NMR spectra of **150** were fully assigned in both d_6 -dimethyl sulfoxide (DMSO) and d_4 -methanol (CD_3OD) (Appendix C). Complete carbon-proton connectivities were established by several HMQC experiments and, in some cases, with a combination of results from several other 2-D experiments; this information is summarized in Table III. The complex methylene proton signals at 1.38 ppm corresponding to H-13 and H-14 observed in DMSO are the only remaining ambiguities in these spectra. The dimeric nature of eusynstyelamide gave rise to many signals that were degenerate or nearly so, particularly in the

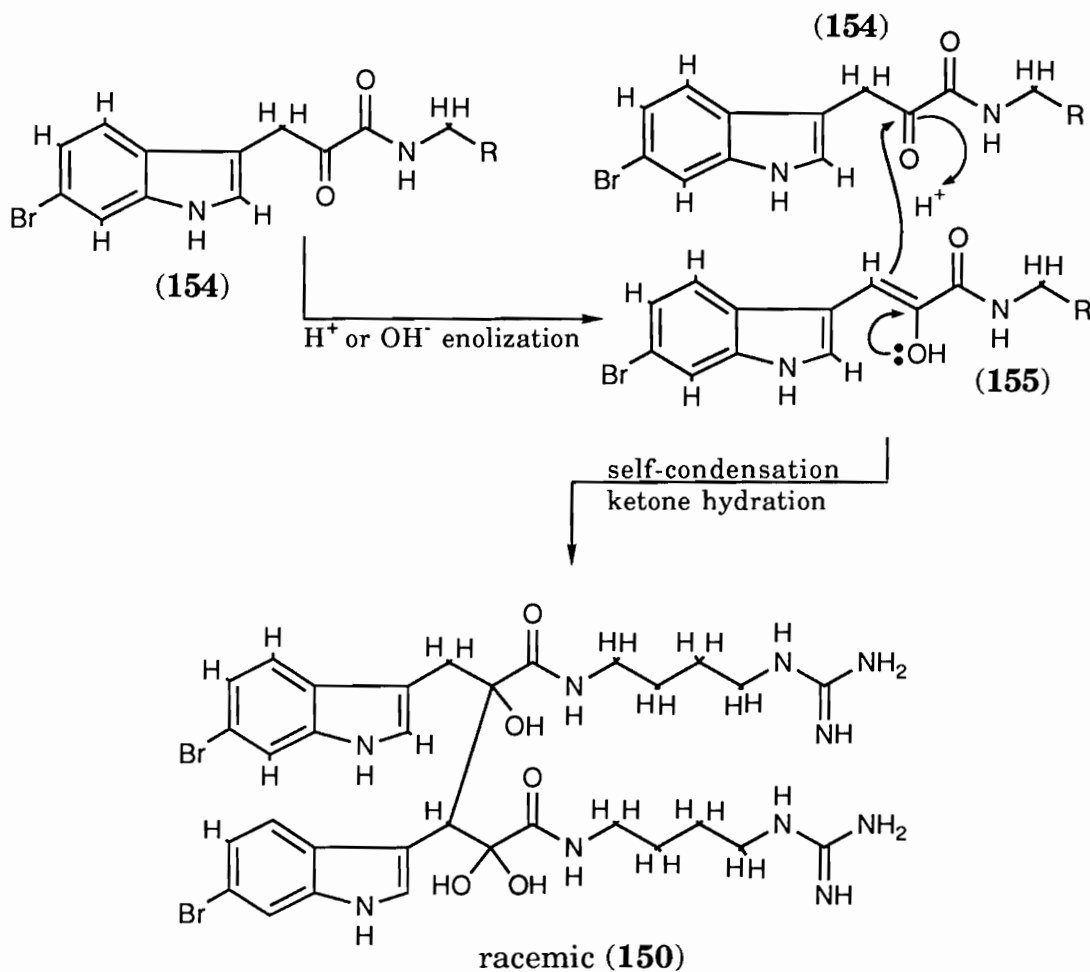


Figure 30. Theoretical formation of eusynstyelamide via self-condensation of an achiral precursor.

aliphatic regions. Spectra collected in DMSO allowed observation of correlations involving exchangeable proton signals, many of which were crucial to the structure determination of **150**. Unfortunately, the peaks in these spectra were broader due to the relatively high viscosity of DMSO, and the peaks were not very well dispersed. The spectra gathered in CD_3OD contained fewer degenerate signals, narrower lines, and better dispersion of signals, resulting in better resolution.

Table III
 ^1H and ^{13}C NMR Assignments of Eusynstyelamide

Position	d_6 -DMSO		CD_3OD	
	^{13}C : δ (mult) ^{a,b}	^1H : δ (mult, J) ^c	^{13}C : δ (mult) ^{b,d}	^1H : δ (mult, J) ^e
1		NH- 11.2 (br s)		
2	126.0 (d)	6.83 (br s)	127.1 (s)	6.92 (s)
3	108.3 (s)		110.5 (s)	
3a	126.9 (s)		128.3 (s)	
4	120.7 (d)	7.0 (d 8.5)	121.4 (d)	6.85 (d 8.5)
5	120.8 (d)	6.75 (dd 8.25, 1.75)	122.8 (d)	6.67 (dd 8.5, 2.75)
6	113.4 (s)		115.68 (s)	
7	113.6 (d)	7.47 (d 2.1)	114.82 (d)	7.43 (d 2.0)
7a	136.7 (s)		138.5 (s)	
8	28.5 (t)	2.65, 3.20 (d 14)	29.3 (t)	2.96, 3.44 (d 15)
9	78.9 (s)	OH- not observed	81.5 (s)	
10	174.1 (s)		177.2 (s)	
11		NH- not observed		
12	38.1 (t)	3.15, 3.12 (cm)	39.5 (t)	3.26, 3.27 (d 6.5)
13*	26.0 (t)	1.38 (m)	27.2 (t)	1.51 (m 6.5, 2)
14*	25.12 (t)	1.38 (cm)	26.41 (t)	1.50 (cm)
15	40.4 (t)	3.05 (cm)	42.04 (t)	3.15, 3.19 (cm)
16		NH- 7.89 (br s)		
17	157.0 (s)		158.6 (s)	
18		NH- 11.4 (br s)		
19	125.6 (d)	7.4 (br s)	126.8 (d)	7.61 (s)
20	105.4 (s)		107.0 (s)	
20a	127.9 (s)		129.2 (s)	
21	121.3 (d)	7.3 (d 9)	122.4 (d)	7.22 (d 9)
22	120.8	6.94 (dd 8, 1.5)	122.9 (d)	7.02 (dd 9, 1.75)
23	113.4 (s)		115.85 (s)	
24	113.6 (s)	7.56 (d 1.5)	114.86 (d)	7.57 (d 1.75)
24a	135.9 (s)		137.8 (s)	
25	47.4 (d)	3.59 (s)	49.85 (d)	3.58 (s)
26	91.9 (s)	OH- 7.14 (br s)	93.7 (s)	
27	171.6 (s)		173.5 (s)	
28		NH- 8.17 (dd 2,2)		
29	38.4 (t)	2.80, 2.95 (cm)	39.7 (t)	2.8, 3.1 (cm)
30	25.34 (t)	0.93, 1.10 (cm)	26.84 (t)	1.09, 1.12 (cm)
31	25.32 (t)	0.93, 1.11 (cm)	26.46 (t)	0.95, 0.97 (cm)
32	40.2 (t)	2.94 (cm)	41.95 (t)	2.89, 2.91 (t 7.5)
33		NH- 7.80 (br s)		
34	156.9 (s)		158.5 (s)	

Table III, continued

- ^a measured at 125 MHz; referenced to DMSO-*d*₆ (δ39.5).
^b multiplicity determined by DEPT experiment.
^c measured at 500 MHz; referenced to residual DMSO (δ2.49).
^d measured at 125 MHz; referenced to CD₃OD (δ49.0).
^e measured at 500 MHz; referenced to residual CHD₂OD (δ3.30).
* These assignments may be interchanged.
-

The proton spectrum of **150** recorded in DMSO displayed signals corresponding to exchangeable protons at 11.4 and 11.2 ppm. Also observed was a complex but adequately resolved aromatic and exchangeable proton region from 8.2 to 6.7 ppm. The aromatic region appeared to be superimposed on two large broad exchangeable peaks from 7.6-7.3 and 7.25-7.0 ppm, consistent with the chemical shift of guanidine imino and amino protons; these broad humps were not observed in the proton spectra taken in CD₃OD. Poorly dispersed signals corresponding to heterosubstituted aliphatic protons were observed in the regions from 3.6-2.5 and 1.4-0.9 ppm. As mentioned, these upfield regions showed much better resolution in CD₃OD. Consequently several of the key 1-D assignments and 2-D correlations involving signals of aliphatic protons (except for those which involve exchangeable protons) were analyzed in the CD₃OD spectra. Conspicuously absent from the proton spectra were signals corresponding to the α -protons of amino acids in the region from 5.0-6.0 ppm.

All but four of the signals in the ¹³C NMR spectra of eusynstyelamide occurred as pairs of signals, attributable to the molecule's dimeric nature. Those signals that were not paired correspond to carbons in the asymmetric regions of eusynstyelamide, i.e., the portion of the molecule in which one dipeptide subunit of **150** attaches to the other. Signals consistent with amide and guanidine functionalities were observed near 171 and 157 ppm, respectively. The sixteen signals corresponding to two aromatic indole systems were observed from 138 to 107 ppm. Four signals corresponding to nitrogen substituted methylene carbons were observed in pairs at 42 and 49 ppm, and four signals of aliphatic methylene carbons were clustered between 26 and 27 ppm. The four "unique" (unpaired) signals in

the carbon spectra were those for aryl methylene and methine carbons at 28.5 and 47.4 ppm respectively, and for two heterosubstituted quaternary sp^3 carbons at 78.9 and 91.9 ppm.

The most straightforward task in the structure elucidation of **150** was the complete assignment of the signals in the aromatic region of the spectrum. The simplest proton spin systems were those corresponding to the two 3,6 disubstituted indole systems, which were established by the results of COSY45 and DQCOSY experiments in DMSO and CD_3OD . These correlations are shown in Figure 31. An 8.5 Hz doublet at 6.84 ppm (H-4) is ortho coupled to a doublet of doublets ($J=8.5, 2.75$ Hz) at 6.66 ppm (H-5). H-5 displays meta coupling to a doublet at 7.42 ppm (H-7). These coupling constants and chemical shifts are typical of 6-bromoindole systems, and compare favorably with values reported for citorellamine (**122**), eudistomin G (**123**) and eudistomin K (**124**).^{116,118,119} H-2 appears as a sharp singlet at 6.83 ppm in the CD_3OD proton spectrum; a broad exchangeable signal at 11.2 ppm (H-1) was shown to couple to H-2, which was a broadened singlet at 6.92 ppm in the DMSO proton spectrum. The proton spin systems of the other indole heterocycle were established in the same way.

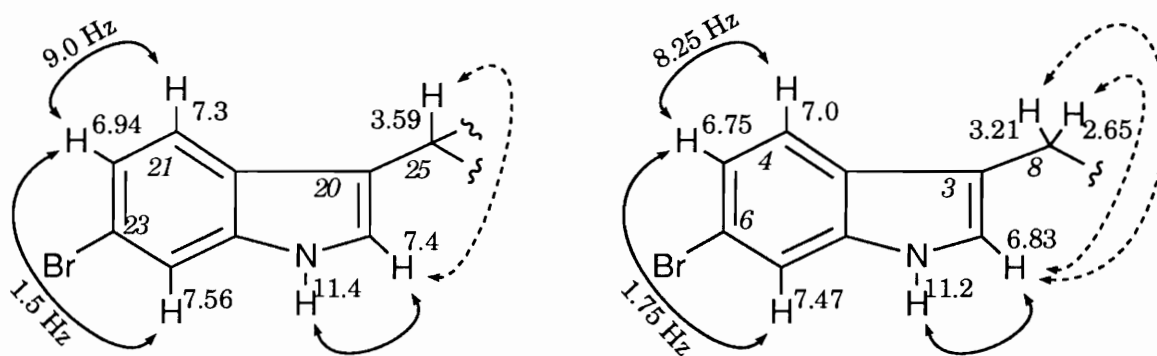


Figure 31. Indole proton spin systems of eusynstyelamide by COSY and COSY45.

Complete carbon assignments of the indole moieties were made by interpretation of DEPT, HMQC and HMBC experiments performed in both DMSO and CD₃OD. The significant HMBC correlations discussed are summarized in Figure 32. One of the two degenerate carbon signals at 113.6 ppm was established as the methine (C-7) which bears the 2.1 Hz doublet proton at 7.47 ppm (H-7) by HMQC. The carbons bearing H-4 and H-5 must be assigned C-4 and C-5 by virtue of the COSY data establishing the H-7 to H-5 to H-4 proton spin system. 3-Bond correlations observed in the HMBC spectra from quaternary carbon signals at 108.3 and 126.9 ppm to H-1 established these carbons as C-3 and C-3a; in 3-alkyl indoles, C-3 routinely gives rise to the furthest upfield signal, generally occurring between 105 and 109 ppm.¹¹⁶ Further correlations from the quaternary carbon signal at 136.7 and C-3 to H-4 allowed assignment of C-7a as this downfield carbon and strengthened the assignment of C-3. The indole ring was unequivocally established as 6-substituted by a combination of results including a correlation from C-7 at 113.6 ppm to H-1 and from C-3 to H-4. Two more HMBC correlations from C-7a to both H-4 and H-2 supported the assignment of C-7a. C-6 was assigned based on weak 2-bond correlations from the quaternary signal at 114.82 ppm to H-7 and H-5 and a very strong 3-bond correlation from 114.82 to H-4. The other indole encompassing C-18 through C-24a was assigned in an analogous fashion.

The substituents at the 3-position of both indoles were established by interpretation of HMBC and COSY45 data (Figure 32). Strong 3-bond HMBC correlations from the unique methylene carbon signal at 28.5 ppm to H-2 allowed assignment of C-8. HMQC established H-8 and H-8' as diastereotopic 15.0 Hz doublets at 3.44 and 2.96 ppm. HMBC correlations from C-2, C-3 and

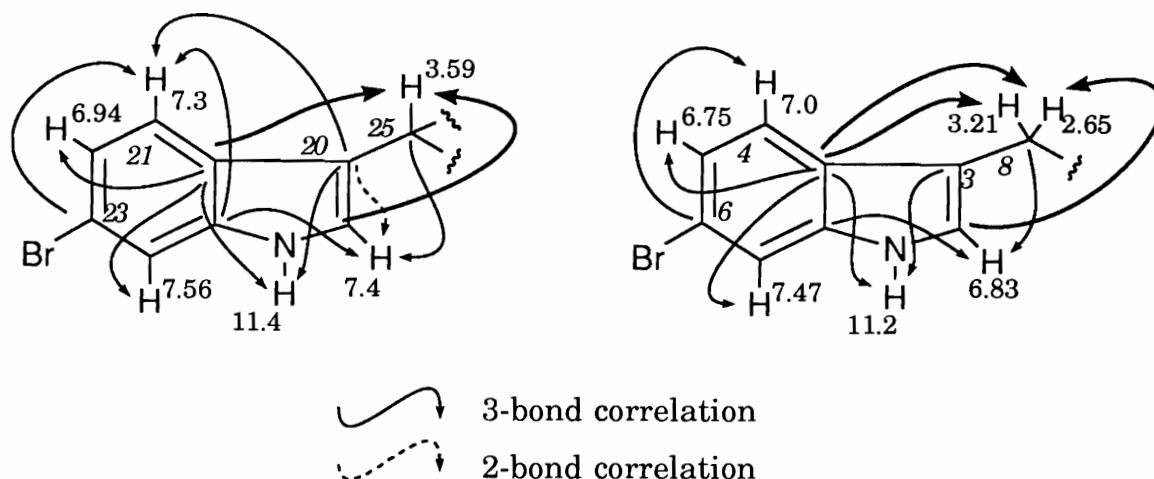


Figure 32. HMBC correlations observed for the indole moieties of eusynstyelamide.

C-3a to both H-8 and H-8' supported assignment of methylene C-8 as the 3-position substituent of the indole group. The substitution pattern of the other indole was determined in the same way. A strong 3-bond HMBC correlation from the unique methine carbon signal at 49.85 ppm to H-19 (7.4 ppm) established this methine as C-25. HMBC correlations from C-19, C-20 and C-20a to H-25 supported assignment of methine C-25 as the 3-position substituent of the second indole unit. Finally, allylic coupling observed in the CD₃OD COSY45 spectrum of eusynstyelamide between H-2 and both H-8 and H-8' and between H-19 and H-25, confirmed the identity of the 3-alkyl substituent of both indoles.

The next step of the structure elucidation of **150** was assignment of the aliphatic systems. The extreme polarity and immobility of eusynstyelamide on a variety of solid chromatographic supports, a positive Sakaguchi test for aliphatic guanidine groups, and relatively broad carbon signals at 157 ppm (3-5 Hz) all indicated that the aliphatic systems consisted

of guanidine nitrogen substituted methylene chains.^{153,154} Each system was found to be a decarboxylated arginine residue consisting of two nitrogen substituted methylenes and two aliphatic methylenes. The four aliphatic methylene carbons of eusynstyelamide gave rise to overlapped or nearly degenerate signals in the carbon spectra, extremely complex proton multiplets, and complicated spin systems in the 2-D COSY45 spectra. For instance, particular pairs of geminal methylene protons gave rise to signals that differed by as little as 0.01 ppm. Needless to say, in most cases visual inspection of splitting patterns for the purpose of determining the coupling relationships between these signals was useless.

Observations from several experiments were combined to resolve several ambiguities in the NMR data sets. We used HMBC, DQCOSY and COSY45 experiments during this process to help assign the aliphatic proton spin systems of eusynstyelamide. These correlations are summarized in Figure 33. One advantage of the COSY45 experiment is that the diagonal signal is minimized by a pulse sequence that selects against zero quantum coherence. The result of this is that geminal and 3-bond scalar coupling correlations between protons of very similar chemical shifts may sometimes be observed. For instance, the COSY45 spectrum of **150** in CD₃OD shows the 8 Hz geminal coupling between two proton signals at 3.19 and 3.15 ppm, which allowed us to infer that the coupled signals at 3.15 and 3.19 both correspond to the protons attached to C-15.

The DQCOSY spectrum of **150** (Appendix C) displayed correlations between a broad exchangeable singlet at 7.80 ppm (H-33) and methylene protons at 2.94 ppm (H-32) and between a sharp exchangeable triplet at 8.17 ppm (H-28) to two methylene signals (H-29) at 2.80 and 2.95 ppm. These two

sets of methylene protons were assigned to carbons at 40.2 ppm (C-32) and 38.4 ppm (C-29) by virtue of correlations observed in the HMQC spectrum; these chemical shifts are indicative of substitution with nitrogen. An HMBC correlation from the broad guanidine carbon signal at 156.9 to H-33 established this quaternary center as C-34. Finally, 2- and 3-bond HMBC correlations from the carbonyl signal at 171.6 ppm to H-28 and both H-29 protons established C-27 as an amide. Correlations observed in the COSY45 spectrum incorporate H-30 and H-31 into spin systems with each other and with H-29 or H-32, respectively. The detailed knowledge of this proton environment afforded by the COSY45 data removed ambiguities in the assignment of H-30 and H-31 to their respective carbons in the HMQC experiment. Furthermore, all expected HMBC correlations were observed for this entire chain of four methylene groups and the accompanying exchangeable protons H-33 and H-28.

Analogous correlations observed in these spectra in DMSO enabled us to assign the signals corresponding to the other aliphatic system consisting of C-10, C-12 and H-12, C-15 and H-15, H-16, and C-17. The amide

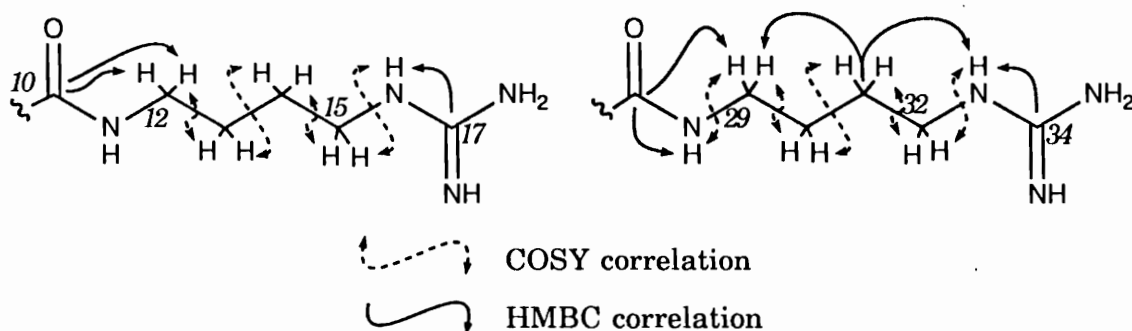


Figure 33. The decarboxylated arginine moieties of eusynstyelamide.

proton H-11 was not observed. Fortunately, unambiguous HMQC correlations permitted assignment of both protons H-12 to C-12. Strong 3-bond correlations in the HMBC experiment from the carbonyl at 174.1 to both methylenes H-12 allowed assignment of C-10 as an amide carbonyl. The chemical shifts of C-10, C-12 and H-12, and the parallel construction of the other decarboxylated arginine in **150** allowed us to infer amide N-11 was positioned as shown (Figure 33).

The remaining aliphatic methylene carbons C-13 and C-14 were indistinguishable. HMBC correlations from C-13 and C-14 to both H-12 and H-15 confirmed that they were indeed part of this aliphatic chain. The protons borne by C-13 and C-14, however, are almost fully degenerate in both solvents. COSY data strengthened the inclusion of H-13 and H-14 into the spin system, but were not helpful in determining unequivocally the identities of either of these methylene groups.

The final task in the structure elucidation of eusynstyelamide was to arrange C-8, C-9, C-25 and C-26 in such a way that the mass spectral data and chemical shifts of these carbons were satisfied. This turned out to be the most puzzling aspect of this project, because the mass spectral data and NMR data initially led to divergent conclusions regarding the structure of **150**.

The carbon atoms near the site of dimerization were relatively straightforward to assign. The connectivities observed in HMBC experiments are indicated in Figure 34. In particular, strong 3-bond correlations observed in the CD₃OD HMBC spectrum from amide C-10 and methylene C-8 to H-25 and a weaker 2-bond correlation from the quaternary signal at 81.5 ppm (C-9) allowed assignment of C-9 and C-25 as the linkage points of

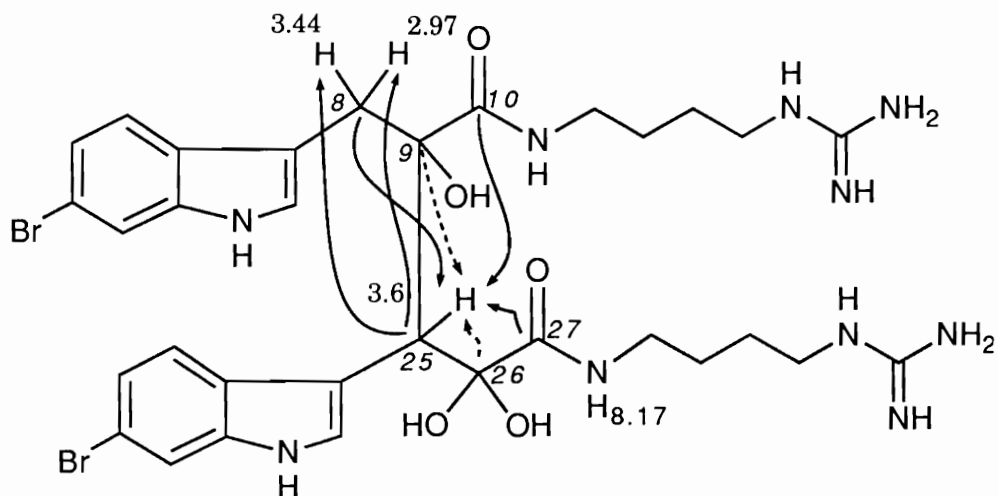


Figure 34. HMBC correlations relating the two dipeptide halves of eusynstyelamide.

the dimer halves of **150**. The chemical shift of C-9 indicates that it is hydroxylated. Further 2- and 3-bond correlations to H-25 from C-27 and C-26 and to both methylenes H-8 from C-25 strengthen this arrangement considerably. C-26 is the only other possible site of attachment to the other half of the molecule according to HMBC data; if this were the case, atom pairs C-10 & H-25 and C-25 & H-8 would be related by four bonds, and we would not expect to see the strong correlations that were observed.

The hybridization and functionalization of C-26 were very unclear at this point. The molecular formula derived from mass spectral data indicated the presence of 17 degrees of unsaturation. The two indole moieties each incorporate six DBE, and each amide and guanidine group incorporates another, for a total of 16 DBE. Only one oxygen atom and one DBE remained unaccounted for in the molecular formula of the ionized species.

The obvious conclusion from these data was that C-26 was a ketone and that C-26 and C-27 comprise an α -keto amide. Such a functionality is found in several recently described compounds, including polyandrocarpamides A - C (**133** - **135**), isolated from the taxonomically and geographically similar Philippino tunicate *Polyandrocarpa* sp. and several recently isolated cyclic peptides from sponges, including cyclotheonamide A (**66**), orbiculamide A (**68**) and keramamides B - D (**69** - **71**).^{58-60,131} The presence of the α -keto amide functional group in the polyandrocarpamides provided a chemotaxonomic precedent within this family of organisms; for these reasons, it was postulated that eusynstyelamide might incorporate this functional group.

The chemical shifts of both C-26 and C-27, however, were grossly inconsistent with this assignment. The polyandrocarpamides and most of the Theonella-derived cyclic peptides share similar chemical shifts for the α -keto amide moiety, in which the amide appears around 161 ppm and the ketone appears around 196 ppm. The salient feature of this group of compounds was the solvent labile nature of the α -keto amide of **66** (Figure 35).

In the hygroscopic solvent DMSO, the α -keto amide group in **66** behaved like those in **133** - **135** and peptides **68** - **71**. When the NMR spectra of **66** were collected in D₂O, the ketone group was hydrated as a geminal diol. The ketone hydrate gave rise to NMR signals at 97.4 and 174.7 ppm. These values are typical of an sp³ hybridized quaternary carbon substituted with two heteroatoms and an amide carbon, respectively. In fact, these values also agree closely with the chemical shifts observed for C-26 and C-29 in eusynstyelamide. Finally, HMBC correlations indicative of coupling between the exchangeable proton signal at δ 7.14 (-OH 26) and C-27 provided

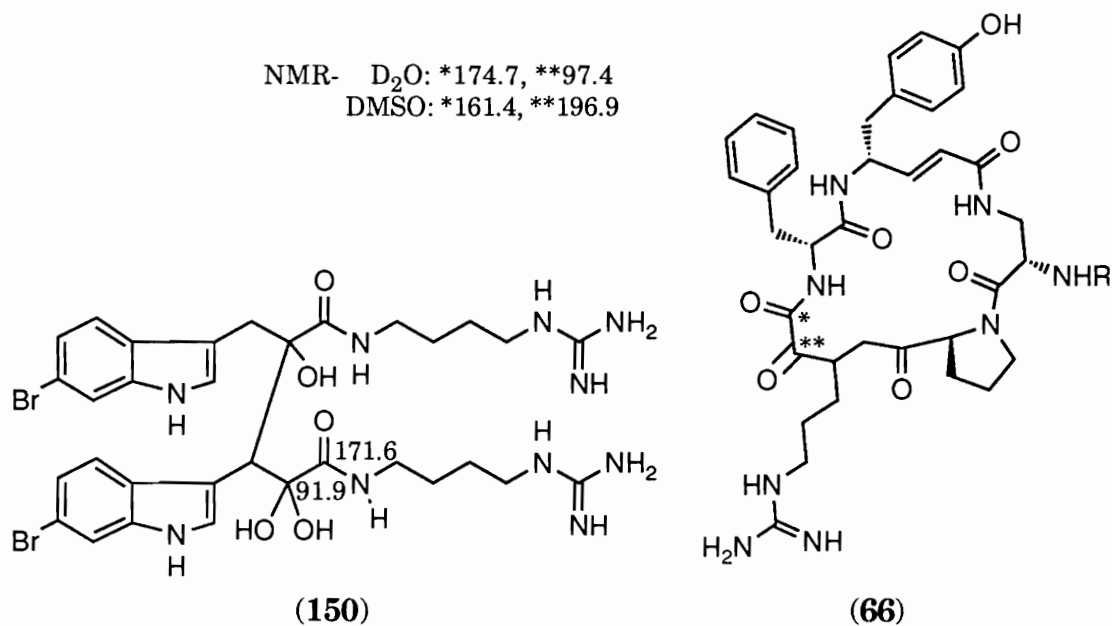


Figure 35. Comparison of α -keto amides and ketone hydrates in eusynstyelamide and cyclotheonamide A.

compelling evidence that C-26 was not a ketone. Therefore, the structure of **150** in solution incorporates an α -keto amide hydrate.

The ionization and fragmentation scheme shown in Figure 36 was proposed to account for the major peaks observed in the FAB spectra of eusynstyelamide. Dehydration of the geminal diol to the α -keto amide (**156**) appears to be a requisite event preceding or during the ionization of eusynstyelamide.

Compound **156** has a molecular mass of 786 a.m.u. and can be protonated, undergo halogen-hydride exchange, and fragment by loss of one arginine groups or into monomers of identical mass and formula, as shown. The labile nature of ketone hydrate **150** during ionization precluded

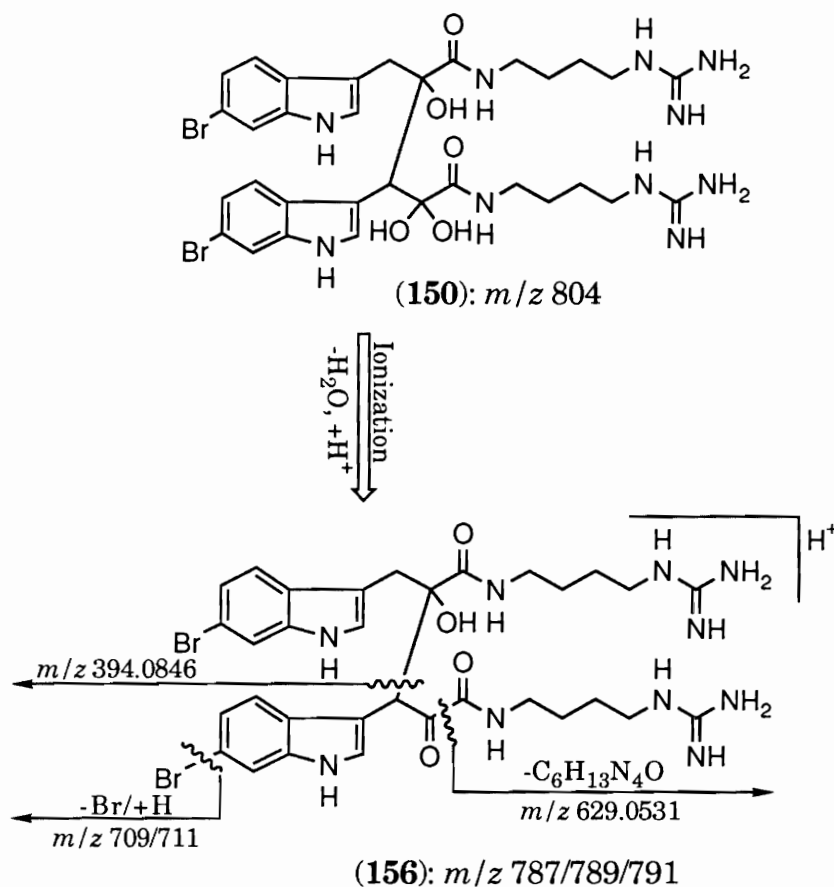


Figure 36. Mass spectral fragmentation pathways of eusynstyelamide.

precluded observation of an ion peak pattern at m/z 805/807/809 using a variety of mass spectral ionization methods, including FAB from 3-NBA and glycerol matrices and electrospray ionization with several solvent mixtures and pH conditions.

Other Experiments with Eusynstyelamide

Increasing the volatility of **150** could conceivably increase its ionization potential enough to allow observation of the ketone hydrate in mass spectroscopy experiments. To this end, conversion of the guanidine groups

to 4,6-dimethylpyrimidines with 2,4-pentanedione was attempted under a variety of base and acid-catalyzed conditions.¹⁵⁵ Isolation of the blocked compound was never accomplished, and in some cases the starting material was not recovered.

In an effort to confirm the hybridization of C-32 by chemical means and to increase the likelihood of crystallizing **150**, we attempted to convert the sp^3 ketone hydrate to a tosylhydrazone. A methanol solution of eusynstyelamide was stirred with 5-10 equivalents of *p*-toluene sulfonylhydrazide and catalytic amounts of either a mineral acid, such as hydrochloric acid, or a Lewis acid, such as boron trifluoride etherate. All attempts to form or isolate the resultant tosyl hydrazone failed.

Several different schemes for crystallizing eusynstyelamide were tried over a period of 6 months in an effort to obtain a sample suitable for x-ray crystallography. None of these was successful, although a saturated methanol solution of **150** infused with benzene vapor for 6 to 8 weeks provided twinned pyramidal cones.

Biological Activity of Eusynstyelamide

Eusynstyelamide exhibited almost no antimicrobial activity, and had extremely low cytotoxicity against HCT-116 cells, with an IC_{50} between 50 and 100 $\mu\text{g/mL}$ in vitro. Pure **150** was found to be remarkably inactive in all other assays available to us.

V. EXPERIMENTAL

General Experimental Procedures

Reagent and spectrophotometric grade solvents were all freshly distilled before use. Chemical reagents were used directly from the supplier.

NMR spectra were recorded on IBM AF 200 or Varian Unity 500 nuclear magnetic resonance spectrometers, operating at 200 MHz and 500 MHz respectively for ^1H . Chemical shifts are reported on the δ -scale and are referenced to residual protonated solvent.

Ultraviolet spectra were recorded on a Beckman DU-8 spectrophotometer in 10 mm cells with either chloroform or methanol as sample and reference solvents. Optical rotary dispersion was measured in a 50 mm cell with a Jasco DIP-370 polarimeter, set at an appropriate wavelength. Colored compounds were measured with integration times of up to one minute. Infrared spectra were recorded on a Perkin Elmer 1600 Fourier transform spectrophotometer calibrated with a polystyrene reference at 1601 cm^{-1} , as neat films deposited on sodium chloride plates. CD spectra were recorded on a Jasco J40-A automatic recording spectropolarimeter, using 10 mm UV cells. Samples were adjusted to less than 1.0 absorbance units at maximum absorbance in the UV spectrum and then directly measured for CD effect.

Low and high resolution fast atom bombardment mass spectra were obtained at either the Department of Medicinal Chemistry or Department of

Chemistry mass spectrometry service facilities at the University of Utah. Mass measurements made in the Department of Medicinal Chemistry were performed on a Varian MAT-731 equipped with an Ion Tech atom gun. Mass measurements made in the Department of Chemistry were performed on a Finnigan MAT 95 High Resolution mass spectrometer equipped with the Finnigan MAT ICIS II operating system. Samples were dissolved in either glycerol or 3-nitrobenzyl alcohol liquid matrices.

HPLC separations were performed using a Waters/Millipore system equipped with a model 501 solvent pump, U6K sample injector and R401 differential refractometer detector. All solvents were filtered and degassed through 0.45 μm nylon filters under aspirator vacuum. Dynamax analytical and preparative columns with in-line guard cartridges were purchased from Rainin Instrument Co., Emeryville, CA.

Preparative LH-20 and reverse phase column chromatography was monitored either by inspection of visible colored fractions, or by monitoring column eluate with an ISCO V⁴ absorbance detector set at 310 nm. Bakerbond octadecasilyl (C₁₈) and amino (NH₂) bonded phase flash column media were purchased from VWR Scientific, Salt Lake City, Utah.

The Chemistry of *Fasciospongia* sp.

Collection and Identification of the Sponge

The yellow, brown and purple mossy sponge was collected by SCUBA from -5 to -15m near Mamanutha Island in the Fijian archipelago in November 1986. The animals were immediately frozen and remained so until investigated in the lab in October 1990. The sponge was identified as

Fasciospongia sp. by Ms. Mary Kay Harper, Scripps Institute of Oceanography, La Jolla, CA.

Isolation of Mamanuthaquinone

The frozen sponge sample (18 g dry weight) was pulverized and extracted with methanol (4 x 300 mL). The deep purple extract was filtered and dried in vacuo to give 1.4 grams of dark brown oil. A small portion of this oil was taken in aqueous methanol and subjected to a standard solvent partition scheme, resulting in hexane, carbon tetrachloride, chloroform and aqueous extracts. Thin layer chromatography (silica gel stationary phase; 40% ethyl acetate/60% hexane mobile phase) showed all four partitions contained the same major component (orange when wetted with solvent system, purple when dry on plate, strongly UV active). Approximately 600 mg of the crude oil was subjected to silica flash column chromatography with 39.5% ethyl acetate/60% hexane/0.5% acetic acid to yield 253 mg of an orange oil. This oil was further purified by either HPLC (Dynamax Si, same solvent system as the flash column) or LH-20 column chromatography eluting with methanol to give 243 mg of mamanuthaquinone (**50**) as an orange oil.

Mamanuthaquinone (50). Orange oil, 4.0% yield from dry weight; $[\alpha]_{546} -31^\circ$ (CHCl₃, c 0.058); IR (neat) ν_{\max} 3337, 2930, 1647, 1607, 1456, 1381, 1350, 1314, 1234, 1212, 1036 cm⁻¹; UV (CHCl₃) λ_{\max} 430 nm (ϵ 620) and 298 nm (ϵ 1435); FABMS (glycerol) m/z 359 (MH⁺), 358 (M⁺), 191 (M⁺ - C₈H₇O₄); HRFABMS (glycerol) found m/z 359.2223 (MH⁺) (C₂₂H₃₁O₄; Δ 0.1 mmu), m/z 358.2146 (M⁺) (C₂₂H₃₀O₄; Δ 0.2 mmu); ¹H and ¹³C NMR (see Table I and Appendix A).

Rearrangement of Mamanuthaquinone and Ilimaquinone

An authentic sample of ilimaquinone (**32**) was kindly provided by Dr. Brent Copp, who isolated **32** during his postdoctoral tenure in our lab. Twenty mg (0.056 mMol) of mamanuthaquinone (**50**) were placed in a 20 mL scintillation vial, and the solvent removed in vacuo. A magnetic stir bar was added, and the quinone dissolved with stirring in 7 ml benzene (freshly distilled over LAH), under N₂ at 10 °C. Five to ten drops boron trifluoride etherate solution were delivered via syringe over 30 seconds, whereupon the solution changed from orange to burgundy. After 30 minutes, the mixture was taken up in 20 ml hexane, washed (3X5 mL) with water, dried over MgSO₄, filtered, and the solvents removed in vacuo to yield a yellow-orange powdery precipitate. HPLC purification (Dynamax Si column, same acidified solvent system as **50** above) yielded 5.0-6.5 mg of the rearranged quinone sesquiterpenoid (**151_m**). Identical reaction conditions with 20 mg of **32** led to similar yields of the same rearranged quinone sesquiterpenoid (**151_i**).

Rearranged quinone sesquiterpenoids. Yellow powder; FABMS (glycerol) *m/z* 359 (MH⁺), 358 (M⁺); Typical color change from orange to purple upon basification; Optical rotary dispersion- **151_m**: $[\alpha]_{546} +28.3^\circ$ (c 0.092, CHCl₃), **151_i**: $[\alpha]_{546} +31.5^\circ$ (c 0.108, CHCl₃); UV (CHCl₃) λ_{\max} 430 nm (ϵ 620); CD curves (CHCl₃) of both rearrangement products exhibited $\Delta\epsilon_{\max}$ 347 nm, $\Delta\epsilon_{\min}$ 400 nm, and nodes ($\Delta\epsilon=0$) at 374 nm, and were nearly identical in amplitude; ¹H NMR (500 MHz, CDCl₃) δ 0.75 (d, J=7 Hz, 3H), 0.80 (s, 3H), 0.93 (s, 3H), 0.97 (s, 3H), 1.3-1.6 (m), 1.8-2.2 (m), 2.56 (d, J=13.2 Hz, 1H), 2.68 (d, J=13.2 Hz, 1H), 3.84 (s, 3H), 5.83 (s, 1H), 7.3 (s, 1H); ¹³C NMR (125 MHz,

CDCl₃) δ 15.4, 19.9, 20.7, 21.9, 25.8, 26.5, 27.9, 28.9, 32.2, 34.3, 34.5, 39.9, 42.7, 56.8, 102.1, 117.9, 131.4, 134.9, 152.8, 161.4, 182.3, 182.6.

The Chemistry of an Unidentified Fijian Sponge of Mixed

Axinellidae and *Jaspidae* Taxonomy

Collection and Identification of the Sponge

The unidentified crunchy tan mottled orange encrusting sponge was collected by SCUBA from -7 to -10m near Mbenga Island in the Fijian archipelago in November 1986 and recollected in November 1987, January 1990, and January 1992. The animals were immediately frozen and kept this way until investigated. A sample of the sponge was sent to Dr. Avril Ayling, Queensland, Australia. Dr. Ayling placed the sponge in the Order *Epipolasida*, which has been considered a “problematic group” for some time by systematists. This Order has characteristics similar to the *Axinellidae* and is currently being reworked. Spicules of the sponge were further examined by Mary Kay Harper at Scripps Institute of Oceanography, La Jolla, California. She has determined that the spicules have characteristics of both *Jaspidae* and *Axinellidae* Families, as well as unidentified morphological traits. Descriptions of this organism prepared by Dr. Patricia Bergquist have appeared in the literature associated with the bengamides.⁶⁹ Because this specimen contains organizational and chemotaxonomic traits typical of both Axinellid and Jaspid sponges, we believe this specimen represents an epizoid association of two separate species, and that one or both of them may be undescribed at this point.

Isolation of Epipolasidamide

The frozen sponge was lyophilized or worked up frozen (45 g dry weight), homogenized with 100 mL MeOH, and extracted exhaustively with MeOH. The combined extracts were filtered, reduced in vacuo, and the resulting dark brown salty oil was taken in 250 mL 20% aqueous MeOH. This solution was subjected to a solvent partitioning scheme as follows: extraction with hexanes (4 X 75 mL), extraction with carbon tetrachloride (7 X 50 mL), addition of 75 mL water followed by extraction with chloroform (6 X 75 mL), addition of 75 mL water followed by extraction with ethyl acetate (5 X 100 mL). Solvents were removed, and the partitions were submitted for testing against HCT-116 cells. The highest activity was pooled in the carbon tetrachloride partition, which was found to contain bengamide A and several related compounds that were not characterized. Slightly lower activity was found in the chloroform and ethyl acetate fractions, which were pooled and reduced in vacuo. The brown residue was applied to a flash column containing 8 g of slurry packed amino bonded-phase medium. The column was eluted at 2-3 mL/min with a mobile phase of 73% ethyl acetate/25% methanol/2% triethylamine. Less polar fractions contained small amounts of **80**. Fractions containing **88**, as determined by silica gel TLC (80% chloroform/20% methanol mobile phase) were pooled, and the solvents were removed in vacuo to give a pale green glassy solid.

An alternative separation protocol in which the chloroform/ethyl acetate derived brown oil was applied to a reverse phase flash column and eluted with a step gradient from 50% aqueous methanol to methanol yielded a related compound in crude form which appeared to be the demethyl ana-

log of **88** by 1-D proton NMR. This labile compound decomposed before we were able to characterize it.

The green glassy solid containing **88** was further purified by HPLC (Dynamax NH2 column, same solvent system as the amino flash column above), yielding epipolasidamide (**88**) as a colorless glassy solid (21 mg).

Epipolasidamide (**88**). Colorless glassy solid, 0.047% yield of dry weight; $[\alpha]_{405} -111.1^\circ$ (Methanol, c 0.054); IR (neat) ν_{\max} 3210, 1670, 1643, 1553, 1486, 1422, 1378, 1276, 1196 and 1034 cm^{-1} ; UV (methanol) λ_{\max} 277.2 nm (ϵ 12,360), 228.0 nm (ϵ 9504), and 206.4 nm (ϵ 9485); CD (methanol) $\Delta\epsilon_{\max}$ 245 nm, $\Delta\epsilon_{\min}$ 218 nm, node($\Delta\epsilon=0$) 230 nm; FABMS (glycerol) m/z 341 (MH^+), 343 ($(\text{M}+2)\text{H}^+$); FABMS (glycerol, negative ion detection mode) m/z 339 ($(\text{M}-\text{H})^-$), 341 ($(\text{M}+2-\text{H})^-$), 260 ($(\text{M}-\text{Br})^-$); HRFABMS (glycerol) found m/z 341.0246 (MH^+) ($\text{C}_{12}\text{H}_{14}\text{N}_4\text{O}_3\text{Br}$; Δ .35 mmu); ^1H and ^{13}C NMR (see Table II and Appendix B).

Molecular Modeling, Dynamics and Minimization of Epipolasidamide

Molecular dynamics calculations were performed on a Silicon Graphics Iris 4D-25 workstation equipped with the QUANTA/CHARMm software package. All energy terms were calculated. Molecular dynamics calculations were run at 1000 K and involved 1000 steps of heating (1 ps), 1000 steps of equilibration (1 ps), and 10 ps of simulation during which 200 data sets were stored.

Energy minimization calculations utilized an adopted basis Newton-Raphson algorithm, followed by conjugate gradient minimization. The dielectric constant was set to 45 to simulate solvation in DMSO. The simulation data sets were inspected to find the most conformationally divergent

forms of **88**. Four of these were minimized into two distinct local minima. Data sets 2050 and 6650 converged to a conformer in which the hydroxyl proton H-11 eclipses the cyclopentyl "C" ring of **88**. Data sets 11,350 and 12,000 converged to a conformer in which H-11 eclipses the hydantoin "D" ring of **88**. These two conformers differed in free energy by 0.014 Kcal/Mol, a negligible energy barrier on the NMR time scale. The dihedral angle described by H7-C7-C12-H12 was nearly identical in both conformers, -94.2 and -94.6 degrees respectively.

The Chemistry of *Eusynstyela misakiensis*

Collection and Identification of the Tunicate

The pink, rusty-colored colonial tunicate *Eusynstyela misakiensis* was collected from depth of -10 to -20m on reefs off the Northern shore of Siquijor Island, near Negros of the Philippines archipelago in April 1991. The animals were immediately frozen and remained so until used. A voucher of this organism was collected in April 1992, relaxed with menthol in sea water for a short time, and preserved in 10% formalin in sea water. The tunicate voucher was identified by Dr. Francoise Monniot, Laboratoire de Biologie des Invertébrés Marins et Malacologie, Paris, France. The organism *Eusynstyela misakiensis* described in the literature appears almost identical in color and organization to the Philippino sample of the tunicate *Eusynstyela misakiensis* studied in our lab.¹⁵⁰

Isolation of Eusynstyelamide

Frozen animals (56 g dry wt. after extraction) were homogenized in a blender with 300 mL methanol and soaked overnight. The homogenate was further extracted with MeOH (3 X 300 mL) and the combined extracts were

filtered and reduced in vacuo to give an orange-brown residue. This residue was taken in 40% aqueous methanol and extracted exhaustively with hexane (100, 70, 50 and 50 mL), carbon tetrachloride (60, 60, and 40 mL), chloroform (100, 70 and 60 mL) and ethyl acetate (3 x 75 mL). The aqueous partition was reduced in vacuo to give a brown salty residue. This residue was triturated with cold methanol (2 x 30 mL), yielding upon reduction 1.3 g tan foam. This material was subjected to flash column chromatography with Bakerbond C18 bonded phase media as the stationary phase. The column was eluted first with 50% aqueous methanol to remove the salts and 935 mg of tan foam and then exhaustively with methanol to yield 86 mg of a dark green glassy solid. TLC of this material proved impossible on all types of plates, including reversed phase. The highly polar metabolite **150** remained at the origin; acidification of the mobile phase produced only slight mobility. A positive Sakaguchi test of the extremely strong UV chromophore indicated the compound contained guanidine groups.¹⁵⁴ Acidified gradient reverse phase separation was ruled out when it was found that **150** decomposed with prolonged contact with highly acidic media. Flash column chromatography of this material was performed twice on Bakerbond octadecyl bonded phase media with a stepwise gradient of 40% aqueous methanol to 100% methanol. The fraction that eluted at 25% aqueous methanol gave 89.5 mg of brown **150** containing material. Pure **150** was separated from a more lipophilic material and a closely related compound by gel-permeation chromatography on an LH-20 column eluted with 0.1% TEA in methanol. Column eluate was monitored by UV detection. **150** containing fractions were pooled and reapplied twice to another LH-20 column

eluted with 0.2% TFA in methanol, yielding eusynstyelamide (**150**) as a pale brown oil (50.8 mg).

Eusynstyelamide A (**150**). Pale brown oil, 0.091% yield of dry weight; $[\alpha]_{405} +125.6^\circ$ (methanol, c 0.226); IR (neat) ν_{\max} 3500-3000, 2946, 1694, 1682, 1674, 1668, 1660, 1652, 1645, 1634, 1622, 1615, 1574, 1558, 1538, 1456, 1417, 1337, 1173, 1109, 1048, 1024, 1004 and 896 cm^{-1} ; UV (methanol) λ_{\max} 206 nm (ϵ 50,893), 224 nm (ϵ 69,417), 285 nm (ϵ 12,357); CD (methanol) $\Delta\epsilon_{\min}$ 231 nm, $\Delta\epsilon=0$ (node) 224 nm, $\Delta\epsilon_{\max}$ 215 nm; FABMS (3-nitrobenzyl alcohol) m/z 787/789/791 ($\text{MH}^+ - \text{H}_2\text{O}$, 22.2/38.8/20.1% of base peak height), m/z 629/631/633 ($(\text{MH}^+ - \text{H}_2\text{O}) - \text{C}_6\text{H}_{13}\text{N}_4\text{O}$, 19.5/39.3/19.5% of base peak height), m/z 394/396 ($(\text{MH}^+ - \text{H}_2\text{O})/2 + \text{H}$, 66.7/65.3% of base peak height); FABMS (glycerol) m/z 787/789/791 ($\text{MH}^+ - \text{H}_2\text{O}$, 1.5/3/1.5% of base peak height), m/z 709/711 ($(\text{MH}^+ - \text{H}_2\text{O}) - \text{Br} + \text{H}$, 1.1/1.1% of base peak height), m/z 629/631/633 ($(\text{MH}^+ - \text{H}_2\text{O}) - \text{C}_6\text{H}_{13}\text{N}_4\text{O}$, 1/2/1% of base peak height), m/z 551/553 ($(\text{MH}^+ - \text{H}_2\text{O}) - \text{C}_6\text{H}_{13}\text{N}_4\text{O} - \text{Br} + \text{H}$, 1/1% of base peak height), m/z 394/396 ($(\text{MH}^+ - \text{H}_2\text{O})/2 + \text{H}$, 5/5% of base peak height); HRFABMS (3-nitrobenzyl alcohol) m/z 787.1661 ($\text{MH}^+ - \text{H}_2\text{O} : \text{C}_{32}\text{H}_{41}^{79}\text{Br}_2\text{N}_{10}\text{O}_4$ requires 787.1679; Δ 1.8 mmu), m/z 394.0846 ($(\text{MH}^+ - \text{H}_2\text{O})/2 + \text{H} : \text{C}_{16}\text{H}_{21}^{79}\text{BrN}_5\text{O}_2$ requires 394.0875; Δ 2.9 mmu), m/z 629.0531 ($(\text{M}^+ - \text{H}_2\text{O}) - \text{C}_6\text{H}_{13}\text{N}_4\text{O} : \text{C}_{26}\text{H}_{27}^{79}\text{Br}_2\text{N}_6\text{O}_3$ requires 629.0507; Δ 2.4 mmu); ^1H and ^{13}C NMR (see Table III and Appendix C).

APPENDIX A

NMR AND CD SPECTRA OF MAMANUTHAQUINONE
AND THE REARRANGED QUINONE
SESQUITERPENOID

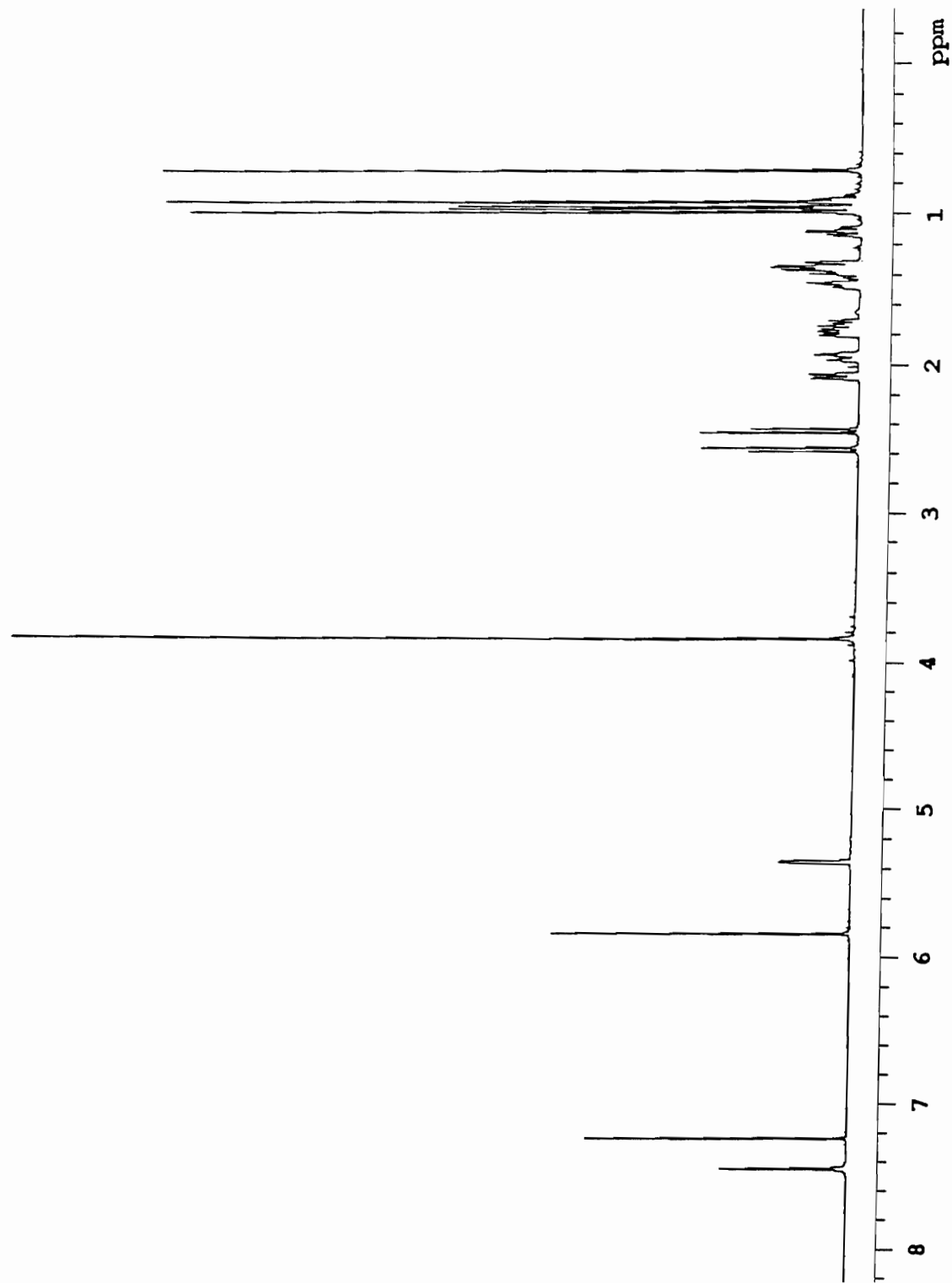


Figure 37. 500 MHz ^1H NMR spectrum of mamanuthaquinone (50).

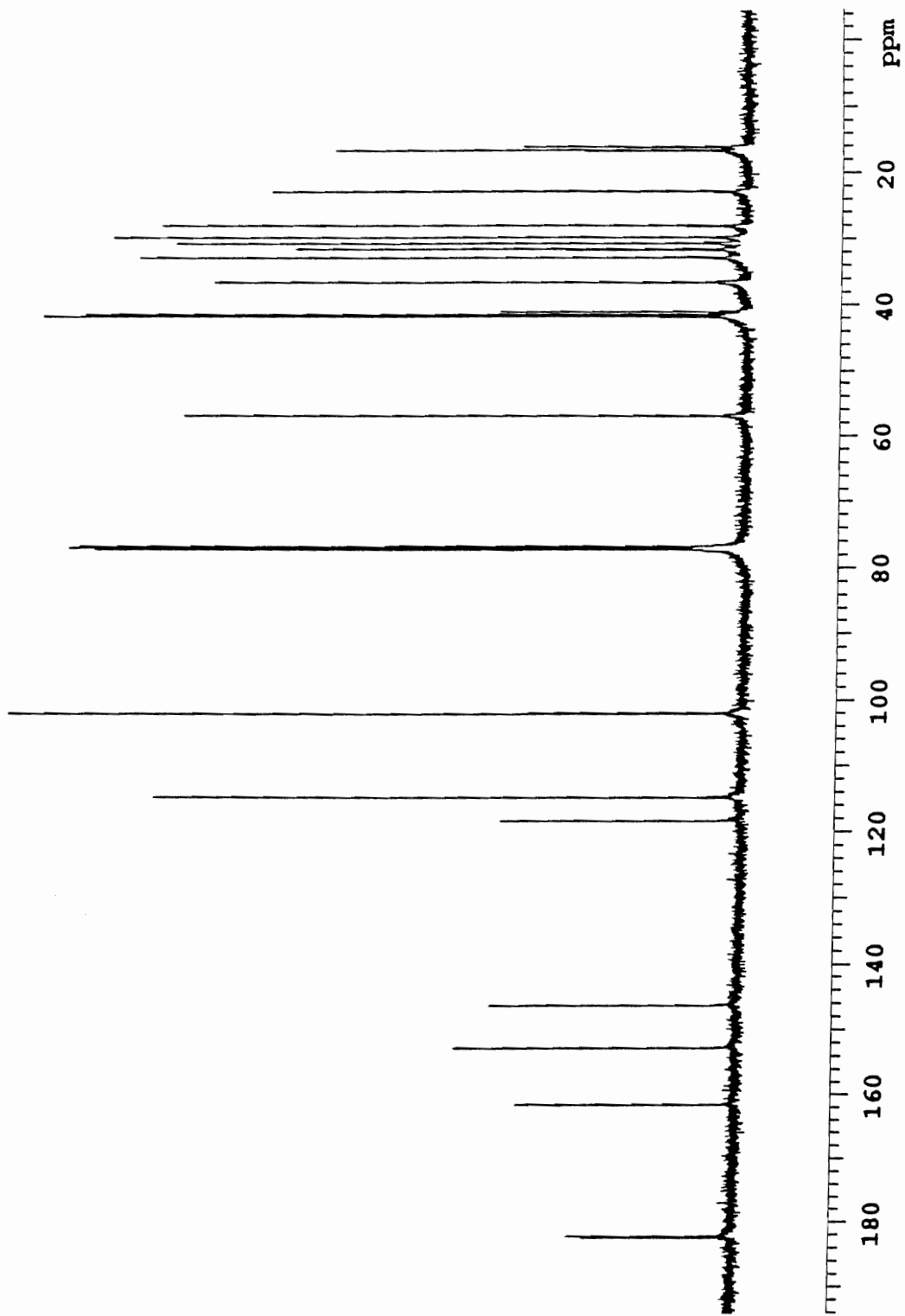


Figure 38. 125 MHz ¹³C NMR spectrum of maminuthaquinone (50).

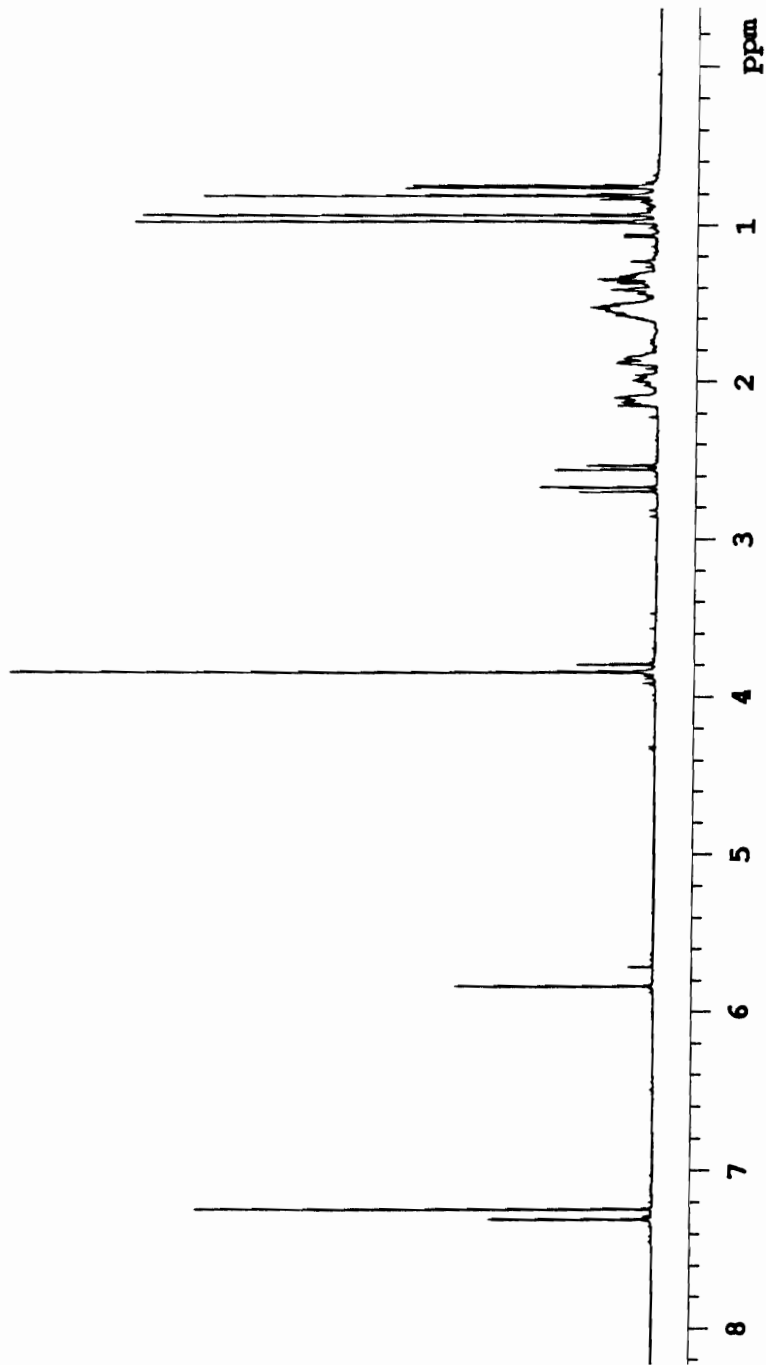


Figure 39. 500 MHz ^1H NMR spectrum of rearranged maminuthaquinone (151_m).

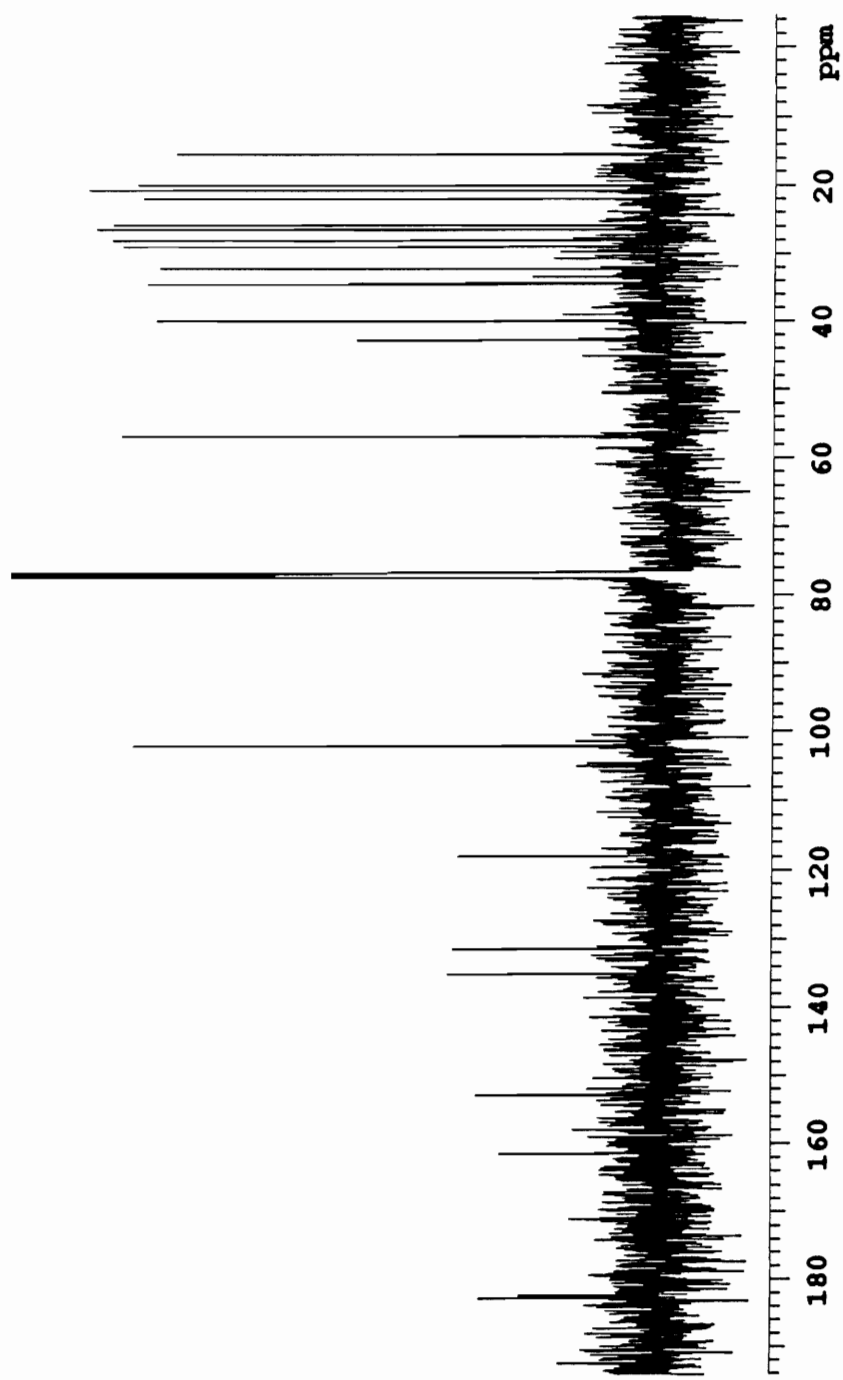


Figure 40. 125 MHz ^{13}C NMR spectrum of rearranged mamanuthaquinone (**151_m**).

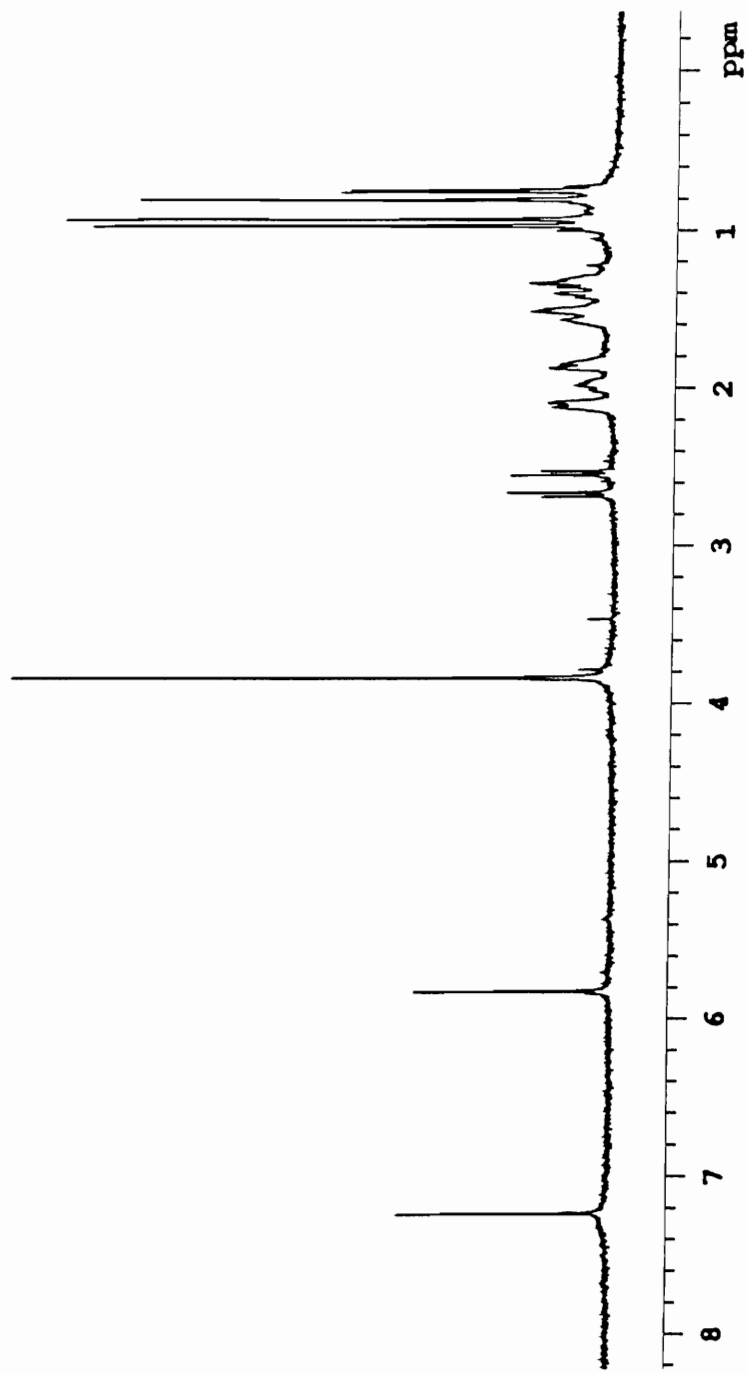


Figure 41. 500 MHz ^1H NMR spectrum of rearranged ilimaquinone (151_i).

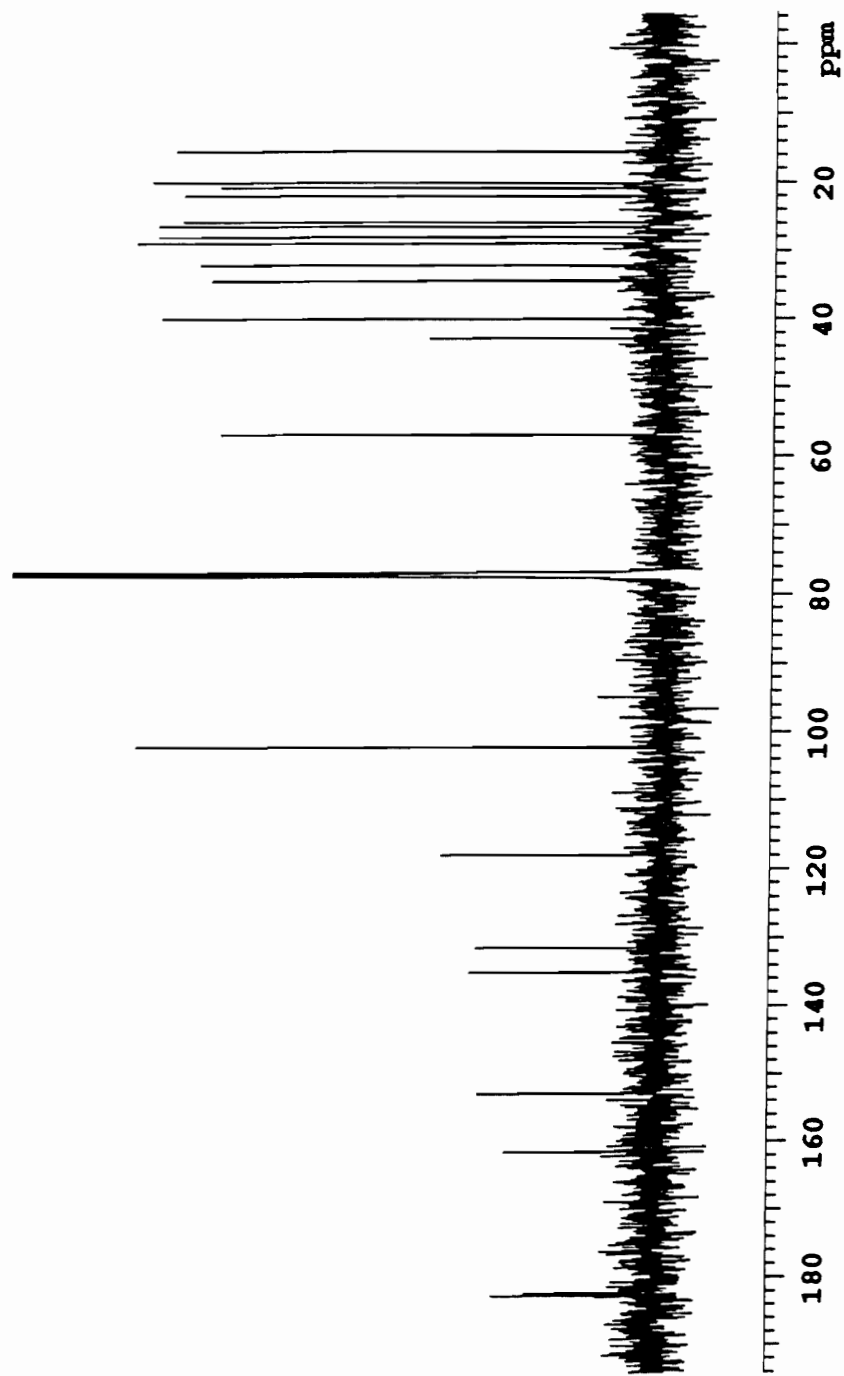


Figure 42. 125 MHz ^{13}C NMR spectrum of rearranged ilimaquinone (**151i**)

Rearranged Quinones, cd 17 jan 1991

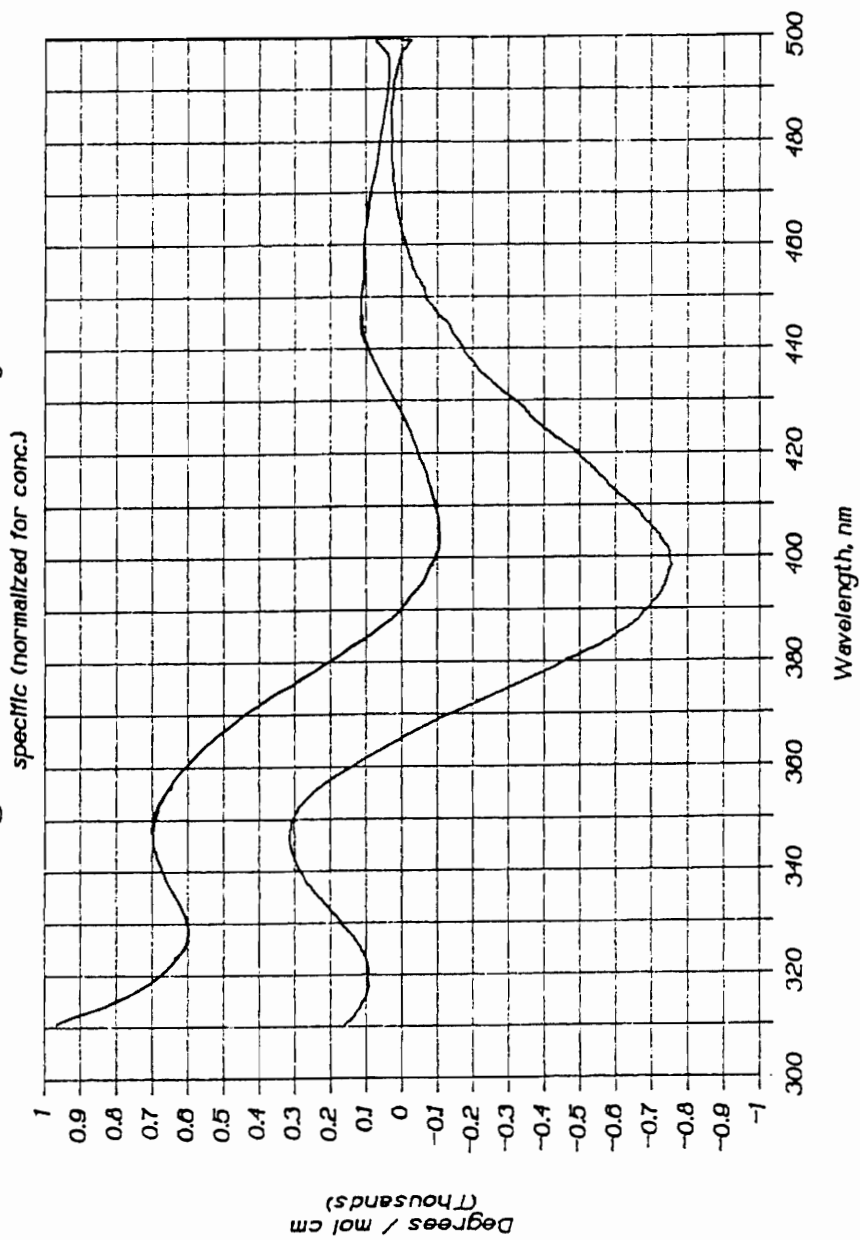


Figure 43. CD spectra of rearranged quinones 151_m and 151_i.

APPENDIX B

NMR AND CD SPECTRA OF EPIPOLASIDAMIDE

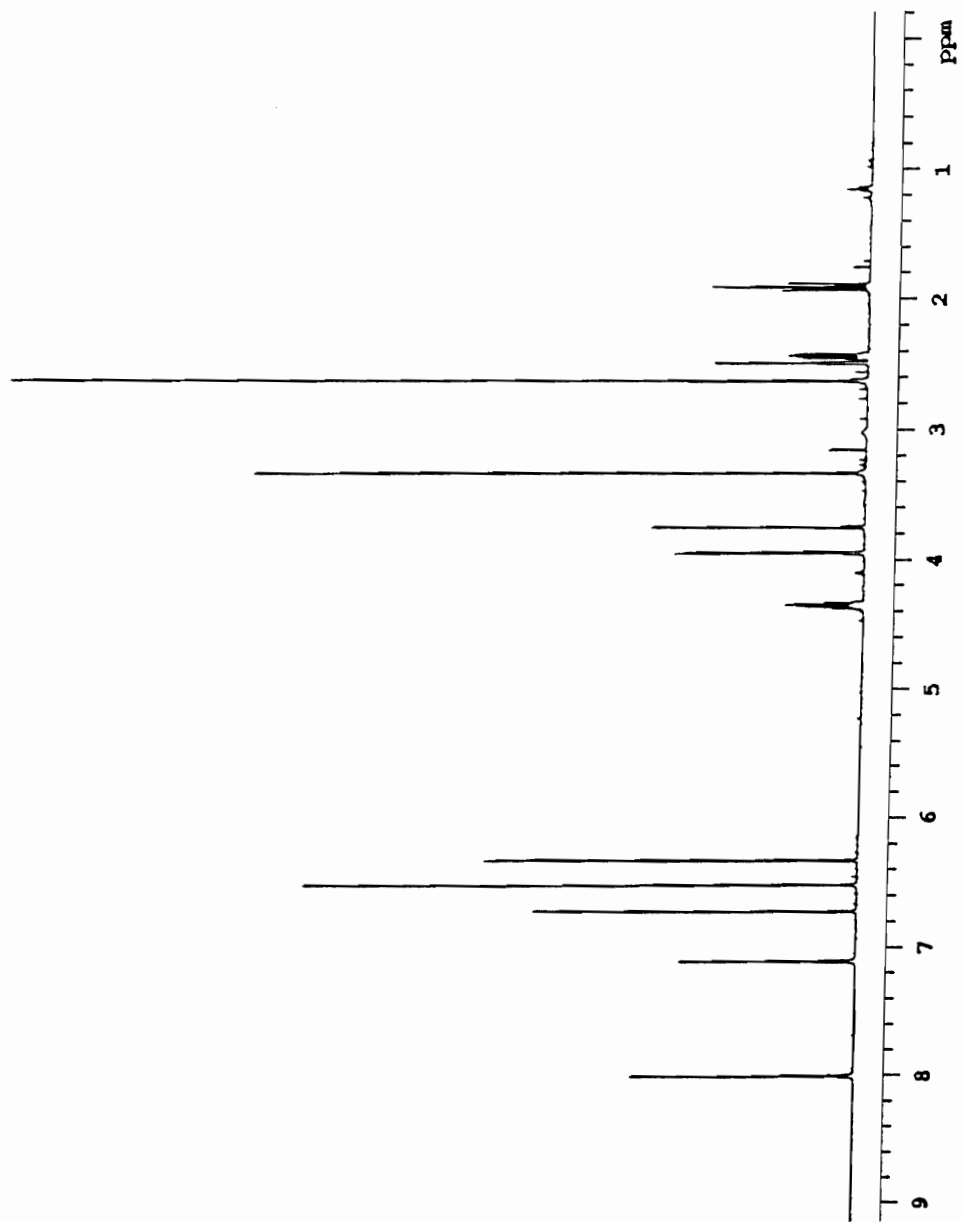


Figure 44. 500 MHz ^1H spectrum of epipolamidamide (88) recorded in d_6 -DMSO.

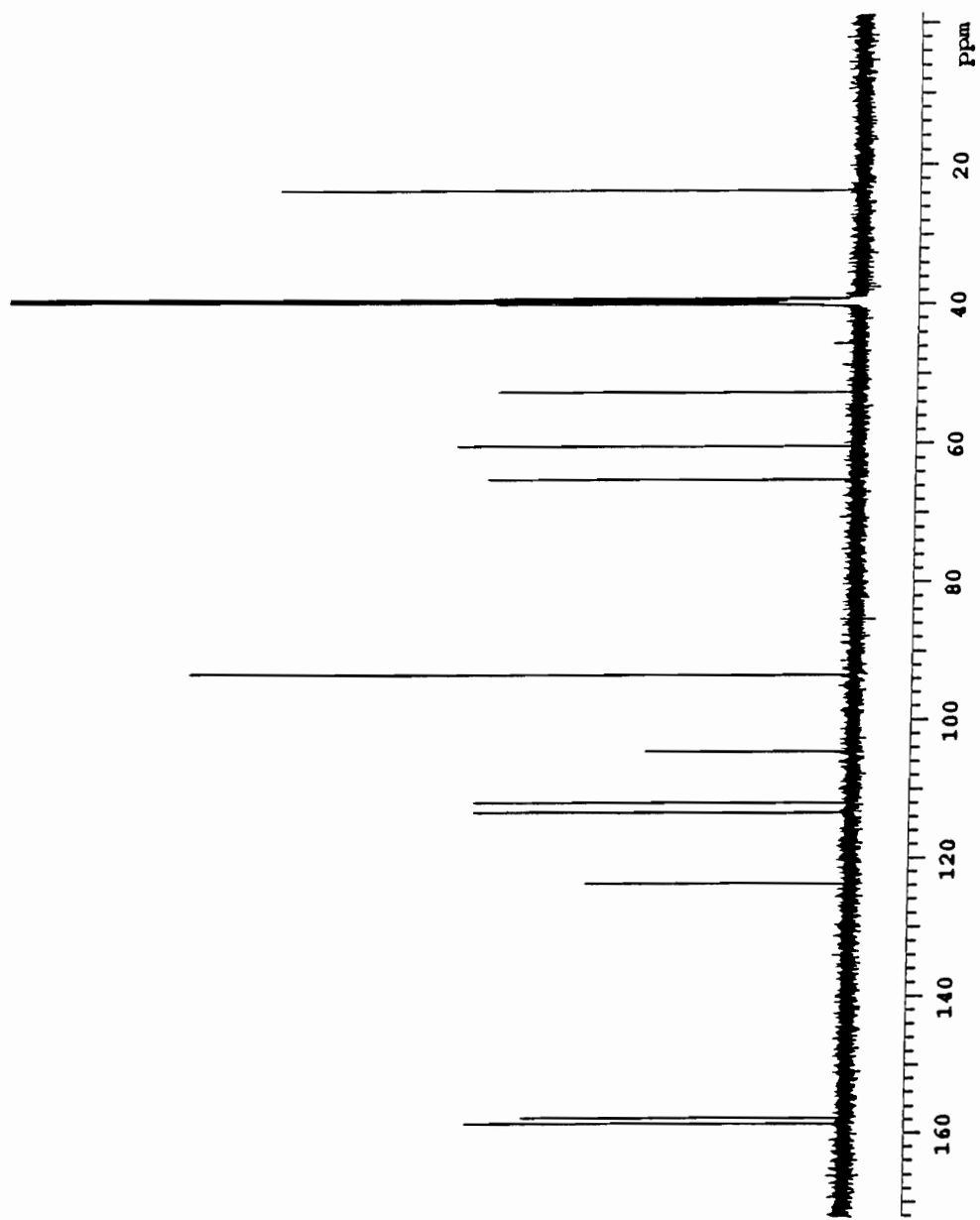


Figure 45. 125 MHz ^{13}C spectrum of epipolasisidamide (88) recorded in d_6 -DMSO.

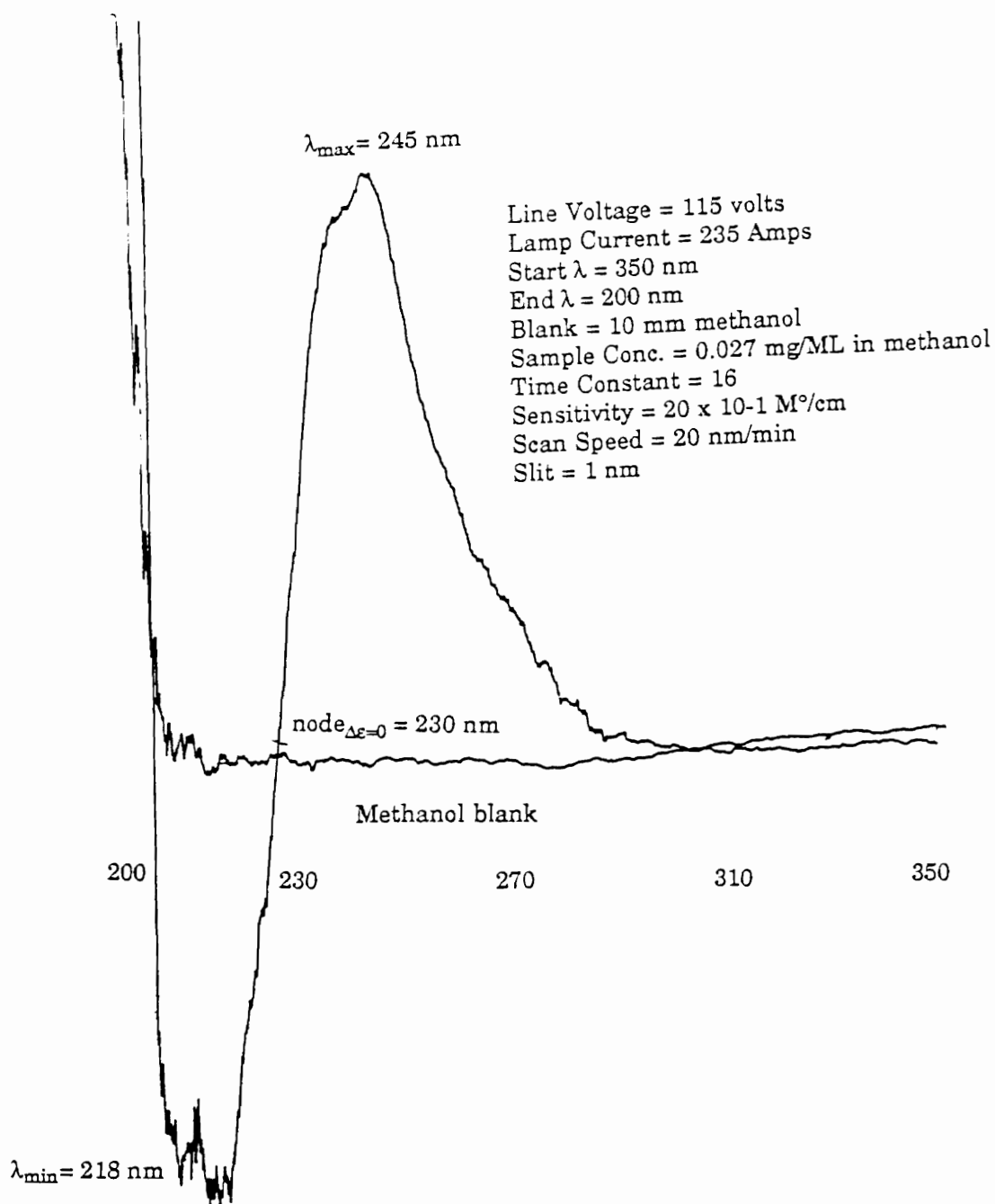


Figure 46. CD Spectrum of epipolasidamide (88) recorded in methanol.

APPENDIX C

NMR AND CD SPECTRA OF EUSYNSTYELAMIDE

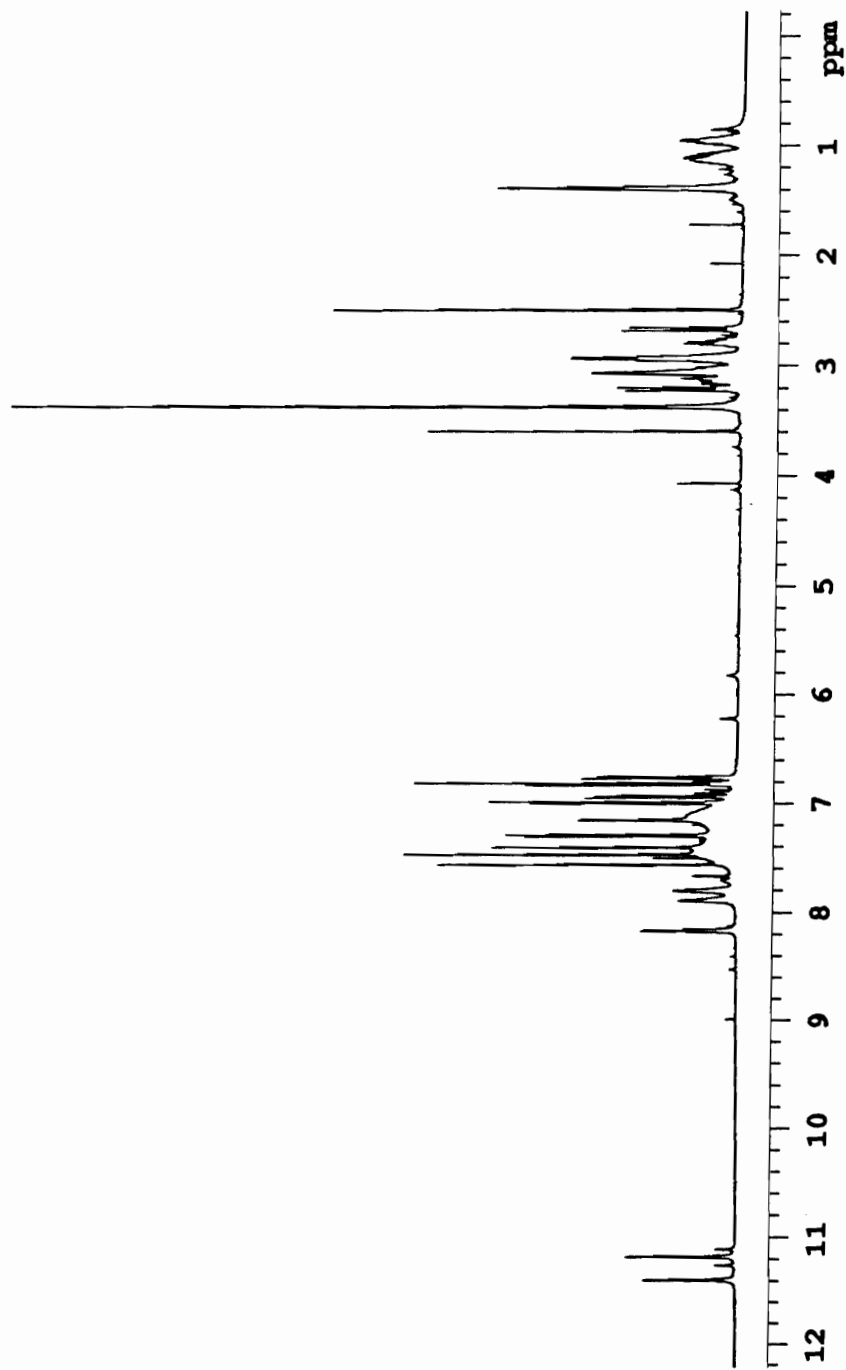


Figure 47. 500 MHz ^1H spectrum of eusynstyelamide (150) recorded in d_6 -DMSO.

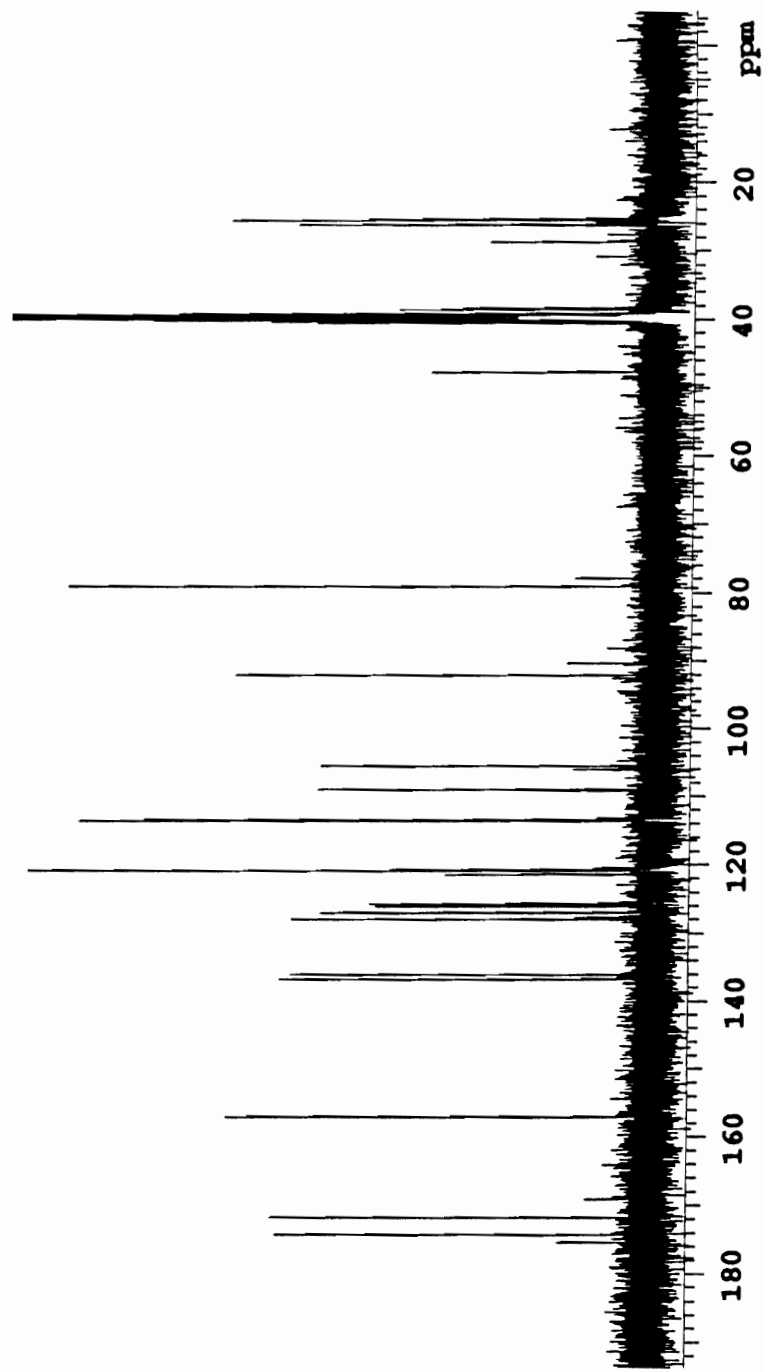


Figure 48. 125 MHz ^{13}C spectrum of eusynstyelamide (150) recorded in d_6 -DMSO.

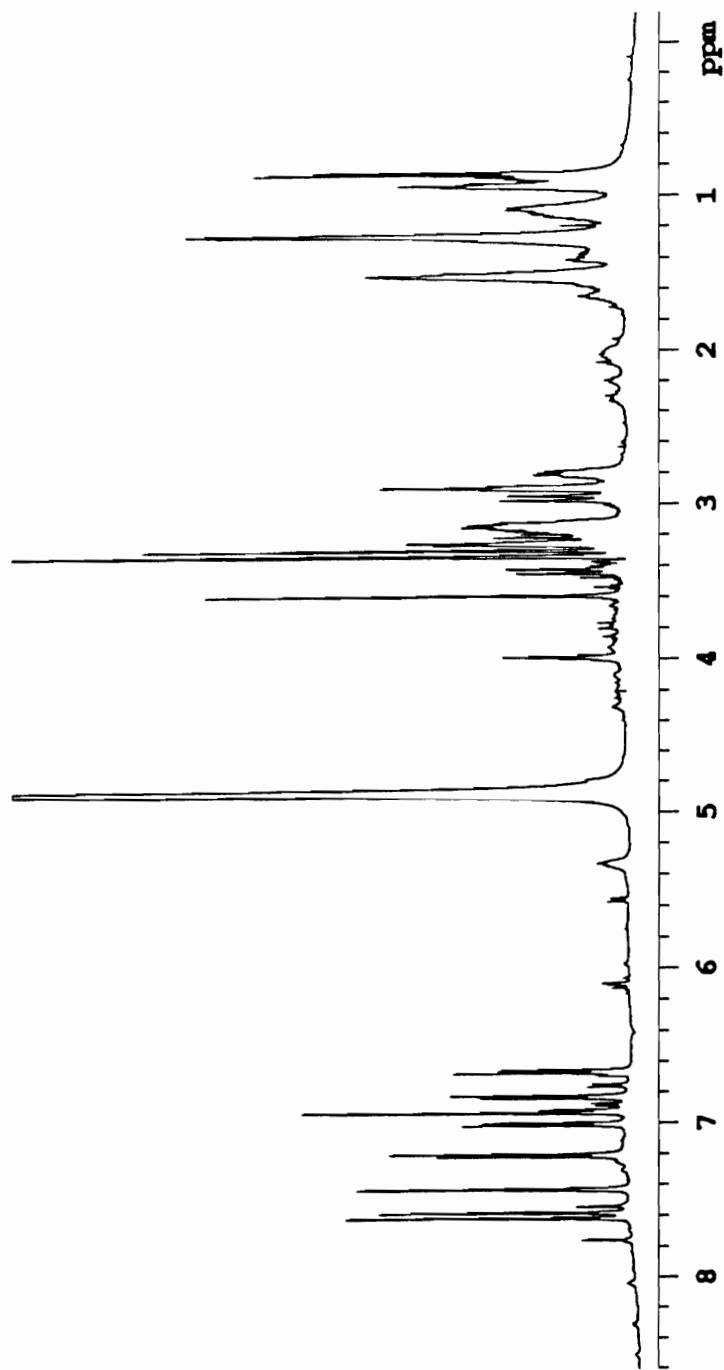


Figure 49. 500 MHz ^1H spectrum of eusynstyelamide (150) recorded in d_4 -methanol.

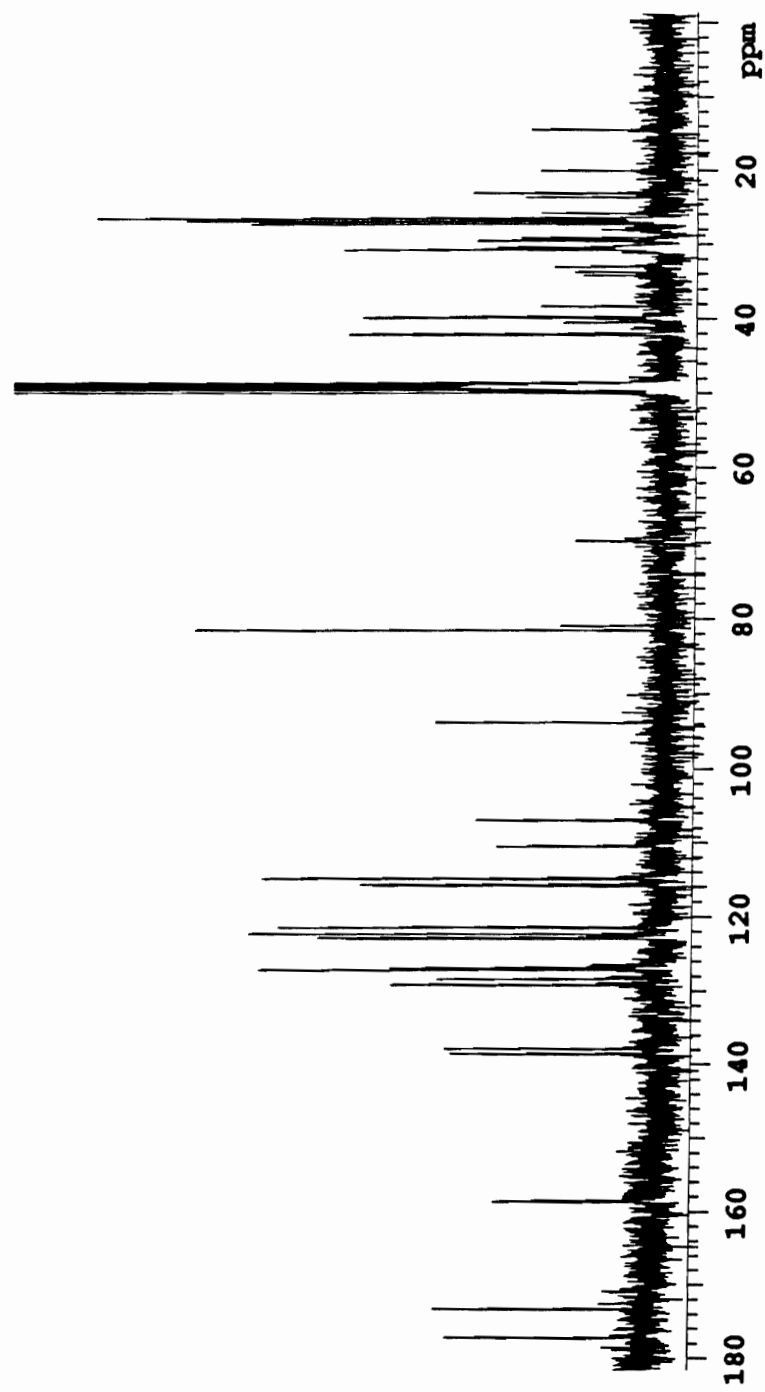


Figure 50. 125 MHz ^{13}C spectrum of eusynstyelamide (150) recorded in d_4 -methanol.

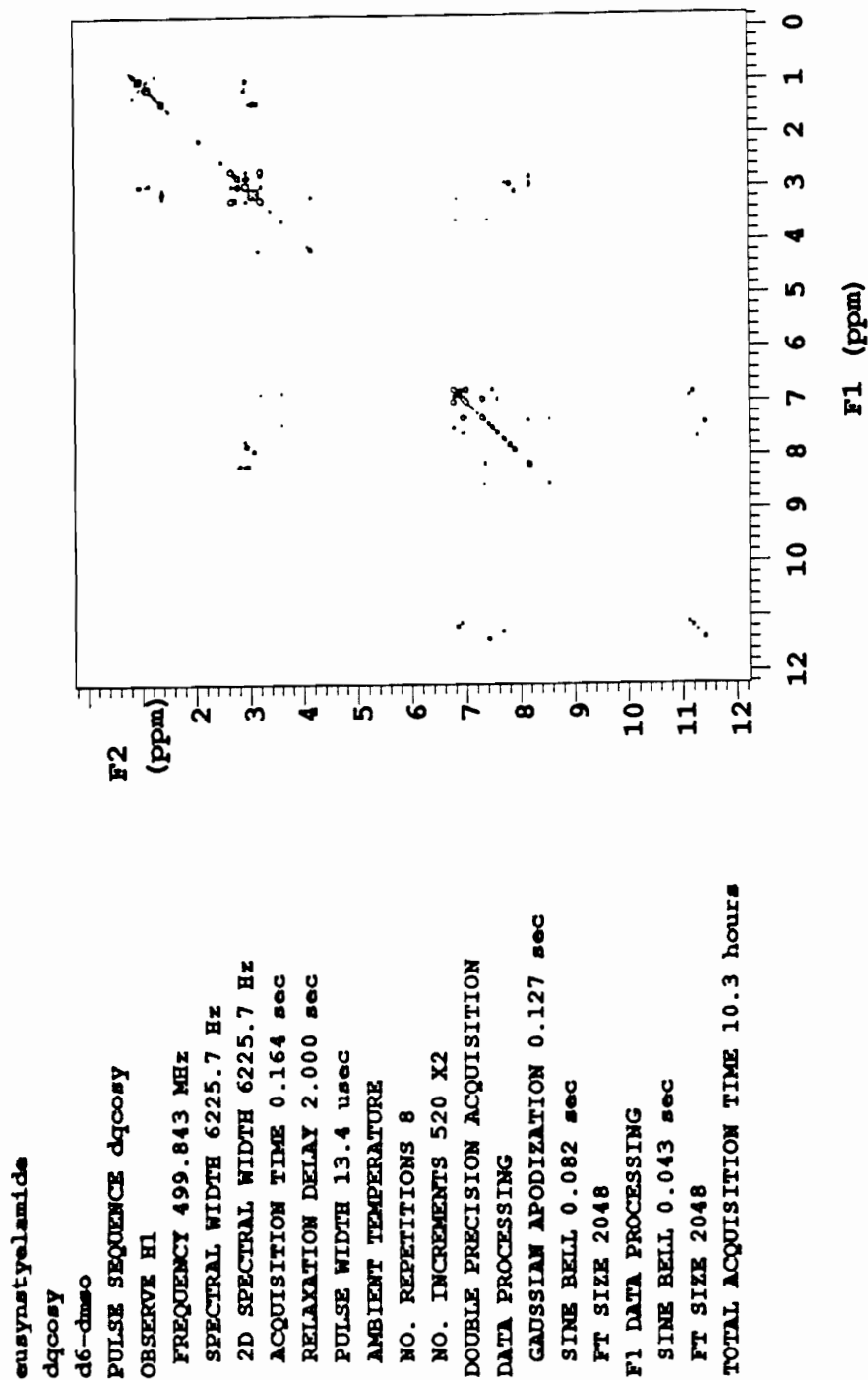


Figure 51. 500 MHz DQCOZY spectrum of eusynstyelamide recorded in d_6 -DMSO.

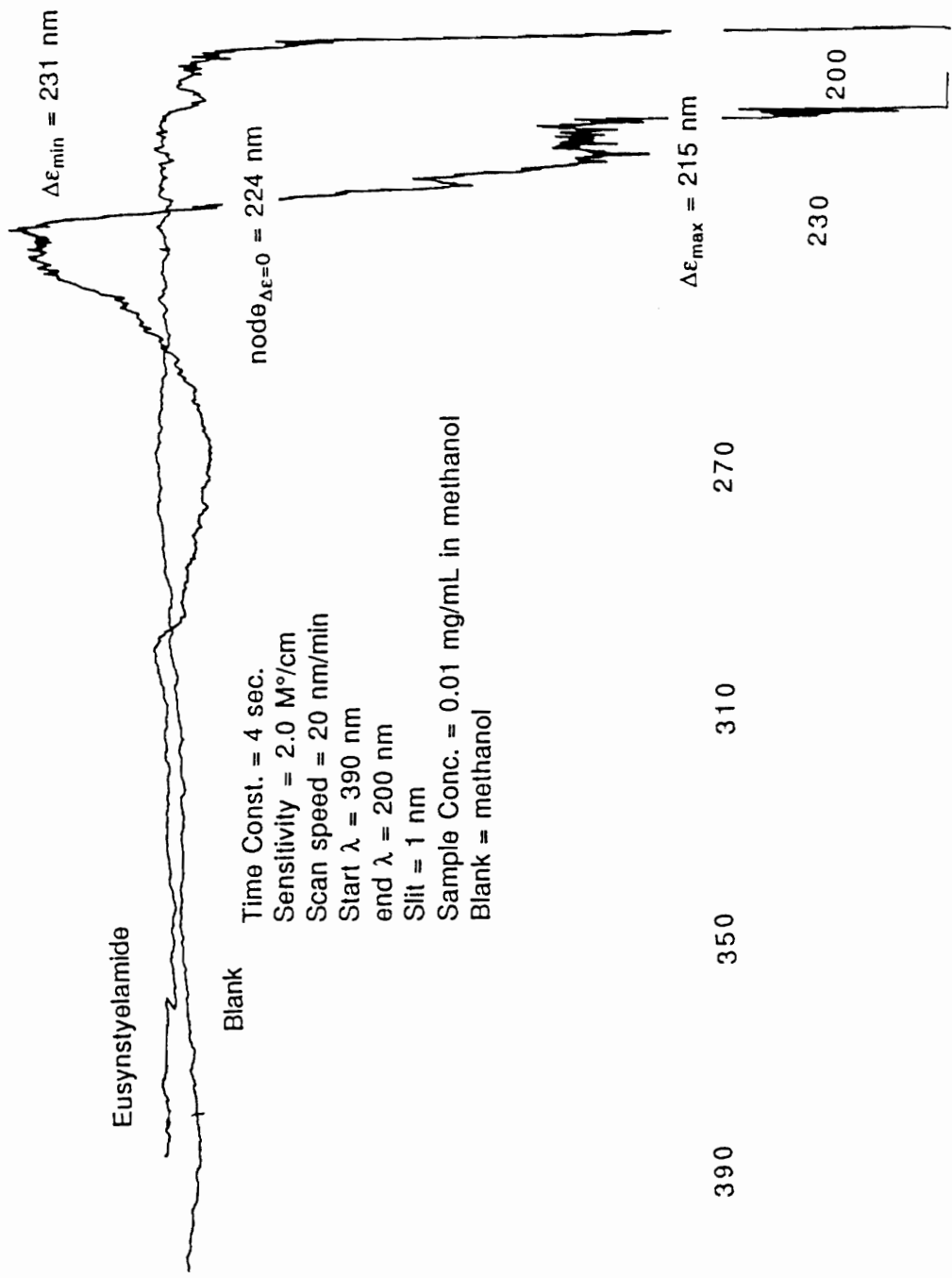


Figure 52. CD spectrum of eusynstyelamide (150) recorded in methanol.

REFERENCES

1. Bergmann, W.; Feeney, R. J. *J. Am. Chem. Soc.* **1950**, *72*, 2809.
2. Bergmann, W.; Feeney, R. J. *J. Org. Chem.* **1951**, *16*, 981.
3. Bergmann, W.; Burke, D. C. *J. Org. Chem.* **1955**, *20*, 1501.
4. Bergmann, W.; Watkins, J. C.; Stempien, M. F., Jr. *J. Org. Chem.* **1957**, *22*, 1308.
5. Cohen, S. S. *Prospect. Biol. Med.* **1963**, *6*, 215.
6. Cohen, S. S. *Prog. Nucleic Acid Res. Mol. Biol.* **1963**, *5*, 1.
7. Cohen, S. S. *Med. Biol.* **1976**, *54*, 299.
8. Faulkner, D. J. *Nat. Prod. Rep.* **1991**, *8*, 97.
9. Faulkner, D. J. *Nat. Prod. Rep.* **1990**, *7*, 269.
10. Faulkner, D. J. *Nat. Prod. Rep.* **1988**, *5*, 613.
11. Faulkner, D. J. *Nat. Prod. Rep.* **1987**, *4*, 539.
12. Faulkner, D. J. *Nat. Prod. Rep.* **1984**, *1*, 251.
13. Faulkner, D. J. *Nat. Prod. Rep.* **1986**, *3*, 1.
14. Faulkner, D. J. *Nat. Prod. Rep.* **1984**, *1*, 551.
15. Kazlauskas, R.; Murphy, P. T.; Quinn, R. J.; Wells, R. J. *Tetrahedron Lett.* **1976**, 2635, and references cited therein.
16. Baker, J. T. *Pure & Appl. Chem.* **1976**, *48*, 35.
17. Cimino, G.; De Stefano, S.; Minale, L. *Tetrahedron* **1972**, *28*, 1579.
18. Faulkner, D. J. *Tetrahedron Lett.* **1973**, 3821.
19. Kernan, M. R.; Cambie, R. C.; Bergquist, P. R. *J. Nat. Prod.* **1991**, *54*, 265.
20. Cimino, G.; De Stefano, S.; Minale, L.; Fattorusso, E. *Tetrahedron* **1971**, *27*, 4673.

21. Fattorusso, E.; Minale, L.; Sodano, G.; Trivellone, E. *Tetrahedron* **1971**, *27*, 3909.
22. Umeyama, A.; Shoji, N. ; A., S.; Ohizumi, Y.; Kobayashi, J. *Aust. J. Chem.* **1989**, *42*, 459.
23. Bergquist, P. R. *N.Z. J. Zool.* **1980**, *7*, 443.
24. Cambie, R. C.; Craw, P. A.; Bergquist, P. R.; Karuso, P. *J. Nat. Prod.* **1988**, *51*, 331.
25. de Silva, E. D.; Scheuer, P. J. *Tetrahedron Lett.* **1980**, *21*, 1611.
26. Blankemeier, L. A.; Jacobs, R. S. *Fed. Proc.* **1983**, *42*, 374.
27. de Freitas, J. C.; Blankemeier, L. A.; Jacobs, R. S. *Experientia* **1984**, *40*, 864.
28. Kobayashi, J.; Ohizumi, Y.; Nakamura, H.; Hirata, Y. *Tetrahedron Lett.* **1986**, *27*, 2113.
29. Albericci, M.; Braekman, J. C.; Daloze, D.; Tursch, B. *Tetrahedron* **1982**, *38*, 1881.
30. Braekman, J. C.; Daloze, D.; Bertau, R.; Macedo de Abreau, P. *Bull. Soc. Chim. Belg.* **1982**, *91*, 791.
31. Madaio, A.; Piccialli, V.; Sica, D. *J. Nat. Prod.* **1990**, *53*, 565.
32. Madaio, A.; Notaro, G.; Piccialli, V.; Sica, D. *J. Nat. Prod.* **1990**, *53*, 565.
33. Enwall, E. L.; van der Helm, D.; Hsu, I. N.; Pattabhiraman, T.; Schmitz, F. J.; Spraggins, R. L.; Weinheimer, A. J. *J. Chem. Soc., Chem. Commun.* **1972**, 215.
34. Kazlauskas, R.; Murphy, P. T.; Ravi, B. N.; Sanders, R. L.; Wells, R. J. *Aust. J. Chem.* **1982**, *35*, 69.
35. Capon, R. J.; Faulkner, D. J. *J. Org. Chem.* **1985**, *50*, 4771.
36. Bonini, C.; Cooper, C. B.; Kazlauskas, R.; Wells, R. J.; Djerassi, C. *J. Org. Chem.* **1982**, *48*, 2108.
37. Nakamura, H.; Deng, S.; Kobayashi, J.; Ohizumi, Y. *Tetrahedron* **1986**, *42*, 4197.

38. Kernan, M. R.; Cambie, R. C.; Bergquist, P. R. *J. Nat. Prod.* **1991**, *54*, 269.
39. Kazlauskas, R.; Murphy, P. T.; Warren, R. G.; Wells, R. J.; Blount, J. F. *Aust. J. Chem.* **1978**, *31*, 2635.
40. Cimino, G.; De Stefano, S.; Minale, L. *Tetrahedron* **1972**, *28*, 1315.
41. Cimino, G.; De Stefano, S.; Minale, L. *Experientia* **1972**, *28*, 1401.
42. Fenical, W., Food Drugs from the Sea Symposium, Puerto Rico, 1974.
43. Capon, R. J. *J. Nat. Prod.* **1990**, *53*, 753.
44. Luibrand, R. T.; Erdman, T. R.; Vollmer, J. J.; Scheuer, P. J.; Finer, J.; Clardy, J. *Tetrahedron* **1979**, *35*, 609.
45. Capon, R. J.; MacLeod, J. K. *J. Org. Chem.* **1987**, *52*, 5059.
46. Djura, P.; Stierle, D. B.; Sullivan, B.; Faulkner, D. J. *J. Org. Chem.* **1980**, *45*, 1098.
47. Swersey, J. C.; Barrows, L. R.; Ireland, C. M. *Tetrahedron Lett.* **1991**, *32*, 6687.
48. Carté, B.; Rose, C. B.; Faulkner, D. J. *J. Org. Chem.* **1985**, *50*, 2785.
49. Schmitz, F. J.; Lakshmi, V.; Powell, D. R.; van der Helm, D. *J. Org. Chem.* **1984**, *49*, 241.
50. Nakamura, M.; Ohizumi, Y.; Cheng, J.; Nakamura, H.; Hirata, Y.; Sasaki, T.; Kobayashi, J. *J. Org. Chem.* **1988**, *53*, 2855.
51. Kobayashi, J.; Murayama, T.; Ohizumi, Y.; Ohta, T.; Nozoe, S.; Sasaki, T. *J. Nat. Prod.* **1989**, *52*, 1173.
52. Kashman, Y.; Fishelson, L.; Ne'eman, I. *Tetrahedron* **1973**, *29*, 3655.
53. Matsunaga, S.; Fusetani, N.; Konosu, S. *Tetrahedron Lett.* **1984**, *25*, 5165.
54. Matsunaga, S.; Fusetani, N.; Konosu, S. *J. Nat. Prod.* **1985**, *48*, 236.
55. Matsunaga, S.; Fusetani, N.; Konosu, S. *Tetrahedron Lett.* **1985**, *26*, 855.
56. Gulavita, N. K.; Gunasekera, S. P.; Pomponi, S. A.; Robinson, E. V. *J. Org. Chem.* **1992**, *57*, 1767.

57. Zabriskie, T. M. Ph. D. Thesis, University of Utah, 1989.
58. Fusetani, N.; Matsunaga, S.; Matsumoto, H.; Takebayashi, Y. *J. Am. Chem. Soc.* **1990**, *112*, 7053.
59. Fusetani, N.; Sugawara, T.; Matsunaga, S. *J. Am. Chem. Soc.* **1991**, *113*, 7811.
60. Kobayashi, J.; Itagaki, F.; Shigemori, H.; Ishibashi, M.; Takahashi, K.; Ogura, M.; Nagasawa, S.; Nakamura, T.; Hirota, H.; Ohta, T.; Nozoe, S. *J. Am. Chem. Soc.* **1991**, *113*, 7812.
61. de Silva, E. D.; Williams, D. E.; Anderson, R. J.; Klix, H.; Holmes, C. F.; Allen, T. M. *Tetrahedron Lett.* **1992**, *33*, 1561.
62. Botes, D.; Tuinman, A.; Wessels, P. L.; Viljoen, C.; Kruger, H.; Williams, D. H.; Santikarn, S.; Smith, R. J.; Hammond, S. *J. Chem. Soc. Perkin Trans. I* **1984**, 2311.
63. Botes, P. B.; Wessels, P. L.; Kruger, H.; Runnegar, M. T.; Santikarn, S.; Smith, R. J.; Barna, J. C.; Williams, D. H. *J. Chem. Soc. Perkin Trans. I* **1985**, 2747.
64. Zabriskie, T. M.; Klocke, J. A.; Ireland, C. M.; Markus, A. H.; Molinski, T. F.; Faulkner, D. J.; Xu, C.; Clardy, J. *J. Am. Chem. Soc.* **1986**, *108*, 3123.
65. Scott, V. R.; Boehme, R.; Matthews, T. R. *Antimicrob. Agents Chemother.* **1988**, *32*, 1154.
66. Crews, P.; Manes, L. V.; Boehler, M. *Tetrahedron Lett.* **1986**, *27*, 2797.
67. Chan, W. R.; Tinto, W. F.; Manchand, P. S.; Todaro, L. J. *J. Org. Chem.* **1987**, *52*, 3091.
68. de Silva, E. D.; Anderson, R. J.; Allen, T. M. *Tetrahedron Lett.* **1990**, *31*, 489.
69. Quiñoà, E.; Adamczeski, M.; Crews, P.; Bakus, G. J. *J. Org. Chem.* **1986**, *51*, 4497.
70. Adamczeski, M.; Quiñoa, E.; Crews, P. *J. Am. Chem. Soc.* **1988**, *110*, 1598.
71. Keifer, P. A.; Schwartz, R. E.; Koker, M. E.; Hughes, R. G., Jr.; Rittschof, D.; Rinehart, K. L. *J. Org. Chem.* **1991**, *56*, 2965.

72. Ireland, C. M.; Molinski, T. F.; Roll, D. M.; Zabriskie, T. M.; McKee, T. C.; Swersey, J. C.; Foster, M. P. In *Bioorganic Marine Chemistry*; P. J. Scheuer, Ed.; Springer-Verlag: Berlin, 1989; Vol. 3, pp 1-46.
73. Forenza, S.; Minale, L.; Riccio, R.; Fattorusso, E. *J. Chem. Soc., Chem. Comm.* **1971**, 1129.
74. Garcia, E. E.; Benjamin, L. E.; Fryer, R. I. *J. Chem. Soc., Chem. Comm.* **1973**, 78.
75. Kobayashi, J.; Ohizumi, Y.; Nakamura, H.; Hirata, Y. *Experientia* **1986**, *42*, 1176.
76. Braekman, J. C.; Dalozze, D.; Moussiaux, B.; Stoller, C.; Deneubourg, F. *Pure Appl. Chem.* **1989**, *61*, 509.
77. Chevolut, L.; Padua, S.; Ravi, B. N.; Blyth, P. C.; Scheuer, P. J. *Heterocycles* **1977**, *7*, 891.
78. Sharma, G. M.; Burkholder, P. R. *J. Chem. Soc., Chem. Commun.* **1971**, 151.
79. Sharma, G. M.; Magdoff-Fairchild, B. *J. Org. Chem.* **1977**, *42*, 4118.
80. Fedoreyev, S. A.; Utkina, N. K.; Ilyin, S. G.; Reshetnyak, M. V.; Maximov, O. B. *Tetrahedron Lett.* **1986**, *27*, 3177.
81. Nakamura, H.; Ohizumi, Y.; Kobayashi, J. *Tetrahedron Lett.* **1984**, *25*, 2475.
82. Nakamura, H.; Wu, H.; Kobayashi, J.; Ohizumi, Y. *Tetrahedron Lett.* **1983**, *24*, 4105.
83. Walker, R. P.; Faulkner, D. J.; van Engen, D.; Clardy, J. *J. Am. Chem. Soc.* **1981**, *103*, 6773.
84. Sesin, D. F.; Ireland, C. M.; Gaskell, S. J. *Bull. Soc. Chim. Belg.* **1986**, *95*, 853.
85. Sesin, D. F.; Ireland, C. M. *Tetrahedron Lett.* **1984**, *25*, 403.
86. McKee, T. C. Ph. D. Thesis, University of Utah, 1990.
87. Paul, V. J.; Lindquist, N.; Fenical, W. *Mar. Ecol. Prog. Ser.* **1989**, *59*, 109.
88. Young, C. M.; Bingham, B. L. *Mar. Biol.* **1987**, *96*, 539.

89. Lindquist, N.; Fenical, W.; Sesin, D. F.; Ireland, C. M.; Van Duyne, D. G.; Forsyth, C. J.; Clardy, J. *J. Am. Chem. Soc.* **1988**, *110*, 1308.
90. Andersen, R. J.; Faulkner, D. J.; He, C.; Van Duyne, G. D.; Clardy, J. *J. Am. Chem. Soc.* **1985**, *107*, 5492.
91. Bruening, R. C.; Oltz, E. M.; Furukawa, J.; Nakanishi, K.; Kustin, K. *J. Am. Chem. Soc.* **1985**, *107*, 5298.
92. Bruening, R. C.; Oltz, E. M.; Furukawa, J.; Nakanishi, K.; Kustin, K. *J. Nat. Prod.* **1986**, *49*, 193.
93. Strohal, P.; Tuta, J.; Zvonimir, K. *Limnol. Oceanogr.* **1969**, *14*, 265.
94. Levine, E. P. *Science* **1961**, *133*, 1352.
95. Nakanishi, K. In *Biomedical Importance of Marine Natural Products*; D. G. Fautin, Ed.; California Academy of Science: San Francisco, 1988; Vol. 13, pp 59-67.
96. Carter, G. T.; Rinehart, K. L. *J. Am. Chem. Soc.* **1978**, *100*, 7442.
97. Kobayashi, J.; Cheng, J. F.; Ohta, T.; Nakamura, H.; Nozoe, S.; Hirata, Y.; Ohizumi, Y.; Sasaki, T. *J. Org. Chem.* **1988**, *53*, 6147.
98. Kikuchi, Y.; Ishibashi, M.; Sasaki, T.; Kobayashi, J. *Tetrahedron Lett.* **1991**, *32*, 797.
99. Foster, M. P.; Maynes, C. L.; Dunkel, R.; Pugmire, R. J.; Grant, D. M.; Kornprobst, J.; Verbist, J.; Biard, J.; Ireland, C. M. *J. Am. Chem. Soc.* **1992**, *114*, 1110.
100. Gouiffes, D.; Juge, M.; Grimaud, M.; Welin, L.; Sauviat, M. P.; Barbin, Y.; Laurent, D.; Roussakis, C.; Hénichart, J. P.; Verbist, J. F. *Toxicon.* **1988**, *26*, 1129.
101. Gouiffes, D.; Moreau, S.; Helbecque, N.; Bernier, J. L.; Hénichart, J. P.; Barbin, Y.; Laurent, D.; Verbist, J. F. *Tetrahedron* **1988**, *44*, 451.
102. Degnan, B. M.; Hawkins, C. J.; Lavin, M. F.; McCaffrey, E. J.; Parry, D. L.; Watters, D. J. *J. Med. Chem.* **1989**, *32*, 1354.
103. Rinehart, K. L., Jr.; Gloer, J. B.; Hughes, R. G., Jr.; Renis, H. E.; McGovern, J. P.; Swynenberg, E. B.; Stringfellow, D. A.; Kuentzel, S. L.; Li, L. H. *Science* **1981**, *212*, 933.
104. Gloer, J. B. Ph. D. Thesis, University of Illinois, Urbana-Champaign, 1983.

105. Rinehart, K. L.; Gloer, J. B.; Cook, J. C., Jr.; Mizsak, S. A.; Scahill, T. A. *J. Am. Chem. Soc.* **1981**, *103*, 1857.
106. Rinehart, K. L. *Science* **1982**, *218*, 254.
107. Canonico, P. G.; Pannier, W. L.; Huggins, J. W.; Rinehart, K. L. *Antimicrob. Agents Chemother.* **1982**, *22*, 696.
108. Jiang, T. L.; Liu, R. H.; Salmon, S. E. *Cancer Chemother.* **1983**, *11*, 1.
109. Montgomery, D. W.; Zukoski, C. F. *Transplant* **1985**, *40*, 49.
110. Rinehart, K. L.; Kishore, V.; Nagarajan, S.; Lake, R. J.; Gloer, J. B.; Bozich, F. A.; Li, K.; Maleczka, R. E.; Todsén, W. L.; Munro, M. H.; Sullins, D. W.; Sakai, R. *J. Am. Chem. Soc.* **1987**, *109*, 6846.
111. Rinehart, K. L.; Kishore, V.; Bible, K. C.; Sakai, R.; Sullins, D. W.; Li, K. *J. Nat. Prod.* **1988**, *51*, 1.
112. Kobayashi, J.; Cheng, J.; Kikuchi, Y.; Ishibashi, M.; Yamaura, S.; Ohizumi, Y.; Ohta, T.; Nozoe, S. *Tetrahedron Lett.* **1990**, *32*, 4617.
113. Kindo, T.; Ohgi, T.; Goto, T. *Agric. Biol. Chem.* **1977**, *41*, 1501.
114. Danswan, G.; Kennewell, P. D.; Tully, W. R. *J. Heterocyclic Chem.* **1989**, *26*, 293.
115. Niwa, H.; Yoshida, Y.; Yamada, K. *J. Nat. Prod.* **1988**, *51*, 343.
116. Roll, D. M.; Ireland, C. M. *Tetrahedron Lett.* **1985**, *26*, 4303.
117. Moriarty, R. M.; Roll, D. M.; Ku, Y.; Nelson, C.; Ireland, C. M. *Tetrahedron Lett.* **1987**, *28*, 749.
118. Rinehart, K. L.; Kobayashi, J.; Harbour, G. C.; Hughes, R. G., Jr.; Mizsak, S. A.; Scahill, T. A. *J. Am. Chem. Soc.* **1984**, *106*, 1524.
119. Kobayashi, J.; Harbour, G. C.; Gilmore, J.; Rinehart, K. L. *J. Am. Chem. Soc.* **1984**, *106*, 1526.
120. Finzer, K. F.; Cardellina, J. H. *Tetrahedron Lett.* **1987**, *28*, 925.
121. Adesanya, S. A.; Chbani, M.; Pais, M.; Debitus, C. *J. Nat. Prod.* **1992**, *55*, 525.
122. Heitz, S.; Durgeat, M.; Guyot, M.; Brassy, C.; Bachet, B. *Tetrahedron Lett.* **1980**, *21*, 1457.

123. Moquin, C.; Guyot, M. *Tetrahedron Lett.* **1984**, *25*, 5047.
124. Moquin-Patthey, C.; Guyot, M. *Tetrahedron* **1989**, *45*, 3445.
125. Guyot, M.; Meyer, M. *Tetrahedron Lett.* **1986**, *27*, 2621.
126. Hogan, I. T.; Sainsbury, M. *Tetrahedron* **1984**, *40*, 681.
127. Helbecque, N.; Berbier, J. L.; Henichard, J. P.; Moquin, C.; Guyot, M. *Cancer Biochem. Biophys.* **1987**, *9*, 271.
128. Cheng, M. T.; Rinehart, K. L. *J. Am. Chem. Soc.* **1978**, *100*, 7409.
129. Carté, B.; Faulkner, D. J. *Tetrahedron Lett.* **1982**, *23*, 3863.
130. Rinehart, K. L.; Harbour, G. C.; Graves, M. D.; Cheng, M. T. *Tetrahedron Lett.* **1983**, *24*, 1593.
131. Lindquist, N.; Fenical, W. *Tetrahedron Lett.* **1990**, *31*, 2521.
132. Doddrell, D. M.; Pegg, D. T.; Bendall, M. R. *J. Magn. Res.* **1982**, *48*, 323.
133. Bendall, M. R.; Pegg, D. T.; Doddrell, D. M. *J. Magn. Res.* **1983**, *52*, 81.
134. Aue, W. P.; Bartholdi, E.; Ernst, R. R. *J. Chem. Phys.* **1976**, *64*, 2229.
135. Piantini, U.; Sørensen, O. W.; Ernst, R. R. *J. Am. Chem. Soc.* **1982**, *104*, 6800.
136. Bax, A.; Summers, M. F. *J. Am. Chem. Soc.* **1986**, *108*, 2093.
137. Braunschweiler, L.; Ernst, R. R. *J. Magn. Res.* **1983**, *53*, 521.
138. Edwards, M. W.; Bax, A. *J. Am. Chem. Soc.* **1986**, *108*, 918.
139. Kinns, M.; Summers, M. F. *J. Magn. Reson.* **1984**, *56*, 518.
140. Loya, S.; Hizi, A. *FEBS Lettrs.* **1990**, *269*, 131.
141. Weislow, O. W.; Kiser, R.; Fine, D.; Bader, J. *J. Natl. Cancer Inst.* **1989**, *81*, 577.
142. Bergquist, P. R. *Sponges*; University of California Press: Berkeley and Los Angeles, 1978.
143. Carmely, S.; Kashman, Y. *Tetrahedron Lett.* **1987**, *28*, 3003.

144. Carmely, S.; Ilan, M.; Kashman, Y. *Tetrahedron* **1989**, *45*, 2193.
145. Pretsch, E.; Seibl, J.; Simon, W.; Clerc, T. *Tables of Spectral Data for Structure Determination of Organic Compounds*, 2nd ed.; Springer-Verlag: Berlin, 1989.
146. Karplus, M. *J. Chem. Phys.* **1959**, *30*, 11.
147. Karplus, M. *J. Am. Chem. Soc.* **1963**, *85*, 2870.
148. Abraham, R. J.; McLauchlan, K. A. *Mol. Phys.* **1962**, *5*, 513.
149. Bystrov, V. F. *Prog. NMR Spec.* **1976**, *10*, 41.
150. Monniot, C.; Monniot, F. *Coral Reef Ascidiens of New Caledonia*; 1st ed.; ORSTOM: Paris, 1991; Vol. XXX, pp 247.
151. Nakamura, T.; Nagaki, H.; Kinoshita, T. *Bull. Chem. Soc. Jpn.* **1985**, *58*, 2798.
152. Sethi, S.; Nelson, C. C.; McCloskey, J. A. *Anal. Chem.* **1984**, *56*, 1975.
153. Sakaguchi, S. *J. Biochem.* **1950**, *37*, 231.
154. Stahl, E. *Thin-Layer Chromatography A Laboratory Handbook*, 2nd International Student ed.; Springer-Verlag: Berlin, 1969.
155. Shemyakin, M. M.; Ovchinnikov, Y. A.; Vinogradova, E. I.; Feigina, M. Y.; Kiryushkin, A. A.; Aldanova, N. A.; Alakhov, Y. B.; Lipkin, V. N.; Rosinov, B. V. *Experientia* **1967**, *23*, 428.